The use of laser light scattering to study solution crystallization phenomena in polyolefins

by
Margaretha Brand

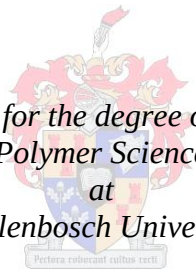

Dissertation presented for the degree of Doctor of Philosophy (Polymer Science) at Stellenbosch University

Promoter: Prof Albert J. van Reenen
Faculty of Science
Department of Chemistry and Polymer Science

December 2012

Declaration

By submitting this thesis electronically, I declare that the entirety of the work contained therein is my own, original work that I am the owner of the copyright thereof (unless to the extent otherwise stated) and that I have not previously in its entirety or in part submitted it for obtaining any qualification.

Date: December 2012

Abstract

An instrument, named solution crystallization analysis by laser light scattering (SCALLS), that measures the solution melting and crystallization of polymers in solution was developed further in this study. The instrument was tested in a theoretical study to evaluate the Flory-Huggins relationship of melting point depression in solution of copolymers. It was found that the solvent interaction parameter for propylene/higher 1-alkene copolymers, with low comonomer content is dependent on the comonomer type. It was also showed that the melting point depression is dependent on both the type and amount of comonomer included in the copolymer. The instrument was further developed to include a total of three lasers with different wavelengths. Initial problems with laser interference was rectified by the introduction of dichroic mirrors to direct the laser light to the relevant detectors and broad pass filters in front of the the detectors to ensure that only the relevant laser light passes through. For homogenous polypropylene samples it was found that even though a slower cooling rate increases the relative peak temperatures as well as the relative temperature differences between the peaks, detail in the peak profiles is the same for the faster cooling rate. The subsequent heating analysis does show that there is a definite dependence on the cooling rate. The ZNPP-4 sample shows that the appearance of a shoulder in the heating analysis becomes more defined as a peak if the preceding cooling analysis is slower. Complex impact-polypropylene samples, differing only in the amount of ethylene were analysed and even small differences between samples were detected. The possible application of the SCALLS instrument was investigated. It was proven that the instrument can be used as a screening method for prep-TREF to determine the fractionation temperatures.

Opsomming

'n Instrument, genoem oplossing kristallisasie-analise deur laser lig verstrooiing (SCALLS), wat die smeltpunt asook die kristallisasie temperatuur in oplossing kan meet is verder ontwikkel in hierdie studie. Die Flory-Huggins verhouding oor die smeltpunt depressie in oplossing van ko-polimere is ondersoek in ‘n teoretiese studie. Daar is bevind dat die oplossing interaksie parameter vir propileen/hoër 1-alkeen kopolimere, met lae ko-monomeer inhoud is afhanklik op die ko-monomeer tipe. Dit is ook getoon dat die smeltpunt depressie afhanklik is van beide die tipe en hoeveelheid ko-monomeer in die ko-polimeer. Die instrument is verder ontwikkel om 'n totaal van drie lasers met verskillende golflengtes in te sluit. Aanvanklike probleme met laser inmenging is reggestel deur die bekendstelling van dichromatiese spieëls wat die laser lig na die regte ooreenstemmende detektor rig en filters voor die detektors verseker dat net die relevante laser lig die detektor bereik. Vir homogene polipropileen monsters is dit bevind dat selfs al is die analises gedoen teen ‘n stadiger afkoelings tempo wat lei tot ‘n verhoging in die piek kristallisasie temperatuur asook die relatiewe temperatuur verskille tussen die lasers, bly die detail in die piek profiele dieselfde as wat gesien word met ‘n vinniger afkoelings tempo. Die daaropvolgende verhitting analise toon dat die analise definitief afhanklik is op die voorafgaande afkoelings analise. Die ZNPP-4 monster toon dat die voorkoms van 'n skouer in die verwarming-analise word meer gedefinieerd en ‘n piek word gevorm soos die voorafgaande afkoelings tempo verlaag. Komplekse impak-polipropileen monsters, wat net verskil in die hoeveelheid etileen inhoud is geanaliseer en verskille is bepaal. Moontlike toepassings van die SCALLS instrument is ondersoek. Dit is bewys dat die instrument gebruik kan word om die fraksionering temperature vooraf te bepaal vir prep-TREF.

This thesis is dedicated to my Mother

-Thank you Mom-

Acknowledgements

I wish to express my sincere gratitude and thanks to the following people:

Prof AJ van Reenen for his on-going guidance and support throughout this and the previous study. Without him I would not have accomplished everything that I did.

Prof EG Rohwer, Dr PH Neethling, Eben Shields, Johan Germishuizen and **Gerhard Louwrens** from the laser research institute at the department of Physics at Stellenbosch University for all the help and guidance throughout the study

The **Olefins** research group

Erinda, Aneli, Margie, Deon, Jim and **Calvin** for administrative and technical assistance

To all my friends that made it fun, either by just making me laugh, going for a hike or going out in town. So thank you **Elana, Phillip, Gareth B, Francois, Adele, Karl, Liesl, Gunter, Kriegler, Danelle, Hanlie, Jacques, Kenneth, Lise, Hennie, Madeleine, Freda, Divann, Pritish, Rassie, Wilma** and everyone that I forgot due to my scatterbrain.

To my family: my **Mom, Liezl** and **Willem** for endless support and encouragement and to **Pedri**, which is always amazed at the experiments I can show him even though he is determined to become an engineer.

Table of Contents

List of Figures

List of equations

List of Tables

Abbreviations

High temperature gel permeation chromatography	HT-GPC
2,6-di-tert-butyl-4-methylephenol	BHT
Nuclear magnetic resonance	NMR
Fourier transform infra-red	FT-IR
Differential scanning calorimetry	DSC
Crystallization analysis fractionation	CRYSTAF
Preparative temperature rising elution fractionation	prep-TREF
Solution crystallization analysis by laser light scattering	SCALLS
1,2,4-trichlorobenzene	TCB
Light amplification by stimulated emission of radiation	laser
Crystallization elution fractionation	CEF
Isotactic polypropylene	iPP
Weight average molecular weight	Mw
Polydispersity index	PDI
Diphenyl-dimethoxysilane	DPDMS
Methyl-phenyl-dimethoxysilane	MPDMS
Propylene random copolymers	EPR
Ethylene propylene copolymers	EPC
Ziegler-Natta polypropylene	ZNPP
Impact polypropylene	ICPP
Number average molecular weight	Mn

Chapter 1

Introduction and Objectives

1.1 Introduction

Material science is essentially the study of the relationship between the structure and the properties of the material in question. In the case of polymeric materials, this is no different. In the case of thermoplastic, semi-crystalline polymers, the morphology of the material is largely described by the extent and nature of the crystalline structures present.

The crystallinity and crystallization of polymers can be studied in a variety of ways. Crystallization from the melt (and melting phenomena) can be studied by thermal analysis techniques, for example by differential scanning calorimetry (DSC). Additionally information might be obtained from scattering experiments (particularly from Wide Angle X-ray Diffraction (WAXD) and Small Angle X-ray Scattering (SAXS). This is particularly useful in determining overall crystallinity as well as differences in crystalline structure between chemically similar polymers.

Several techniques have been used[1,2] to study the crystallization of polymers from solution; and in particular to relate the chemical heterogeneity of these polymers (particularly the polyolefins) to the crystallization data that could be obtained. Crystallization from dilute solution is obviously completely different from that which occurs from the melt, as polymer chains in solution have a far greater degree of freedom of movement than those entangled chains in a viscous polymer melt. Yet it appears as if techniques like Crystallization Analysis Fractionation (CRYSTAF), Temperature Rising Elution Fractionation (TREF)[2] and Crystallization Elution Fractionation[3] (CEF) are commonly used to relate the molecular heterogeneity (or homogeneity) of common polyolefins like LLDPE and isotactic PP to the crystallization behavior of these polymers from solution (the theory and practice of these techniques will be discussed in more detail in Chapter 2).

A number of theories have been developed that describe the crystallization of polyolefins from the melt[4-6] and some of these theories and equations (like the Flory-Huggins equation) have been adapted to crystallization from dilute solutions (please refer to Chapter 3 for details).

It seems that there is a need to investigate the effect of molecular parameters on the results that are obtained from standard techniques like CRYSTAF, TREF and CEF In the recent past, our laboratory developed an instrument, based on the original work of Li et al[7] which we named Solution Crystallization Analysis by Laser Light Scattering (SCALLS)[8,9]

The scope of the research reported on in this thesis involves the development and testing of the SCALLS instrument over the past few years. To this end the aim and objectives of this study can be defined as follows:

1.2 Aim

To develop, expand and test the SCALLS instrument to the point where the instrument could be utilized to reproducibly obtain crystallization data within the family of commercially available polyolefins.

1.3 Objectives

Within the broad scope of the aim as set out in point 1.2 we set ourselves the following objectives:

- After completion of the first phase of the development of the instrument, to test the instrument in a theoretical study of solution crystallization and melting. To this end we will evaluate the Flory-Huggins relationship of melting point depression in solution for copolymers.
- Altering the configuration of the instrument to include lasers of differing wavelengths in order to increase the ability of the instrument to detect crystallization events.
- Evaluation of the instrument with multiple lasers with different polymers, and the investigation of possible application with the instrument.

The following information is a brief summary of the rest of the thesis, divided according to chapters.

Chapter 2:

A brief historical overview of the techniques used in this study to analyse polymers.

Chapter 3:

Details of the experimental techniques used in this study and an overview of the research already conducted with the SCALLS instrument.

Chapter 4:

Measuring the solution melting temperature for the very first time offers the ability to study the applicability of the Flory-Huggins equation.

Chapter 5:

Development of the SCALLS instrument by introducing lasers of different wavelengths.

Chapter 6:

Evaluation of the new instrument and investigation of potential new applications of the SCALLS instrument.

Chapter 7:

Summary of the goals achieved during this study.

1.4 References

[1] Monrabal, B. : Microstructure Characterization of Polyolefins. TREE and CRYSTAF. Stud.Surf.Sci.Catal. **, 161**, 35-42 (2006).

[2] Soares, J.B.P.; Anantawaraskul, S. : Crystallization Analysis Fractionation. J.Polym.Sci., Part B: Polym.Phys. **, 43**, 1557-1570 (2005).

[3] Monrabal, B.; Sancho-Tello, J.; Mayo, N.; Romero, L. : Crystallization Elution Fractionation. A New Separation Process for Polyolefin Resins. Macromol.Symp. **, 257**, 71-79 (2007).

[4] Mandelkern, L. *Crystallization of Polymers*, 2nd ed.; Cambridge University Press: Cambridge, UK ; New York, (2002).

[5] Mandelkern, L. *Crystallization of Polymers*, First Edition ed.; American Institute of Physics, (1964).

[6] Alamo, R.G.; Mandelkern, L. : The Crystallization Behavior of Random Copolymers of Ethylene. Thermochim.Acta **, 238**, 155-201 (1994).

[7] Shan, C.L.P.; de Groot, W.A.; Hazlitt, L.G.; Gillespie, D. : A New Turbidimetric Approach to Measuring Polyethylene Short Chain Branching Distributions. Polymer **, 46**, 11755-11767 (2005).

[8] van Reenen, A.J.; Brand, M.; Rohwer, E.G.; Walters, P. : Solution Crystallization Analysis by Laser Light Scattering (SCALLS). Macromolecular Symposia **, 282**, 25 (2009).

[9] van Reenen, A.J.; Rohwer, E.G.; Walters, P.; Lutz, M.; Brand, M. : Development and use of a Turbidity Analyzer for Studying the Solution Crystallization of Polyolefins. J Appl Polym Sci **, 109**, 3238-3243 (2008).

Chapter 2

Historical Background

2.1 Polypropylene

Polypropylene is used in a variety of applications ranging from household appliances, water sports (floating ropes), Tupperware® and even those colourful shopping bags seen in Woolworths®. It is clear that it is a very popular product but also very diverse in its applications. The diverse end products are not only due to different processing techniques; it already starts at the synthesis of polypropylene. Metallocene catalysis ensures a more homogenous polypropylene while Ziegler-Natta catalysis gives rise to heterogeneous polypropylene. Polypropylene is also not just synthesized as a homopolymer, copolymers are obtained by copolymerization with alpha-olefins and reinforced polypropylene or impact polypropylene is obtained by a two-step process. A brief explanation of these processes follows.

2.1.1 Ziegler-Natta catalysis

Development of suitable catalyst ensured that polypropylene could be polymerized in a usable form and not just a wax as was produced in the beginning processes. During the 1950's Karl Ziegler realised that aluminium alkyls can insert ethylene into the metal-carbon bond to form paraffins[1]. Further research showed that group IV transition metal compounds, such as zirconium and titanium halides, activated with main group metal alkyls can polymerize ethylene at low pressure[1]. The following year Giulio Natta used this technology to successfully produce isotactic PP[1]. Propylene is prochiral and thus polypropylene can have different types of stereoregularity. The multiple active sites present in Ziegler-Natta catalysts produce polymers with varying degree of stereoregularity[2]. Polypropylene produced with multiple active sites is called heterogeneous polypropylene.

2.1.1.1 Internal and External electron donors

In this study a range of Ziegler-Natta polymers are analysed. Two different external donors namely diphenyl-dimethoxysilane (DPDMS) and methyl-phenyl-dimethoxysilane (MPDMS), in varying amounts, were added. Studies have shown that the addition of electron donors leads to an increase in isotacticity and molar mass[3-5]. The polydispersity index decreases with the addition of the electron donors. Internal donors competively coordinate with the Ti species on the support to avoid aspecific sites being formed by coordination of the Ti species with the (110) surface[5,6]. Aspecific sites are converted to isospecific sites by coordination of the internal and external donors with the support in the region of the Ti-species[7]. External donors reduce the extraction of the internal donor by the cocatalyst, this is done by the formation of a complex with the cocatalyst. If however extraction still occurs the external donor replaces the extracted internal donor.

2.1.2 Metallocene catalysis

The term metallocene was first used for the compounds of two rings, consisting of five carbons each, bonded together to a central atom to form a sandwich structure used in polymerizing of polymers. Development in the field of catalysis has changed the structure significantly that metallocene now refers to any catalysts to have a single well defined active centre. Kealy and Paulson were the first to report about ferrocene, but Wilkinson was the first to recognize that it was a sandwich structure. Polymerization occurs in the presence of a co-catalyst, usually an aluminoxane. Due to the single active site, polymers are more homogeneous regarding stereoregularity and thus also called homogeneous polymers.

2.1.3 Impact polypropylene synthesis, the two step process

Polymerization of impact PP is a two-step process that takes place in two sequential reactors[8,9]. Isotactic PP is polymerised in the first reactor with a Ziegler-Natta catalyst. The polymer is then transferred to the second reactor, containing both ethylene and propylene, in the presence of the catalyst. In the second reactor ethylene propylene rubber (EPR) is mainly formed. The EPR is mainly contained within the PP matrix. Ethylene-propylene copolymers are also formed; these have various lengths of ethylene and propylene sequences. Ethylene homopolymer is also formed during this step. This leads to a very complex polymer. In this study samples were taken out of the second reactor at increasing time intervals. The first sample was taken before any addition of ethylene, thus isotactic-PP. Subsequent samples that were removed have increasing ethylene content with increasing time spent in the reactor.

2.1.3.1 Degradation of Impact polypropylene

Suzuki et al[10,11] investigated the effect of comonomer content and tacticity on a series of impact PP copolymers with different ethylene contents. It was seen that a decreasing tacticity and increasing ethylene content lead to an increase in oxidation resistance in this series of copolymers. De Goede et al[12] studied the spatial heterogeneity of thermo oxidative degradation of impact polypropylene and showed that samples with lower ethylene content degraded faster at all depths than samples with higher ethylene content.

2.2 Rayleigh and Mie Scattering.

When a portion of incident radiation is diffused in a medium of different refractive index by small particles, it is called scattering[13]. Light Amplification by Stimulated Emission of Radiation or commonly known by its acronym laser is a suitable light source in spectroscopy due to its high spatial and temporal coherence. Scattering of the laser light will occur when it encounters non-uniform

entities in its trajectory. The type of light scattering is defined by the dimensionless size parameter α, which can be defined by Equation 2-1.

Equation 2-1:Light scattering equation defined by the dimensionless parameter α

$$\alpha = \frac{\pi D_p}{\lambda}$$

Where λ is the wavelength of the incident light and πD_p is the circumference of the particle.

The minimum size needed to scatter light is dependent on the wavelength. When the particles are small, relative to the wavelength, Rayleigh's law of scattering will apply[14]. This states that the intensity of the scattered light varies inversely as the fourth power of the wavelength of light and directly as the sixth power of the diameter of the particle. Thus scattering is dependent on two factors, the particle size and the wavelength. Rayleigh scattering can visually be explained by a phenomenon that happens every day, daylight and sunset[13]. During the day, the sky is blue due to sunlight being scattered in the atmosphere. The shorter wavelength, blue in visible spectrum, gets scattered more and thus the sky appear blue. During sunset the sun is closer to the horizon and the light must now pass through more air, Rayleigh scattering is increased for the shorter wavelength, blue colour, to such an extent that the colour cannot be seen. The longer wavelength colours remain and thus sunset appears red/orange. This effectively relates to analysis by laser light. If a blue laser is used a point will be reached were the effective light scattered, ensure that no light passes through to the detector but the longer wavelength lasers will at that point have lower scattering and a signal will still be detected.

2.2.1 A brief overview of the development of crystallization theory

If only the chemical composition is taken into account it would seem that polyolefins are simple materials consisting of only carbon and hydrogen atoms. In reality the complete opposite is true due to the complexity that arises from microstructure, tacticity, molecular weight and polymer architecture. To understand the complexity of the structure and property relationship of polymers multiple experimental techniques, scientific disciplines and theoretical approaches are needed[15]. Polymer properties are affected by the molecular morphology that in turn is affected by the crystallization mechanisms. Information of the crystallization mechanism is obtained by studying the crystallization kinetics[15,16] thus in the end everything is interrelated.

The growth in the field of polymer crystallization is well illustrated by the publication of Leo Mandelkern's book crystallization of polymers. In 1964 the first edition of crystallization of polymers[17] was published as one volume. The second edition[15] published in 2002 consisted of three volumes covering equilibrium concepts, kinetics and mechanisms and lastly the morphology, structure and properties. The broadness of the subject thus caused different research fields to form below it. Even though throughout the years, various research groups have studied different aspects of polymer

crystallization broadening the understanding of polymer crystallization, which I will discuss briefly, there still is a lot of research to be done.

After the discovery in 1957 by P. H. Till that single crystals can be grown from dilute solutions of linear polyethylene [18] Hoffman and Lauritzen presented their theory for the formation of chain-folded crystals in 1960 and 1961 resulting in the Hoffman-Lauritzen theory that is still used today. Throughout the years it has been revisited and modified, even by the authors themselves[19-21] but the core idea is still intact. In 1969 together with Passaglia, Ross, Frolen and Weeks[22] an extensive article regarding the kinetics of polymer crystallization from solution and melt was published. There were three main objectives, the first was to investigate the basic cause of chain folding, secondly to predict the variation of thickness of chain-folded lamellae due to crystallization temperature in fundamental terms and thirdly to predict the thermodynamic properties of the chain-folded crystals that is produced at various temperatures.

The Johnson-Mehl-Avrami-Kolmogorov (JMAK) equation[23,24] is used to describe the kinetics behind the crystallization of polymers, originally for isothermal crystallization but modifications have made it possible to study non-isothermal crystallization[25,26][27]. The equation has two constants, n and k, that can help to describe the type and rate of crystallization and this is described further on in this section. The Ozawa equation[28,29][30] has also been shown to adequately describe the non-isothermal crystallization of polymers and it has even been combined with the JMAK equation[27]. Numerous kinetic studies based on this equation have been done throughout the years.

More recently work has shifted to try and model and predict polymer crystallization. Muthukumar has published work on the modelling of polymer chemistry[31-33] and molecular modelling of nucleation in polymers[34] as well. Soares and Anantawaraskul have done extensive work on the modelling of polymer crystallization in CRYSTAF[35-40].

As can be seen, this is quite an extensive field and thus cannot be discussed in detail here and thus only the brief discussion given.

2.3 Crystallization in solution and in the bulk

A full understanding of complex semi-crystalline polymers cannot be achieved by just analysing the bulk properties. This will only give an average value and no detail on the heterogeneity of the sample is obtained. Fractionation techniques are a necessity to characterize these polymers. The polymer can either be bulk fractionated with subsequent off-line characterization, with multiple characterization techniques fractionation and characterization happens in one on-line step. Polymers are not heterogeneous in just one aspect and depending on the type of polymer can have a distribution in molecular weight, tacticity, chemical composition and comonomer sequence length. There are

quite a few characterization techniques available for fractionation based on the above mentioned distributions and a brief overview of the relevant techniques will be discussed.

2.3.1 TREF

Temperature rising elution fractionation is a two-step process, consisting of a slow cooling step followed by a dissolution step. The polymer is controlled cooled in the first step, where no solvent flow is present, assuring reproducible results according to crystallisability. Control of the cooling step is very important as discussed in the work of Glockner, Bergström, Avela and Wild[41-43]. If proper temperature control is maintained the polymer will crystallize out of solution in decreasing order of crystallizability. Fractions crystallize on top of each other forming, what is best described as, an onion layer structure with the support, if present, as the core layer. If no support was used during the cooling step, one is mixed in before elution. In the second step the polymer is eluted in increasing order of crystallisability from the support at successively higher temperatures. There are two types of TREF experiments, namely analytical TREF and preparative TREF (p-TREF). In principle the two techniques are the same but usually prep-TREF is used when further separate analysis, such as SEC, NMR, DSC; just to name a few are needed. This makes the process a lot slower than analytical TREF but more information is obtained. In comparison larger sample sizes are needed for Prep-TREF than analytical TREF and thus also bigger columns. The other big difference is the temperature profile used. The polymer is eluted at predetermined temperature intervals to obtain fractions in Prep-TREF in comparison to a continuous temperature profile used in analytical TREF.

2.3.2 CRYSTAF

Following on from TREF, Monrabal[44,45] developed a new technique called Crystallization Analysis Fractionation (CRYSTAF). CRYSTAF is a one-step analysis, providing faster analysis than TREF. The instrument consists of five stainless steel vessels inside of an oven. The polymer is dissolved in a suitable solvent, such as 1,2,4 TCB, that is compatible to be used with the infrared detector. The solution is stirred throughout the whole analysis. Crystallization takes place in solution, no support present. Aliquot of samples are taken discontinuously for measurement throughout the cooling process. The sample is filtered through an internal filter and the polymer concentration left in solution is measured in comparison to the concentration of the sample at the beginning of analysis. The number of data points taken is determined by the user but is limited by the solution volume as well as the time needed to take samples. The temperature is lowered at a controlled cooling rate but the end temperature is limited by the solvent used, the solution cannot be lowered below the freezing point of the solvent used and thus for a standard run the temperature is decreased to between 25 °C and 30 °C. The soluble fraction i.e. all polymer left in solution at the end of analysis, is measured relatively to the beginning concentration.

2.3.3 SCALLS

Shan[46] first introduced a new instrument, turbidity fractionation analyser (TFA), to analyse the short chain branching distribution of polyethylenes. A similar instrument was built by Van Reenen et al[47] and the effect of different experimental parameters was tested as well as the response of different types of polymers. A new name was coined for the instrument namely, solution crystallization analysis by laser light scattering, SCALLS[48] for short. Propylene α-olefin copolymers were synthesized and analysed on the instrument. The further development of this instrument is the focus of this work and thus no more will be said about it in this part.

2.3.4 CEF

A new technique called Crystallization Elution Fractionation (CEF) combines the separation power of TREF and CRYSTAF but with faster analysis time. The technique combines the two step analysis of TREF but the physical separation takes place during the cooling cycle as in CRYSTAF. The polymer is crystallized onto a support inside a column but during the cooling cycle a solvent flows through the cell at a low flow rate. The flow rate causes the polymer to move until it reaches its crystallization temperature, crystallizes out of solution and stays at that spot while the polymer still in solution moves forward. As explained in the work of Monrabel[49] et al, this flow rate is very important. The flow rate must be calculated, taken into account the crystallization rate and range as well as the column volume. It is considered an optimal crystallization if the crystallized polymer covers the whole column. When the crystallization cycle is completed the flow is stopped, the column is heated and a higher flow rate is applied to elute the polymer. The fractions will elute in the same order as with CRYSTAF due to the separation occurring in the crystallization step and not in the dissolution step as in TREF.

2.3.5 DSC

DSC analysis usually takes place with a solid state sample but Mirabella[50] tested the melting of poly(ethylene-α-olefin) random copolymers in the presence of a trichlorobenzene as a diluent.

Successive self-nucleation and annealing (SSA) can be performed on a DSC[51,52]. The polymer is subjected to a series of annealing steps after which the melting behaviour is observed. During the annealing steps the polymer is fractionated based on its short chain branching content, molar mass or crystallizability. Chau and Teh[52] analysed ethylene copolymers and found a good correlation between the TREF and SSA data. It was also shown that if interest only lies with the homopolymer fraction, analysis can be performed only above 90°C, decreasing analysis time by half.

2.3.5.1 Determining Avrami constants from DSC

Crystallization consists of two main processes; primary crystallization and secondary crystallization. Primary crystallization is the macroscopic development of crystallinity. This involves primary and secondary nucleation. Secondary crystallization is the crystallization of the interfibrillar melt, rejected and trapped by the primary crystal structure[53]. Crystallization kinetics is not just important for academic purposes but also for industry. During processing the rate of transformation from the melt to semi-crystalline state is important. Just as important is the effect of fillers, additives, anti-static and anti-oxidants, to name a few, on the rate of crystallization. A lot of research has been done on developing a mathematical model to describe macroscopic evolution of crystallinity during isothermal conditions. Kolmogorov, Johnson and Mehl and Evans proposed similar models to the work of Avrami[23,24,53]. Avrami calculates the volume of material that crystallizes as a function of time[54,55]. To be able to apply the Avrami equation to the crystallization of macromolecules some modifications/assumptions are made as mentioned here;

- Nucleation is random.
- All nuclei are formed simultaneously or a constant rate of nucleation is sustained and thus a constant nucleation density
- Linear crystal growth rate is assumed to be constant from nucleation to impingement.
- Impingement leads to a negligible volume fraction of interference

This gives rise to the following general form of the Avrami expression[27,56]

Equation 2-2: Avrami equation in its general form

$$X_t = 1 - \exp(-kt^n)$$

Crystal conversion or relative crystallinity is denoted by X_t , the Avrami exponent by n and the rate parameter by k[25,27].

The Avrami exponent, n, gives an indication of the mechanism of nucleation as well as the geometry of crystal growth and is the value of the slope of the Avrami plots. The rate constant, k, is a combination of the nucleation and growth-rate parameters, obtained from the y-axis intersect of the Avrami plot. Three-dimensional growth gives rise to an Avrami exponent of 4, two-dimensional growth an exponent of 3 and so forth[55].

2.3.6 Solution crystallization according to molecular weight

Polymers can be fractionated according to molecular weight by use of a solvent non-solvent system. Moore and Boden[57] fractionated atactic polypropylene into six fractions by adding acetone, a non-solvent, to a cyclohexane polymer solution. Vilaplana[58] used this technique to preparatively fractionate polymers according to molecular weight, with a preparative CRYSTAF. Paukkeri and

Lehtinen[59] fractionated polypropylene acording to molecular weight by using ethylene glycol monobutyl ether/diethylene glycol monobutyl ether as a solvent/non-solvent pair.

2.3.7 Fractionation according to chemical composition distribution

Recent developments in high-temperature gradient HPLC[60] has made it possible to separate polyethylene-polypropylene blends. The separation was achieved by using ethylene glycol monobutylether (EGMBE) and trichlorobenzene as a mobile phase and silica gel as the stationary phase. A precipitation-redissolution mechanism was achieved for polyethylene (PE) with the use of n-decanol while polypropylene (PP) was eluted in size exclusion mode. Ethylene-propylene-diene terpolymers were separated according to the content of diene by HT-HPLC and HT 2D-LC by Chitta et al[61].

2.4 An overview of the research already conducted on the SCALLS

This thesis is a continuation of the research undertaken towards the MSc degree of the author of this thesis[62]. In order to obviate the necessity of repetition regarding the experimental set-up that lead to the stage where the research and development of the present SCALLS instrument evolved, and which is the topic of this thesis, we thought it necessary to present a brief overview of the work undertaken to date. The simplest way of doing this was to present papers that appeared in the Journal of Applied Polymer Science and Macromolecular Symposia 2009 [47,48]. This provides an overview of the research instrumentation and the experimentation that occurred in the initial stages of the paper. These papers are presented in Appendix A.

2.5 Summary

This concludes the brief summary on crystallization, polymer synthesis and characterization techniques. In this study fully characterised polymers were analysed on a relatively new analytical technique to access the potential of it. In following chapters the experimental techniques will be discussed followed by the results that were obtained.

2.6 References

[1] Karger-Kocsis, J. Polypropylene - an A-Z Reference. (1999).

[2] Virkkunen, V.; Laari, P.; Pitkänen, P.; Sundholm, F. : Tacticity Distribution of Isotactic Polypropylene Prepared with Heterogeneous Ziegler–Natta Catalyst. 1. Fractionation of Polypropylene. Polymer **, 45**, 3091-3098 (2004).

[3] Correa, A.; Piemontesi, F.; Morini, G.; Cavallo, L. : Key Elements in the Structure and Function Relationship of the MgCl2/TiCl4/Lewis Base Zieglerâ''Natta Catalytic System. Macromolecules **, 40**, 9181-9189 (2007).

[4] Chadwick, J.C.; Morini, G.; Balbontin, G.; Camurati, I.; Heere, J.J.R.; Mingozzi, I.; Testoni, F. : Effects of Internal and External Donors on the Regio- and Stereoselectivity of Active Species in MgCl2-Supported Catalysts for Propene Polymerization. Macromolecular Chemistry and Physics **, 202**, 1995-2002 (2001).

[5] Barbé, P.; Cecchin, G.; Noristi, L. The catalytic system Ti-complex/$MgCl_2$. In *Catalytical and Radical Polymerization*.; Anonymous .; Springer Berlin / Heidelberg, 1986; 81, pp. 1-81.

[6] Lim, S.; Choung, S. : Effects of External Electron Donor on Catalyst Active Sites in Propylene Polymerization. J Appl Polym Sci **, 67**, 1779-1787 (1998).

[7] Bukatov, G.D.; Zakharov, V.A. : Propylene Ziegler-Natta Polymerization: Numbers and Propagation Rate Constants for Stereospecific and Non-Stereospecific Centers. Macromolecular Chemistry and Physics **, 202**, 2003-2009 (2001).

[8] Debling, J.A.; Ray, W.H. : Heat and Mass Transfer Effects in Multistage Polymerization Processes: Impact Polypropylene. Ind Eng Chem Res **, 34**, 3466-3480 (1995).

[9] Kittilsen, P.; McKenna, T.F. : Study of the Kinetics, Mass Transfer, and Particle Morphology in the Production of High-Impact Polypropylene. J Appl Polym Sci **, 82**, 1047-1060 (2001).

[10] Suzuki, S.; Boping, L.; Terano, M.; Manabe, N.; Kawamura, K.; Ishikawa, M.; Nakatani, H. : Influence of Primary Structure on Thermal Oxidative Degradation of Polypropylene Impact Copolymer. Polymer Bulletin **, 55**, 141-147 (2005).

[11] Suzuki, S.; Nakamura, Y.; Hasan, A.K.; Liu, B.; Terano, M.; Nakatani, H. : Dependence of Tacticity Distribution in Thermal Oxidative Degradation of Polypropylene. Polymer Bulletin **, 54**, 311-319 (2005).

[12] de Goede, E.; Mallon, P.E.; Rode, K.; Pasch, H. : Spatial Heterogeneity of Thermo-Oxidative Degradation in Impact Poly(Propylene) Copolymers. Macromolecular Materials and Engineering **, 296**, 1018-1027 (2011).

[13] Halliday, D.; Resnick, R.; Walker, J. *Fundamental of Physics*, Fifth Edition ed.; John Wiley & Sons: United States of America, (1997).

[14] Barnett, C.E. : Some Applications of Wave-Length Turbidimetry in the Infrared. - J. Phys. Chem. **, 46**, - 69 (1942).

[15] Mandelkern, L. *Crystallization of Polymers*, 2nd ed.; Cambridge University Press: Cambridge, UK ; New York, (2002).

[16] Mandelkern, L. : The Structure of Crystalline Polymers. Acc. Chem. Res. **, 23**, 380-386 (1990).

[17] Mandelkern, L. *Crystallization of Polymers*, First Edition ed.; American Institute of Physics, (1964).

[18] Till, P.H. : The Growth of Single Crystals of Linear Polyethylene. Journal of Polymer Science **, 24**, 301-306 (1957).

[19] Hoffman, J.D.; Miller, R.L. : Kinetic of Crystallization from the Melt and Chain Folding in Polyethylene Fractions Revisited: Theory and Experiment. Polymer **, 38**, 3151-3212 (1997).

[20] Hoffman, J.D.; Miller, R.L. : Response to Criticism of Nucleation Theory as Applied to Crystallization of Lamellar Polymers. Macromolecules **, 22**, 3502-3505 (1989).

[21] Cheng, S.Z.D.; Lotz, B. : Enthalpic and Entropic Origins of Nucleation Barriers during Polymer Crystallization: The Hoffman–Lauritzen Theory and Beyond. Polymer **, 46**, 8662-8681 (2005).

[22] Hoffman, J.D.; Lauritzen, J.I.; Passaglia, E.; Ross, G.S.; Frolen, L.J.; Weeks, J.J. : Kinetics of Polymer Crystallization from Solution and the Melt. Colloid & Polymer Science **, 231**, 564-592 (1969).

[23] Tomellini, M.; Fanfoni, M.; Volpe, M. : Spatially Correlated Nuclei: How the Johnson-Mehl-Avrami-Kolmogorov Formula is Modified in the Case of Simultaneous Nucleation. Phys. Rev. B **, 62**, 11300-11303 (2000).

[24] Li, J.J.; Wang, J.C.; Xu, Q.; Yang, G.C. : Comparison of Johnson–Mehl–Avrami–Kologoromov (sic) (JMAK) Kinetics with a Phase Field Simulation for Polycrystalline Solidification. Acta Materialia **, 55**, 825-832 (2007).

[25] Qin, J.; Deng, K.; Li, Z. : Melting Behavior, Isothermal and Nonisothermal Crystallization Kinetics of EPPE/mLLDPE Blends. J Appl Polym Sci **, 108**, 3601-3609 (2008).

[26] Hussein, I.A. : Nonisothermal Crystallization Kinetics of Linear Metallocene Polyethylenes. J Appl Polym Sci **, 107**, 2802-2809 (2008).

[27] Li, J.; Zhou, C.; Wang, G.; Tao, Y.; Liu, Q.; Li, Y. : Isothermal and Nonisothermal Crystallization Kinetics of Elastomeric Polypropylene. Polym. Test. **, 21**, 583-589 (2002).

[28] Eder, M.; Wlochowicz, A. : Kinetics of Non-Isothermal Crystallization of Polyethylene and Polypropylene. Polymer **, 24**, 1593-1595 (1983).

[29] Lu, H.; Nutt, S. : Cold-Crystallization Kinetics of Syndiotactic Polystyrene. J Appl Polym Sci **, 89**, 3464-3470 (2003).

[30] Bogoeva-Gaceva, G.; Janevski, A.; Grozdanov, A. : Crystallization and Melting Behavior of iPP Studied by DSC. J Appl Polym Sci **, 67**, 395-404 (1998).

[31] Muthukumar, M. : Modeling Polymer Crystallization. Polym.Mater.Sci.Eng. **, 85**, 195 (2001).

[32] Muthukumar, M. : Modeling Polymer Crystallization. Adv.Polym.Sci. **, 191**, 241-274 (2005).

[33] Muthukumar, M.; Welch, P. : Modeling Polymer Crystallization from Solutions. Polymer **, 41**, 8833-8837 (2000).

[34] Muthukumar, M. : Molecular Modelling of Nucleation in Polymers. Philosophical Transactions: Mathematical, Physical and Engineering Sciences **, 361**, pp. 539-556 (2003).

[35] Anantawaraskul, S.; Soares, J.B.P.; Jirachaithorn, P. : A Mathematical Model for the Kinetics of Crystallization in Crystaf. Macromol.Symp. **, 257**, 94-102 (2007).

[36] Anantawaraskul, S.; Jirachaithorn, P.; Soares, J.B.P.; Limtrakul, J. : Mathematical Modeling of Crystallization Analysis Fractionation of ethylene/1-Hexene Copolymers. J.Polym.Sci., Part B: Polym.Phys. **, 45**, 1010-1017 (2007).

[37] Anantawaraskul, S.; Somnukguandee, P.; Soares, J.B.P.; Limtrakul, J. : Application of a Crystallization Kinetics Model to Simulate the Effect of Operation Conditions on Crystaf Profiles and Calibration Curves. J.Polym.Sci., Part B: Polym.Phys. **, 47**, 866-876 (2009).

[38] Anantawaraskul, S.; Soares, J.B.P.; Jirachaithorn, P.; Limtrakul, J. : Mathematical Modeling of Crystallization Analysis Fractionation (Crystaf) of Polyethylene. J.Polym.Sci., Part B: Polym.Phys. **, 44**, 2749-2759 (2006).

[39] Anantawaraskul, S.; Soares, J.B.P.; Wood-Adams, P.M. : An Experimental and Numerical Study on Crystallization Analysis Fractionation (Crystaf). Macromol.Symp. **, 206**, 57-68 (2004).

[40] Soares, J.B.P.; Monrabal, B.; Nieto, J.; Blanco, J. : Crystallization Analysis Fractionation (CRYSTAF) of Poly(Ethylene-Co-1-Octene) made with Single-Site-Type Catalysts. A Mathematical Model for the Dependence of Composition Distribution on Molecular Weight. Macromol.Chem.Phys. **, 199**, 1917-1926 (1998).

[41] Wild, L.; Ryle, T.R.; Knobeloch, D.C.; Peat, I.R. : Determination of Branching Distributions in Polyethylene and Ethylene Copolymers. Journal of Polymer Science: Polymer Physics Edition **, 20**, 441-455 (1982).

[42] Wild, L.; Glöckner, G. Temperature rising elution fractionation. In *Separation Techniques Thermodynamics Liquid Crystal Polymers*.; Anonymous .; Springer Berlin / Heidelberg, 1991; 98, pp. 1-47.

[43] Bergström, C.; Avela, E. : Investigation of the Composite Molecular Structure of LDPE by using Temperature Rising Elution Fractionation. J Appl Polym Sci **, 23**, 163-171 (1979).

[44] Monrabal, B. : Crystallization Analysis Fractionation: A New Technique for the Analysis of Branching Distribution in Polyolefins. J Appl Polym Sci **, 52**, 491-499 (1994).

[45] Monrabal, B. : Crystallization Based Separations for Semicrystalline Polymers. Abstracts of Papers, 236th ACS National Meeting, Philadelphia, PA, United States, August 17-21, 2008 , ANYL-247 (2008).

[46] Shan, C.L.P.; de Groot, W.A.; Hazlitt, L.G.; Gillespie, D. : A New Turbidimetric Approach to Measuring Polyethylene Short Chain Branching Distributions. Polymer **, 46**, 11755-11767 (2005).

[47] van Reenen, A.J.; Rohwer, E.G.; Walters, P.; Lutz, M.; Brand, M. : Development and use of a Turbidity Analyzer for Studying the Solution Crystallization of Polyolefins. J Appl Polym Sci **, 109**, 3238-3243 (2008).

[48] van Reenen, A.J.; Brand, M.; Rohwer, E.G.; Walters, P. : Solution Crystallization Analysis by Laser Light Scattering (SCALLS). Macromolecular Symposia **, 282**, 25 (2009).

[49] Monrabal, B.; Sancho-Tello, J.; Mayo, N.; Romero, L. : Crystallization Elution Fractionation. A New Separation Process for Polyolefin Resins. Macromol.Symp. **, 257**, 71-79 (2007).

[50] Mirabella, F.M. : Correlation of the Elution Behavior in Temperature Rising Elution Fractionation and Melting in the Solid-State and in the Presence of a Diluent of Polyethylene Copolymers. J.Polym.Sci., Part B: Polym.Phys. **, 39**, 2819-2832 (2001).

[51] Arnal, M.L.; Sánchez, J.J.; Müller, A.J. : Miscibility of Linear and Branched Polyethylene Blends by Thermal Fractionation: Use of the Successive Self-Nucleation and Annealing (SSA) Technique. Polymer **, 42**, 6877-6890 (2001).

[52] Chau, J.; Teh, J. : Successive Self-Nucleation and Annealing in the Solvated State of Ethylene Copolymers. Journal of Thermal Analysis and Calorimetry **, 81**, 217-223 (2005).

[53] Supaphol, P.; Spruiell, J.E. : Application of the Avrami, Tobin, Malkin, and Simultaneous Avrami Macrokinetic Models to Isothermal Crystallization of Syndiotactic Polypropylenes. Journal of Macromolecular Science, Part B **, 39**, 257-277 (2000).

[54] Bruna, P.; Crespo, D.; Gonzalez-Cinca, R.; Pineda, E. : On the Validity of Avrami Formalism in Primary Crystallization. J. Appl. Phys. **, 100**, 054907 (2006).

[55] T Pradell and D Crespo and N Clavaguera and,M.T.Clavaguera. : Diffusion Controlled Grain Growth in Primary Crystallization: Avrami Exponents Revisited. Journal of Physics: Condensed Matter **, 10**, 3833 (1998).

[56] Pineda, E.; Pradell, T.; Crespo, D. : Non-Random Nucleation and the Avrami Kinetics. Philos. Mag. A **, 82**, 107-121 (2002).

[57] Moore, W.R.; Boden, G.F. : Heptane-Soluble Material from Atactic Polypropylene. I. Fractionation and Characterization of Fractions. J Appl Polym Sci **, 9**, 2019-2029 (1965).

[58] Vilaplana, F.; Morera-Escrich, V.; del Hierro-Navarro, P.; Monrabal, B.; Ribes-Greus, A. : Performance of Crystallization Analysis Fractionation and Preparative Fractionation on the Characterization of α-Irradiated Low-Density Polyethylene. J Appl Polym Sci **, 94**, 1803-1814 (2004).

[59] Paukkeri, R.; Lehtinen, A. : Thermal Behaviour of Polypropylene Fractions: 1. Influence of Tacticity and Molecular Weight on Crystallization and Melting Behaviour. Polymer **, 34**, 4075-4082 (1993).

[60] Heinz, L.; Pasch, H. : High-Temperature Gradient HPLC for the Separation of polyethylene–polypropylene Blends. Polymer **, 46**, 12040-12045 (2005).

[61] Chitta, R.; Ginzburg, A.; van Doremaele, G.; Macko, T.; Brüll, R. : Separating Ethylene-Propylene-Diene Terpolymers According to the Content of Diene by HT-HPLC and HT 2D-LC. Polymer **, 52**, 5953-5960 (2011).

[62] Margaretha Brand. : Investigation of molecular weight effects during the solution crystallisation of polyolefins. University of Stellenbosch (2008).

Chapter 3

Experimental

This chapter focuses on the techniques used to characterize the polymers in this study

3.1 Polymerization

The homogeneous polypropylene and the heterogeneous polypropylene samples were synthesized in previous studies. Details regarding the synthesis can be found in the references given. The impact polypropylene reactor grade powders were received from SASOL Polymers (Secunda, South Africa).

3.2 Characterization

This section contains information regarding the techniques used to characterize the polymers as well as details regarding sample preparation.

3.2.1 High temperature gel permeation chromatography (HT-GPC)

Molecular weights were determined on a Polymer Laboratories PL-GPC-220 high temperature chromatograph at elevated temperature, 150 °C with a flow rate of 1 ml/min. The column set is a combination of three, 300 × 7.5 mm PLgel Olexis columns and a PLgel Olexis guard column of the dimensions 50 × 7.5 mm. Samples were dissolved at a concentration of 0.75 mg/ml in 1,2,4-trichlorobenzene and 200µl were injected for analysis. The solvent was stabilized with 0.0125% 2,6-di-tert-butyl-4-methylphenol (BHT), which also functioned as the flow rate marker. Calibration is done with monodisperse polystyrene standards (Polymer Laboratories).

3.2.2 Nuclear magnetic resonance (NMR)

^{13}C NMR spectra were performed on a Varian Unity Inova 600 MHz spectrometer at 120 °C. The pulse angle was 90 degrees with an acquisition and relaxation time of 1.8 and 15 seconds respectively. 1,1,2,2-tetrachloroethane-d_2 with a shift of δ 74.3 was used as an internal reference. Tacticity calculations were determined according to the method described by Busico[1] et al.

3.2.3 Fourier transform infra-red (FT-IR)

Infra-red spectra were obtained on a Nicolet iS10 with an attenuated total reflectance attachment. Infrared spectra were obtained for the reactor grade powder and heat treated impact polyprolyene samples. To ascertain if any degradation is taking place during heat treatment of the impact polypropylene samples the appearance of carbonyl peaks at 1735.7 cm^{-1} were taken as evidence. The appearance of carbonyl peaks at 1735.7 cm^{-1} could be evidence of possible degradation taking place.

3.2.4 Differential scanning calorimetry (DSC)

DSC thermograms were obtained on a TA Instruments Q100 DSC module. The instrument is calibrated with indium metal according to standard methods.

Standard analysis runs:

Heated from 25 °C to 220 °C at a rate of 10 °C/min, isothermal for 5 min, cooled down to -40 °C at a rate of 10 °C/min and lastly heated again to 200 °C at a rate of 10 °C/min.

Melting and crystallization peak temperatures were obtained from these standard runs

Isothermal analysis to determine Avrami constants:

Samples were heated to 10 °C above their melting temperatures, as obtained from the standard analysis runs. Samples were then cooled down at a rate of 30 °C/min to the isothermal crystallization temperature. This was repeated at different crystallization temperatures for each sample. More detail regarding the calculations of the Avrami constant is given in chapter 6.

3.2.5 Crystallization analysis fractionation (CRYSTAF)

A commercial CRYSTAF model 200 supplied by PolymerChar Spain was used for crystallization analysis fractionation. Precisely 20 mg of sample were dissolved in 40 ml 1,2,4-trichlorobenzene. The sample was dissolved at 160 °C for 90 minutes. The sample was then equilibrated at 100 °C for 30 minutes after which it was cooled at a rate of 0.1 °C/min to 30 °C.

3.2.6 Preparative temperature rising elution fractionation (prep-TREF)

To obtain sufficient sample, enough for further analysis, during fractionation a bulk fractionation technique was used. Prep-TREF allows the user to start with relatively large amounts of polymer. In this case 3 grams of polymer was dissolved in 300 ml of xylene with 2% (w/v) Irganox 1010 as a stabiliser. The solution was transferred into a glass reactor positioned in an oil bath heated to 130 °C. A heated support, in this case washed sand-quartz (Sigma Aldrich), was added to the solution, enough to ensure that all the solution was covered. The oil bath was then cooled at a rate of 1 °C/hour to room temperature. Four glass vessels were positioned in the oil bath, and thus four samples could be cooled simultaneously. Afterwards the sample was transferred to a steel column inside a GC oven. The oven was heated to predetermined temperatures at which fractions were collected. Solvent is pumped through the column and the fraction that is dissolved at that temperature elutes with the solvent. To isolate the polymer the solvent was evaporated with the help of a rotary evaporator.

3.2.7 Solution crystallization analysis by laser light scattering (SCALLS)

Polymers are dissolved in 1,2,4-trichlorobenzene at a concentration of 0.5 mg/ml, unless otherwise stated. A standard analysis consists of dissolving the polymers at elevated temperatures, different for each type of polymer, cooling the solution at a rate of 1 °C/min to 100 °C and kept there for 10 minutes to stabilize. The polymer solution is then controlled cooled to 30 °C at a rate of either 0.2 °C/min, 0.4 °C/min or 1 °C/min and kept isothermally for 5 min after which the solution was controlled heated at a rate of 1.5 °C/min to 120 °C. Analyses were repeated 3 times to ensure accuracy and repeatability. The experimental setup can be seen in **Error! Reference source not**

found.. The lasers are positioned on the left hand side and the detectors on the right hand side as marked. Experiments are performed in the dark as can be seen in **Error! Reference source not found.**. To show the lasers light more pronouncedly powder was scattered to highlight the laser beam.

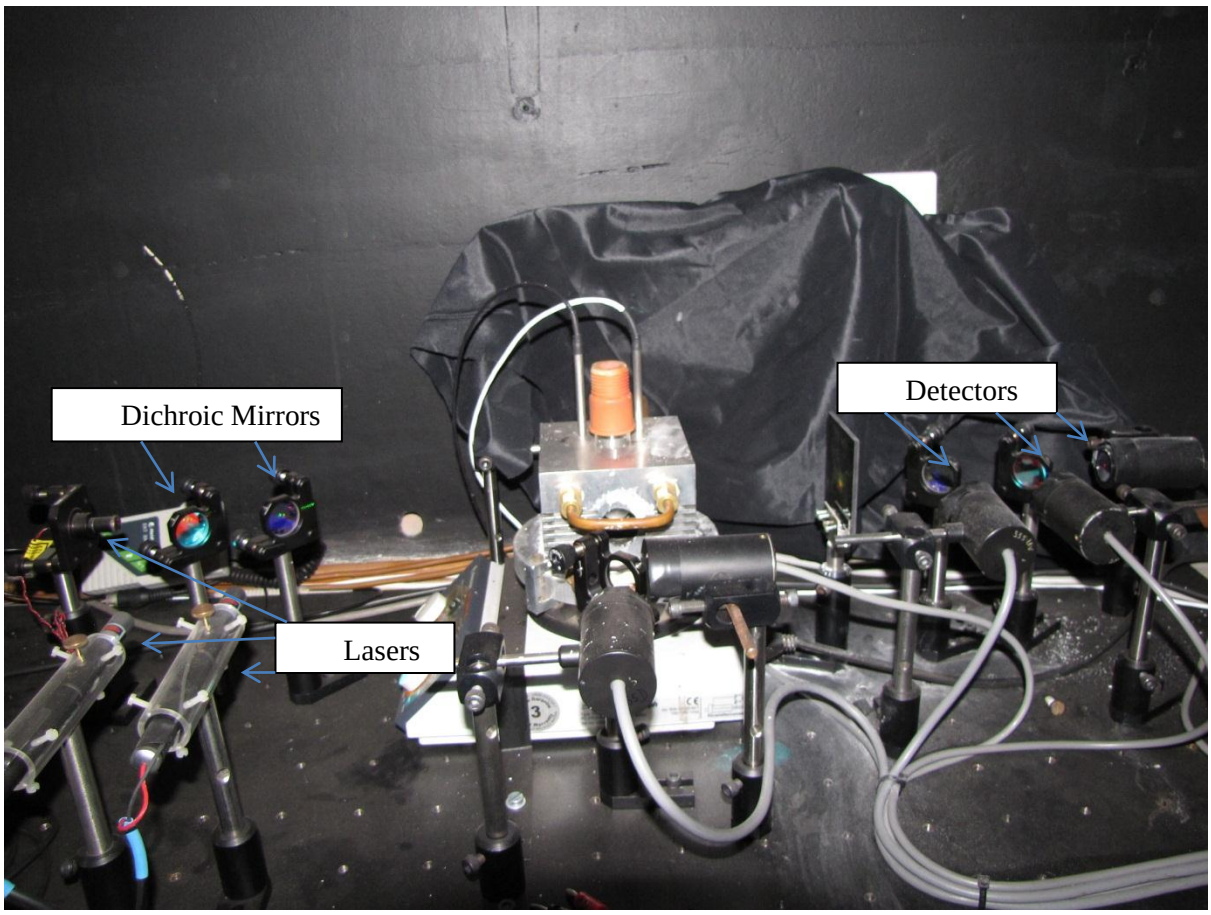

Figure 3.1: Experimental setup of the SCALLS instrument

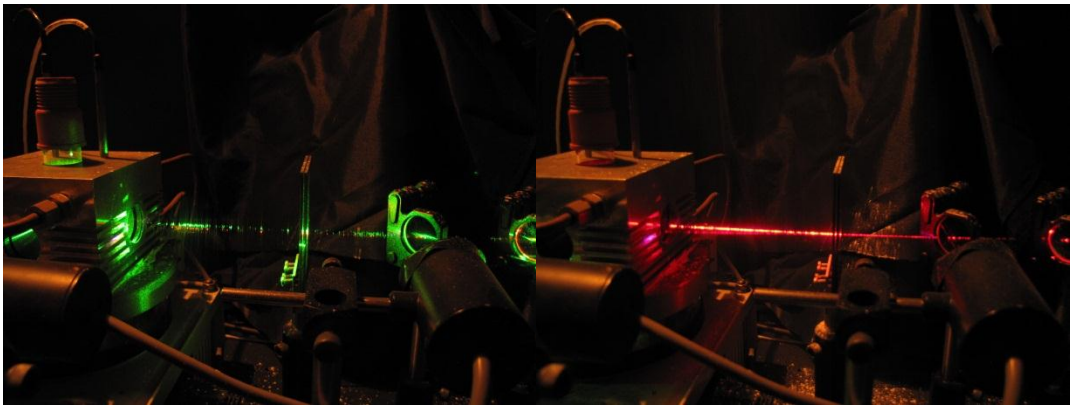

Figure 3.2: Detail of the setup, from the sample to the detectors, to accentuate the lasers powder was scattered over the beam.

3.3 References

[1] Busico, V.; Cipullo, R.; Monaco, G.; Vacatello, M.; Segre, A.L. : Full Assignment of the ^{13}C NMR Spectra of Regioregular Polypropylenes: Methyl and Methylene Region. Macromolecules**,** **30**, 6251-6263 (1997).

Chapter 4

The solution melting temperature of polyolefins and the Flory-Huggins equation: A SCALLS study

The conclusion of the first phase of the development of the SCALLS instrument prompted us to pursue an investigation into the possible application of the instrument in the study of a given aspect of the solution crystallization and melting of the polyolefins. The following is the first draft of a paper that has been submitted to Xpress Polymer Letters following said research.

There might be some duplication regarding the experimental details reported elsewhere in this thesis, but we felt it was suitable for the draft paper to be included here in it's original form.

The solution melting temperature of polyolefins and the Flory-Huggins equation: A SCALLS study.

*Margaretha Brand[1], Albert van Reenen[*1], Erich Rohwer[2] and Pieter Neethlingh[2]*

1. Department of Chemistry and Polymer Science, 2. Laser Physics Institute, University of Stellenbosch, Private Bag X1, Matieland 7602 South Africa

* Corresponding author

E-mail address: ajvr@sun.ac.za

4.1 Summary

Solution crystallization analysis by laser light scattering offers a direct way of measuring the "solution melting" temperature and solution crystallization temperature of polyolefins. The measurement of the solution melting temperature offers the chance to study the applicability of the Flory-Huggins equation in predicting the solution crystallization of the polyolefins.

Keywords: laser light scattering, polyolefins, Flory-Huggins

4.2 Introduction

Crystallization of polyolefins from solution is a useful technique of separating these polymers into distinct fractions. The study of the crystallization of polyolefins from solution is well known, and several techniques to provide information on chemical composition distribution. Crystaf and analytical Tref (*a*Tref) are well known techniques that have been extensively reviewed [1, 2]. Recent developments include crystallization elution fractionation (CEF) reported by Monrabal [3] . CEF affords rapid analysis compared to Crystaf and *a*Tref without a loss in separation quality. We have also recently reported the use of solution crystallization analysis by laser light scattering (SCALLS) [4, 5]. This technique was first described by Shan et al [6], who called the technique "turbidity fractionation analysis".

During SCALLS analyses, a polyolefin solution is cooled in a controlled fashion and crystallization from solution is followed by measuring the intensity of laser beam passing through the solution (or the intensity of scattered light emanating from the solution) during cooling. During a SCALLS experiment, light is scattered as soon as the crystallite size is large enough to scatter the laser light. In previous papers [4, 5] the effect of some experimental parameters and studies on the crystallization of propylene copolymers were reported.

SCALLS differs from a technique like Crystaf in that it measures changes directly and quite rapidly and that it affords the opportunity to measure "solution melting" temperatures as well as solution crystallization temperatures. This is quite simply done by heating the crystallized suspension of polymer in a controlled fashion and once again measuring the intensity of scattered light or the intensity of transmitted light as a function of temperature. In both the cooling and heating modes peak temperatures can be obtained by taking the first derivative of the measured intensities.

The Flory theory for the fusion of a polymer has been applied during the study of the crystallization of polymers in a number of ways. For the melting point depression in a random binary copolymer, for example, Alamo and Mandelkern [7] in their discussion of ethylene/1-alkene copolymers specified that the melting temperature of a copolymer can be described by the relationship

$$\frac{1}{T_m} - \frac{1}{T_m^0} = -\frac{R}{\Delta H_u} \ln p \quad (4.1)$$

Here Tm is regarded as being the melting temperature of the copolymer, and T_m^0 is the melting temperature of the pure homopolymer and ΔH_u is the heat of fusion of the crystallizable unit, and p is the sequence propagation probability of the crystallizable monomer. In an attempt to relate the Flory theory to crystallization results obtained (in solution) by Crystaf, first Monarabal et al [8], and then followed by Brull et al [9] made some assumptions which allowed for the simplification of Equation 1 to:

$$\frac{1}{T_m} - \frac{1}{T_m^0} = \frac{R}{\Delta H_u} \ln[1 - N_2] \quad (4.2)$$

Here N_2 is the molar fraction of the copolymer that is included, and since $\ln[1-N_2] \approx -N_2$ for low values of comonomer the above can be rearranged to:

$$\frac{1}{T_m} - \frac{1}{T_m^0} = -\frac{R}{\Delta H_u} N_2 \quad (4.3)$$

or

$$T_m = T_m^0 - \frac{R[T_m^0]^2}{\Delta H_u} N_2 \quad (4.4)$$

The above (equation 4) can be derived if it is assumed that $T_m.T_m^0 \approx [T_m^0]^2$

Both Monrabal and Brüll demonstrated that plotting peak crystallization data for a series of ethylene and propylene/α-olefin copolymers obtained from Crystaf against the comonomer concentration yielded essentially linear relationships. In the case of the propylene/α-olefin copolymers it was also shown that the data for DSC melting points, DSC peak crystallization temperatures and the Crystaf crystallization peak data, when plotted against the comonomer content, all yielded plots with essentially the same slope. The conclusion was therefore made that the type of comonomer had little effect on the crystallization from solution, but that the amount of comonomer did. This was in contrast to other results [10].

The Flory-Huggins equation for the free energy of mixing was initially developed for concentrated polymer solutions, as was pointed out in the 2005 review on Crystaf and Tref by Soares et al [11]. The equation below was in fact developed to describe the melting point depression in the presence of a diluent (solvent), with T_m being the "solution melting" temperature of the polymer.

$$\frac{1}{T_m} - \frac{1}{T_m^0} = \frac{R}{\Delta H_u}\left(\frac{V_u}{V_1}\right)\left[-\frac{\ln v_2}{x} + \left(1 - \frac{1}{x}\right)v_1 - \chi_1 v_1^2\right]_2 \quad (4.5)$$

Here where $T_m{}^0$ is the melting temperature of the pure polymer, T_m is the equilibrium melting temperature of the polymer in solution, ΔH_u is the heat of fusion per repeating unit, V_u and V_1 are the molar volumes of the polymer repeating unit and diluent, respectively, υ_1 and υ_2 are the volume fractions of the diluent and polymer, respectively, x is the number of segments, and χ_1 is the Flory–Huggins thermodynamic interaction parameter.

In techniques like TREF, CRYSTAF (and SCALLS), the crystallization step occurs in dilute solution, which complicates things as we have a non-uniform distribution of the polymer segments in the solvent. Whilst it is therefore strictly speaking not possible to apply Equation 1 for dilute solutions, Mandelkern [11] states that the change in chemical potential with increasing dilution is so small that Equation 1 is obeyed even in dilute solutions. We can therefor rearrange Equation 5 as follows, whilst substituting the number of repeat units (r) for the number of segments (x). This yields Equation 6:

$$\frac{1}{T_m} - \frac{1}{T_m^0} = \left(\frac{R}{\Delta H_u}\right)\left(\frac{V_u}{V_1}\right)(v_1 - \chi_1 v_1^2) - \frac{R}{\Delta H_u}\left[\frac{ln(v_2)}{r} + \frac{v_1}{r}\right] \quad (4.6)$$

The term on the right-hand side approaches zero if the molecular weight is large, and for polymeric systems we can therefore rewrite Eq 4.6 as

$$\frac{1}{T_m} - \frac{1}{T_m^0} = \left(\frac{R}{\Delta H_u}\right)\left(\frac{V_u}{V_1}\right)(v_1 - \chi_1 v_1^2) \quad (4.7)$$

In the case of dilute solutions of copolymers, we need to rewrite the interaction parameter to reflect the contribution of both monomers.

$$\chi_1 = \upsilon_A \chi_{1A} - \upsilon_A \upsilon_B \chi_{AB} \quad (4.8)$$

In this case χ_1 is the interaction parameter of the binary copolymer with pure solvent, while χ_{1A} and χ_{1B} are the interaction parameters of the corresponding homopolymers with the same solvent. If the chemical nature of the comonomers is very similar, then one could simply use equation 4.5 (or the derived form thereof). We are therefore left with two equations that could be applied, i.e equations 4.3 and 4.7. If the former is applicable, plotting comonomer content (N_2) against $\frac{1}{T_m} - \frac{1}{T_m^0}$ should lead to a straight line, with the slope not affected by the type of comonomer. This would then mean we assume that the nature of the comonomer does not affect the solubility of the polymer in a given solvent. In other words, the right-hand term of equation 4.7 would only be influenced by amount of comonomer, and not the interaction parameter.

Recently our group reported on the solution electrospinning of propylene-1-alkene copolymers, and it appeared that the solubility of these copolymers were, in fact, influenced by the type of comonomer [12].

With the development of solution crystallization analysis by laser light scattering [4, 5] we now have a technique where we can follow both the crystallization from solution of a polyolefin, as well as the solution melting of the same polyolefin. We can, therefor, actually determine the value for T_m, as set out in the Flory-Huggins relationship for polymer solutions. As this is the case we thought it would be interesting to see if the Flory-Huggins equation could be applied to a series of propylene/α-olefin copolymers similar to that which was previously reported on [8]. It is simple to determine the "bulk" melting temperature (T_m^0) of the polymer by DSC, and then the melting point depression in the presence of the solvent, and to plot the difference of the inverse of the solution melting temperature end the inverse of the bulk melting temperature against the comonomer content of a selected number of propylene/α-olefin copolymers. This paper reports the results of this investigation.

4.3 Experimental

4.3.1 The SCALLS instrument

The development and layout of the instrument has been reported previously [4, 13]. A schematic representation of the setup is given in Figure 4.1. The two photodiode detectors at 90° and 270° to the incident laser beam (635 nm diode laser) measure scattered light intensity. The detector in line with the laser beam (denoted as 180° detector) measures a decrease in light intensity as crystallization occurs.

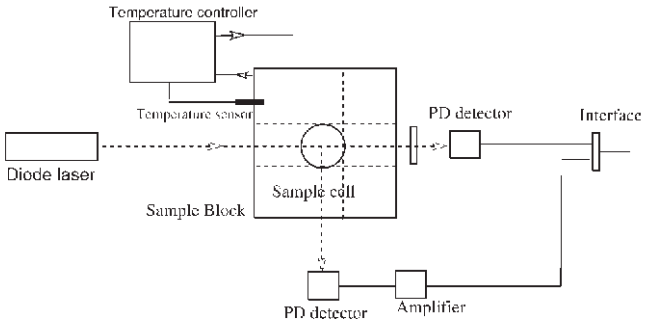

Figure 4.1. Schematic of layout of the SCALLS instrument. Top view [4].

4.3.2 The SCALLS method.

Unless otherwise stated, all heating and cooling experiments in the SCALLS were conducted using a polymer concentration of 0.5 mg/ml in 1,2,4 trichlorobenzene and at a rate of 1.5 °C/minute (heating) and

1 °C/minute (cooling) respectively. Polymer solutions were prepared at 140 °C, equilibrated in the instrument at 100 °C and then cooled from to 30 °C. Controlled heating followed directly afterwards (to 120 °C).

4.3.3 CRYSTAF

Crystaf analysis was performed using a Crystaf model 200 manufactured by PolymerChar. The polymer was dissolved in 1,2,4-trichlorobenzene (TCB) at a concentration of 0.57mg/ml, this accounts to 20mg polymer in 35ml solvent. The polymer solution was kept at 160°C for 90 minutes to ensure complete dissolution and then stabilized at 100°C for 40 minutes. The temperature was then decreased at a rate of 0.1°C/min to a final temperature of 30°C. The decrease in polymer concentration of the solution was measured by an in-line infra-red detector.

4.3.4 Polymers

The propylene copolymers (propylene/1-octene, propylene/1-decene, and propylene/1-octadecene) were synthesized using a metallocene catalyst as previously described[4, 8, 13, 14]. The polymers were subjected to standard characterization techniques. Thermal analyses were done on a TA Instruments Q 100 DSC using a heating and cooling rate of 10 °C/min, while ^{13}C NMR spectra were recorded on a Varian Unity Inova 600 MHz NMR spectrometer (150 MHz, 130 °C tetrachloroethane-d_2 as solvent) and used to calculate comonomer content. Molecular weight determinations were done on a PL 220 GPC at 160 °C in trichlorobenzene as solvent and using 4 PL gel MIXED-B columns. The properties of the polymers that were analyzed are given in Table 4.1. Crystaf experiments were run on a Model 200 (Polychar, Valencia Spain) in 1,2,4 trichlorobenzene as solvent.

4.4 Results and Discussion

The data for the copolymers that were synthesized [14] are given in Table 4.1 It needs to be noted that all the copolymers had molecular weights in excess of 150 000 g/mol, so it should be assumed that the effect of molecular weight on the crystallization process is minimal.

Table 4.1. Summary of the characterization data for the copolymers used in this study.

Polymer Code	Comonomer Type	Comonomer Content (mole %)	Mw (PD)	T_m DSC (°C)	T_m Scalls (°C)
8.1	1-octene	3.12	328700 (2.0)	105	64.21
8.3		1.72	332000 (2.2)	120.39	69.45
8.6		1.27	156000 (3.1)	121.92	74.49
8.4		0.86	456900 (2.2)	133.31	87.67
8.7		0.57	421500 (2.4)	137.89	94.22
8.8		0.47	600200 (2.1)	142.86	94.5
10.1	1-decene	2.38	523700 (2.3)	118.3	63.25
10.3		1.39	372700 (2.4)	123.68	78.25
10.4		1.08	427700 (2.3)	132.05	85.85
10.8		0.47	448800 (2.2)	136.84	91.9
10.6		0.42	466200 (2.1)	138.97	94.6
14.3	1-tetradecene	0.89	639200 (2.2)	127.54	82.3
14.6		0.77	369700 (2.5)	137.35	90.3
14.5		0.68	553500 (2.5)	134.61	89
14.7		0.50	240700 (2.4)	134.38	89.19
14.8		0.26	282700 (2.2)	136.03	94.28
18.2	1-octadecene	2.04	380600 (1.9)	111.02	68.25
18.9		1.49	547400 (2.1)	119.74	74
18.10		1.09	227560 (2.2)	126.39	80.25
18.5		0.81	486200 (2.4)	131	86.5
18.4		0.66	N/D	133.51	88.07
18.6		0.47	279700 (2.4)	138.52	93.24

In the cases where the comonomer content was above 2.50 mole% it was not possible to obtain a solution crystallization temperature for the polymer by SCALLS (or CRYSTAF). If we simply plot, as a first exercise, the comonomer content against the solution melting temperature (following the approach by Brull et al) we do obtain what appears to be a reasonably straight lines, albeit with quite a poor fit (R^2 = 0.88 for the solution melting and R^2 = 0.83 for the solution crystallization).

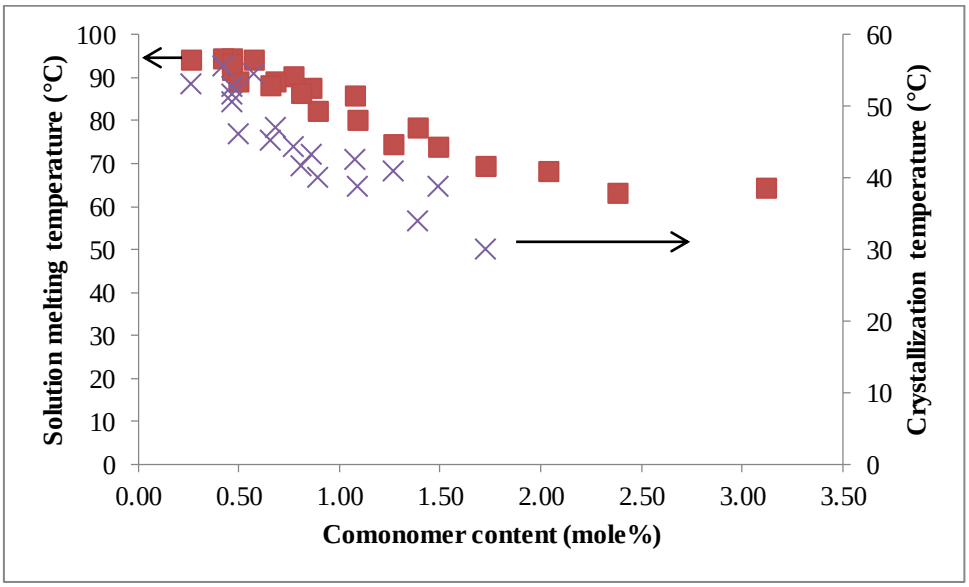

Figure 4.2. Comonomer content (all copolymers) vs solution melting and solution crystallization peak temperatures obtained by SCALLS.

What should happen is for the y intercept at comonomer content = 0 to be about equal to the solution melting temperature of a isotactic polypropylene homopolymer prepared with the same catalyst. This clearly not the case, as the solution melting temperature should be in the region of 107 – 110 °C. In fact, fitting a 2nd order polynomial equation to the some of the data set (see Figure 3) provides a much better fit, and a provides an intercept value of approximately the solution melting as obtained by SCALLS for a metallocene iPP.

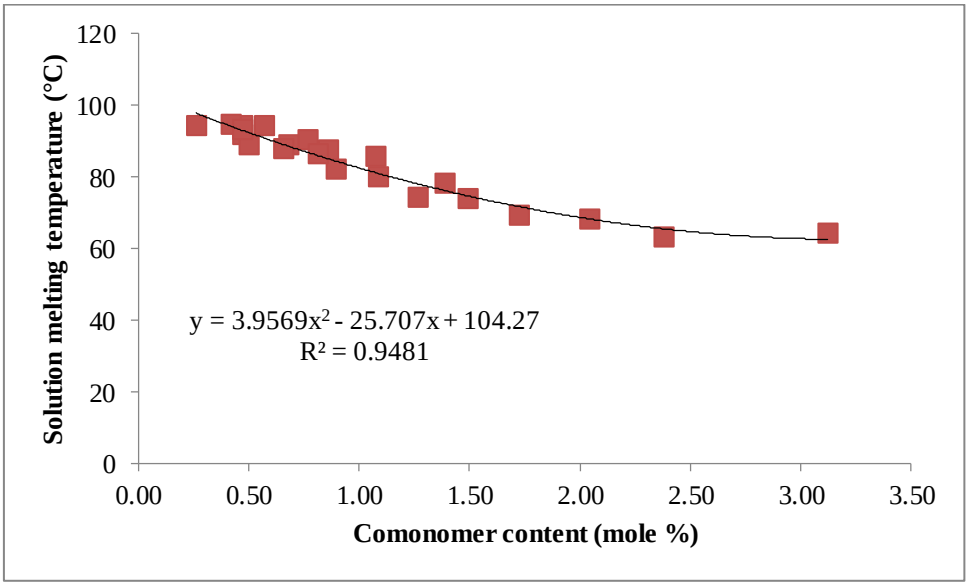

Figure 4.3. Illustration of a 2nd order polynomial fit of a trendline through the data points (solution melting vs comonomer content) of all the copolymers. The equation and regression coefficient is indicated on the plot.

If now plot the individual copolymer series (solution melting vs comonomer content) it becomes obvious that we see a significant deviation from linearity at higher comonomer contents. As an example, Figure 4

shows the data for the C8/C3 copolymer series. A similar, but less significant deviation can be seen for the data set for the C10/C3 copolymers. It was therefor decided to limit, for the purpose of the investigation of the melting point depression as a function of comonomer type and amount, the maximum comonomer content to a value of no greater than 2.50 mole%.

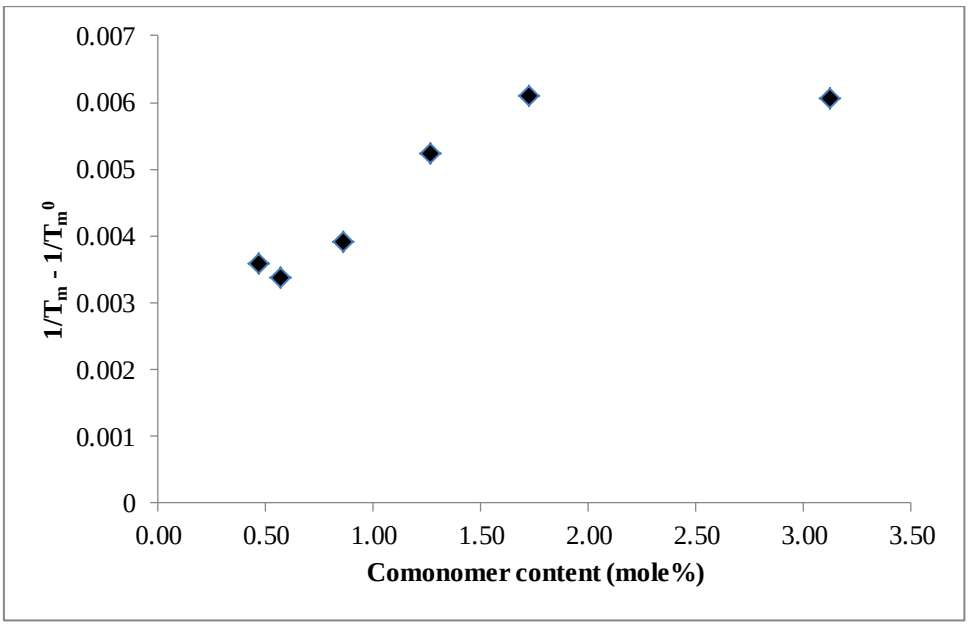

Figure 4.4. The relationship between comonomer content and $\frac{1}{T_m} - \frac{1}{T_m^0}$ for the propylene/1-octene copolymers

If we then plot the individual series of copolymers we see an interesting trend, particularly when we investigate the regression analysis for the different polymers. Examples of the C8/C3 and C18/C3 copolymer series are shown in Figure 4.5 (a) and (b) below.

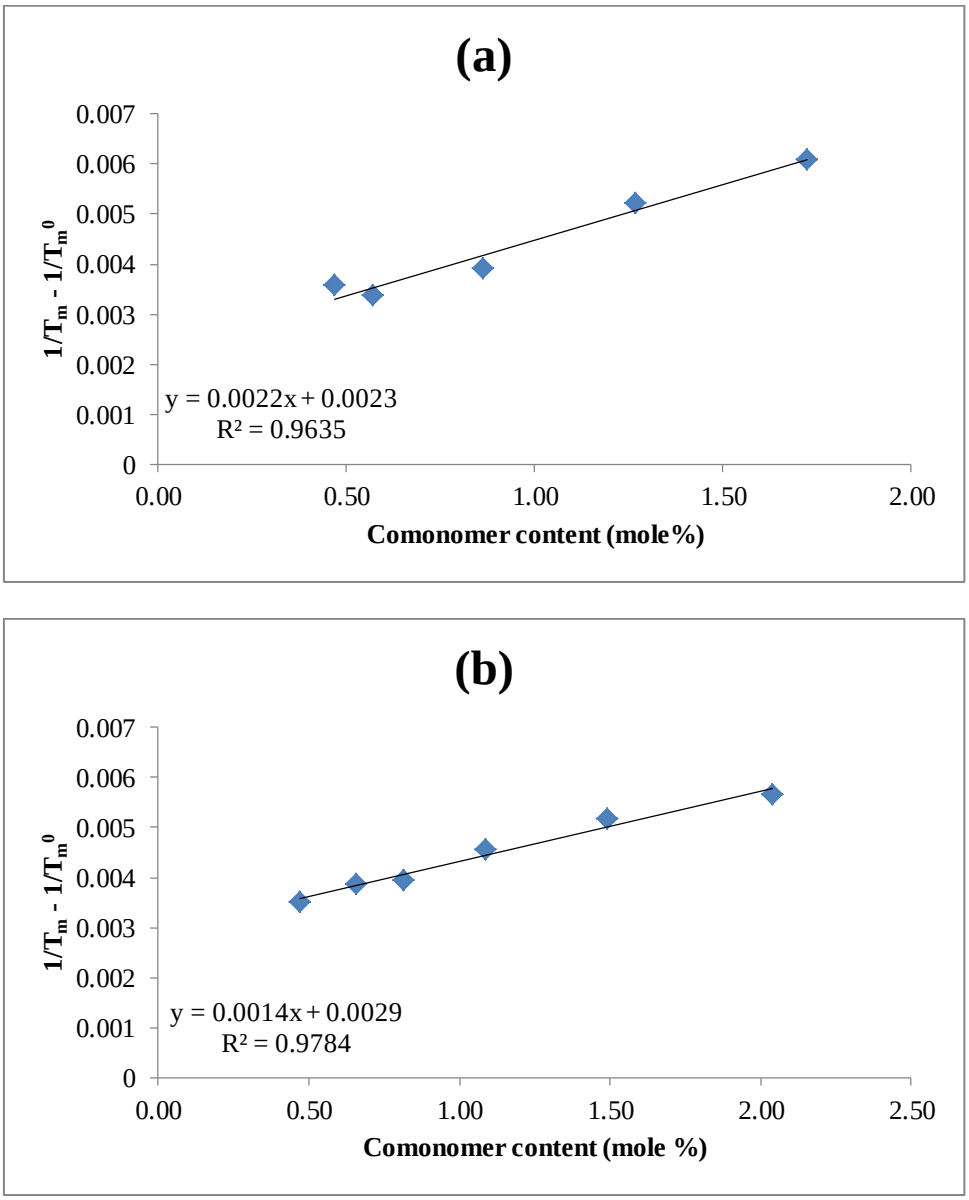

Figure 4.5 The relationship between the comonomer content and $\frac{1}{T_m} - \frac{1}{T_m^0}$ for (a) propylene/1-octene and (b) propylene/1-octedecene copolymers, for low comonomer content (<2.5 mole%).

The regression analysis for all 4 copolymer series yields interesting results, with a clear distinction in the slopes for the C8 and C10 copolymers and the C14 and C18 copolymers (Table 4.2)

Table 4.2. Regression analysis for linear plots of $\frac{1}{T_m} - \frac{1}{T_m^0}$ vs comonomer content.

Comonomer	Linear regression equation
1-octene	y = 0.0022x + 0.0023, R^2 = 0.9635
1-decene	y = 0.0020x + 0.0024, R^2 = 0.9486
1-tetradecene	y = 0.0016x + 0.0029, R^2 = 0.9418
1-octadecene	y = 0.0014x + 0.0029, R^2 = 0.9784

It is quite clear from this table that the slopes decrease as the comonomer content increases. The intercept values for the C8 and C10 copolymers are similar, as are the values for the C14 and C18 copolymers.

From this superficial evaluation it would appear as if the interaction between the solvent and the polymer is influenced by the comonomer type, with the result that the solution crystallization and melting is influenced by both comonomer type and amount. It needs to be stressed that this evaluation was done only for the propylene copolymers. We can do a similar exercise for the solution crystallization data obtained by SCALLS. If we attempt to plot the crystallization point depression as a function of comonomer content, however, it becomes more difficult to attempt to attain a linear relationship as the comonomer size increases. Whilst we may get a reasonably linear response for the C3/C8 copolymers(R^2 = 0.91), the C3/C10 (0.89), C3/C14 (0.87) and C3/C18 copolymers show a significant deviation from linearity. In fact, the C3/C18 copolymers appear to show a levelling off of the crystallization temperature depression as the comonomer content increases (Figure 5)

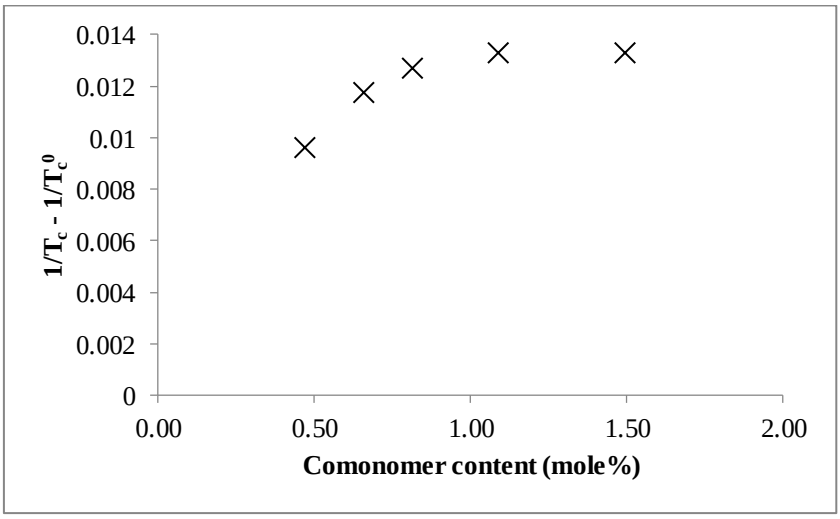

Figure 4.6. Crystallization point depression as a function of comonomer content (1-octadecene copolymers)

It seems clear that the crystallization temperature is affected to a greater degree by the comonomer type than the melting temperature.

4.5 Conclusion

SCALLS is a technique that offers direct measurement of the solution crystallization or solution melting temperature of polymers. It was successfully used to study the applicability of the Flory-Huggins equation for propylene-higher 1-alkene copolymer systems in solution crystallization. It appears that the solvent interaction parameter for the propylene/higher 1-alkene copolymers (with low comonomer content) is dependent on the comonomer type. The melting point depression is clearly dependent on both the type and amount of comonomer included in the copolymer.

4.6 References

1. Anantawaraskul, S.; Soares, J. B. P.; Wood-Adams, P. M. *Adv.Polym.Sci.* **2005**, *Polymer Analysis--Polymer Theory*, 1-54.

2. Soares, J. B. P.; Anantawaraskul, S. *J.Polym.Sci., Part B: Polym.Phys.* **2005**, *13*, 1557-1570.

3. Monrabal, B.; Sancho-Tello, J.; Mayo, N.; Romero, L. *Macromol.Symp.* **2007**, *Polyolefin Characterization*, 71-79.

4. Van Reenen, A. J.; Rohwer, E. G.; Walters, P.; Lutz, M.; Brand, M. *J Appl Polym Sci* **2008**, *5*, 3238-3243.

5. Van Reenen, A. J.; Brand, M.; Rohwer, E. G.; Walters, P. *Macromolecular Symposia* **2009**, 25.

6. Shan, C. L. P.; de Groot, W. A.; Hazlitt, L. G.; Gillespie, D. *Polymer* **2005**, *25*, 11755-11767.

7. Alamo, R.G.; Mandelkern, L. *Thermochim. Acta* **1994**, 238, 155 -201.

8. Monrabal, B.; Blanco, J.; Nieto, J.; Soares, J.B.P. *J. Polym. Sci., Part A, Polym. Chem.* 1999, 37, 89 - 93.

9. Brull, R.; Pasch, H.; Raubenheimer, H.G.; Sanderson, R.D.; Van Reenen, A.J.; Wahner, U.M. *Macromol. Chem. Phys.* **2001,** 202, 1281 - 1288.

10. Da Silva Filho, A.A.; Soares, J.B.P.; De Galland, G.B.; *Macromol. Chem. Phys.* **2000**, 201, 1226 - .

11. Mandelkern, L. *Crystallization of polymers; 2nd Ed*, Cambridge University Press: Cambridge, UK ; 2002 (p90).

12. Van Reenen, A.J.; Keulder, L. *Macromol. Mat. Eng.* **2010**, 295, 666 - 670.

13. Brand, M. Investigation of molecular weight effects during the solution crystallisation of polyolefins, University of Stellenbosch, 2008.

14. Van Reenen, A.J.; Brull, R, Wahner, U.M.; Raubenheimer, H.G., Sanderson, R.D., Pasch, H. J. *Polym. Sci. Part A, Polym. Chem*. **2000**, 38, 4110 - 4118.

Chapter 5

Development of the SCALLS instrument

This chapter focuses on the development from one to three lasers to improve the sensitivity of the instrument

5.1 Introduction:

Studying crystallization of polymers can be done either in solid state or in solution. Well known techniques as Crystaf [1], a-TREF [2] and CEF[3-5] have been extensively reviewed and used in the analysis of polyolefins. As previously reported [6,7] we have developed an instrument to directly study the crystallization of polymers in solution. After the initial development of the SCALLS instrument, which comprised a set-up with a single, 635 nm ("red") laser and photodiode detectors at 90 °, 180 ° and 270 ° (to measure the intensity of transmitted light (180 °) and scattered light (90 °, 270 °) the instrument was developed to include two additional lasers, one of 532 nm ("green") and one of 405 nm ("blue"). The light is scattered as soon as the crystallite size becomes large enough. Introduction of lasers with lower wavelength will thus scatter at smaller crystallite sizes. This chapter discusses the development of the instrument with respect to the addition of these lasers.

5.2 Experimental:

5.2.1 SCALLS Instrument:

The original development of the instrument was discussed and published previously[7]. Further development included the introduction of the extra two lasers of 532 nm and 405 nm, from now on referred to as green and blue laser respectively, and their corresponding detectors. In this regard, the challenge was to be able to utilise all three lasers (635, 532 and 405 nm) simultaneously. We wanted to be able to measure both transmitted and scattered light of all the wavelengths, and to be sure that the scattering due to lasers of differing wavelengths did not interfere with the analysis. As a first attempt, the 405 nm and 532 nm lasers were mounted at 90 ° to the 635 nm lasers. Dichroic mirrors directed the incident laser beams. Broadpass filters in-line with the laser beams were used to ensure that only the required light was recorded by the detector in question. PhotopTM series detectors were used. They combine a photodiode with an operational amplifier in the same package. PhotopTM are general-purpose detectors that have a spectral range from either 350 nm to 1100 nm or 200 nm to 1100nm. Addition of dichroic mirrors direct the laser light to the detectors and filters in front of the detectors only allow the relevant laser light to pass. The technical specifications for the filters are as follow; red, centre wavelength (CWL) = 635 ± 2 nm, full with at half maximum (FWHM), 10 ± 2 nm, green CWL = 530 ± 2nm, FWHM = 10 ± 2nm and blue CWL = 405 ± 2nm, FWHM = 10 ± 2nm. Data was recorded at a rate of 1 point every 10 seconds. The data acquisition card is a NI USB-6009 that provides connection to eight analog input (AI) channels, two analog output (AO) channels, 12 digital input/output (DIO) channels, and a 32-bit counter with a full-speed USB interface. Further processing were performed in Origin 7.5© software.

5.2.2 SCALLS Method:

All samples analysed were dissolved at high temperatures, followed by a cooling cycle, cooling rate used is specified each time, and all samples were subsequently heated at a rate of 1.5 °C/min. The samples were

controlled-cooled from 100°C to 30°C and then heated again after 5 min to 120°C. Samples were dissolved in 1,2,4 trichloro-benzene at a concentration of 0.5 mg/ml at 140°C.

5.2.3 Polymers:

Materials used in the development phase. A "metallocene" isotactic polypropylene (iPP) sample as well as some distinctly heterogeneous PP samples (details below) were used in the development phase of the project. iPP was synthesized using a C_2 symmetric catalyst and hydrogen was used to control molecular weight[8]. Heterogeneous polypropylene was synthesized with a Ziegler-Natta catalyst[9]. Polymers were subjected to standard analysis techniques. Thermal analysis were done on a TA instrument Q100 DSC using a heating and cooling rate of 10°C/min. Molecular weight were determined by a PL 220 GPC at 160°C using trichlorobenzene as a solvent with 4 polystyrene/divinylbenzene copolymer packed columns (PL gel MIXED-B [9003-53-6]). Crystaf experiments were done on a Model 200 (Polymer Char, Valencia, Spain) in TCB as solvent (cooling at 0.1°C/min) from 100°C to 30°C). Characterization data can be seen in Table 5-1.

Table 5-1: Characterization data of the polymers

Sample	Mw	PDI
Homo-PP	35 962	2.7
ZNPP-4	226000	5.9
ZNPP-7	192000	8.8
ZNPP-9	183000	8.5

5.3 Results and Discussion:

5.3.1 Testing of the three lasers

In the first version of the instrument only a 635 nm (red) laser was used to follow the crystallization or dissolution of the polymer in solution. Crystallization or dissolution is measured by the change in intensity of the laser. In theory smaller particles will be detected by a shorter wavelength laser. A 532 nm (green) and 405 nm (blue) laser was added to determine if this theory is valid. The 635 nm laser was left at its original position, in line with the sample and detector. The 532 nm and 405 nm lasers were added at a 90° angle relative to the original red laser. The positioning of the detectors mirrored the position of the lasers. To direct the laser light into the sample and from the sample into the detectors dichroic mirrors were used. It was assumed that the mirrors will direct only the applicable laser signal into the detectors. The first set of experiments was done to evaluate the efficacy of the initial set-up. Unfortunately the mirrors were not as effective as expected and a lot of interference was experienced on the different detectors. This is illustrated in Figure 5.1; it shows the cooling of a homogenous PP sample. The maximum peak temperatures for the three different lasers are all the same. There were two possibilities, either the data is identical for all the

lasers or there is interference i.e. the detectors do not only collect the relevant signals. In order to evaluate this, the analyses were done separately for each of the lasers to determine which possibility is true.

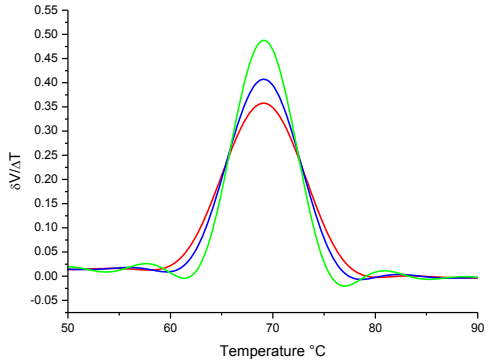

Figure 5.1: Homogenous PP sample analysed with all three lasers, showing interference before addition of the filters

Results for the separate analysis of the three lasers can be seen in Figure 5.2, note that the spectra is not normalised. Clearly it can be seen that the peak temperatures are not the same. There were distinct differences in the peak values (as obtained from the first derivatives of the data) for the 635, 532 and 405 nm lasers. This seemed to indicate that interference from the lasers were responsible for the overlapping curves that we observed in Figure 5.1. It is not practical to analyse samples separately for all three lasers so another solution was needed to this problem.

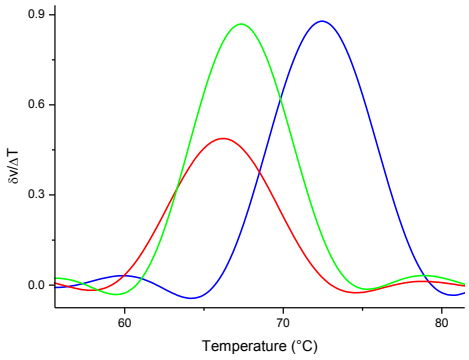

Figure 5.2: Homogenous polypropylene sample analysed separately for the three different lasers

Broad pass filters were added directly in front of the detectors that only allowed the desired wavelength to pass. The homogenous iPP sample was then analysed again, but this time all three lasers were used simultaneously. The data, showed in Figure 5.3 corresponds well with the experimental data obtained from the separate lasers. The basic concept behind the choice of lasers of different wavelengths is that the shortest wavelength (405 nm) should be scattered by smaller particles than the 532 and 635 nm lasers. Then it should be possible to follow the growth of a crystallite from solution. This is clearly shown to be the case (Figure 5.3)

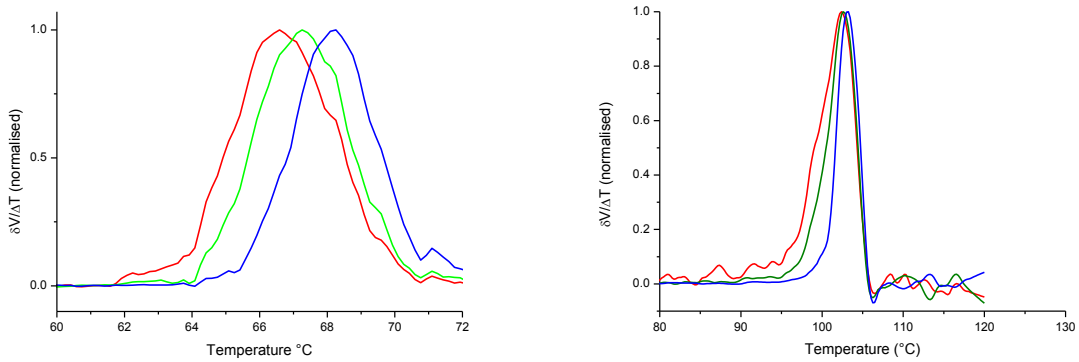

Figure 5.3: SCALLS analysis of a homogenous polypropylene sample analysed at a (a) cooling rate of 1.0 °C/min followed by (b) a 1.5 °C/min heating cycle

While the 405 nm laser is scattered by smaller particles than the 532 and 635 nm lasers, there is limits with respect to scattering of bigger particles. To explain this I draw your attention to Figure 5.4 showing the raw data of the cooling curve. The blue laser not only shows a change in response first but also reaches its minimum response first due to effective scattering. It needs to be noted that the 405 nm laser will, with the intensity that we have used, not be able to detect secondary crystallization events that start at lower temperatures. Combination of the three lasers thus gives detection of particle sizes over a broad range.

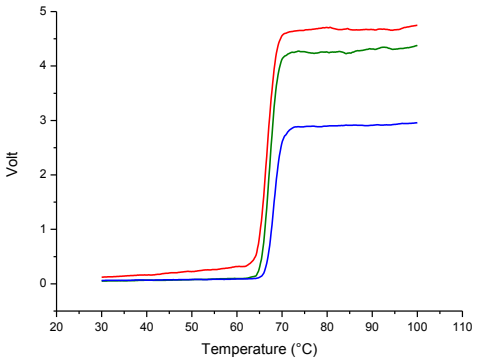

Figure 5.4: Raw data of the homogenous PP sample cooled at a rate of 1°C

5.3.2 Different cooling rates and the effect on the laser response on homogeneous polypropylene

Different cooling rates result in higher peak temperatures as shown previously[6,7]. The samples were analysed at a rate of 0.2°C/min, 0.4°/min and 1°C/min cooling. In Figure 5.5(a) and Figure 5.6(a) a shift in peak maxima, relative to Figure 5.3(a) can be seen, as was expected. There is no clear difference in shape or form of the graphs for the different cooling rates. This must indicate that even though the slower cooling rate changes the peak temperature the particle sizes stays the same, at least for a homogenous sample. If the spherulite sizes are the same similar heating curves, that directly follow the cooling cycles, should be obtained for these samples. This is in fact the case as can be seen in Figure 5.3(b), Figure 5.5(b) and Figure 5.6 (b). Even though there is a shift in the peak melting temperatures the general shape of the graphs stays the same. Data for the reproducibility runs can be found in Table 5-2.

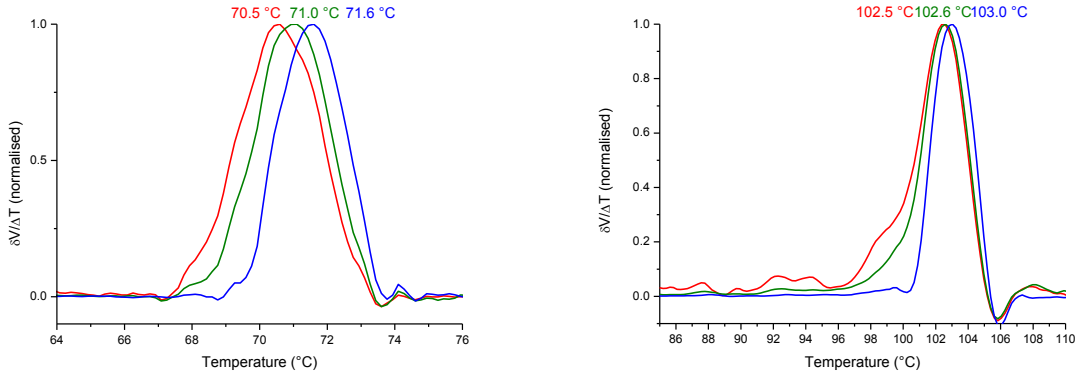

Figure 5.5: SCALLS analysis of a homogenous polypropylene sample analysed at a (a) cooling rate of 0.4 °C/min followed by (b) a 1.5 °C/min heating cycle

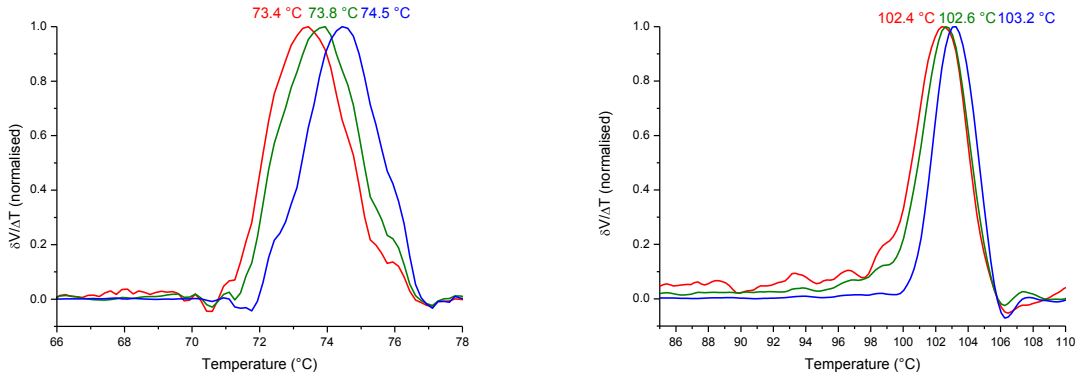

Figure 5.6: SCALLS analysis of a homogenous polypropylene sample analysed at a (a) cooling rate of 0.2 °C/min followed by (b) a 1.5 °C/min heating cycle

5.4 Testing the new system with more complex polymers

It was proven that the system functions properly with a relatively simple polymer regarding molecular weight and tacticity but further testing was needed on more complex polymers. The degree of dependence of the heating cycle on the cooling profile still needed to be determined. The data obtained for the heating cycle cannot fully be trusted when it follows separate cooling cycles due to experimental error that can occur. This problem is overcome with the simultaneous use of all lasers.

5.4.1 Heterogeneous polypropylene

Separate laser analysis of a heterogeneous polypropylene, ZNPP-9, is shown in Figure 5.7. The laser responses of the cooling profile follow the expected trend, but not the heating profile. The order of the laser response are not as expected and cannot be explained. Questions arise about the validity of the data and interesting details such as the lower melting peak around 106 °C cannot be trusted. Fortunately it was later proven that even though the relative position of the laser responses could not be trusted for separate analysis, the finer detail of the responses was indeed true as can be seen in Figure 5.8. The double melting peak is still visible and peak temperatures correspond well, truly astounding if taken into account that these analysis were done 10 months apart. The reproducibility data, for all the polymers in this section can be seen in Table 5-2.

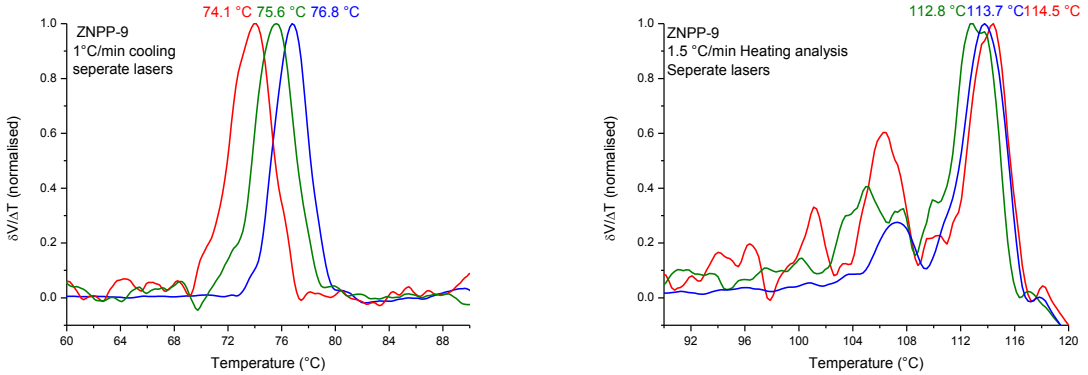

Figure 5.7: SCALLS analysis of a heterogeneous polypropylene, ZNPP-9, analysed separately for the three lasers at (a) a cooling rate of 1 °C/min and (b) a heating rate of 1.5 °C/min

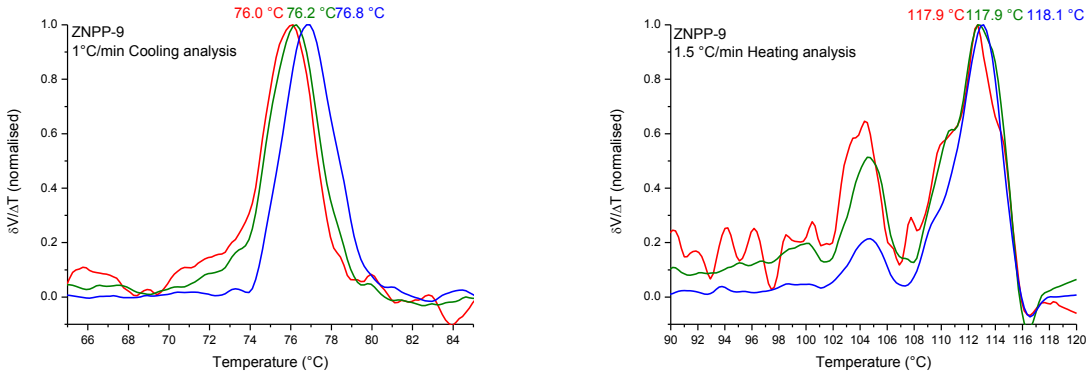

Figure 5.8: SCALLS analysis, of the three lasers simultaneously, for a heterogeneous polypropylene, ZNPP-9, analysed at (a) a cooling rate of 1 °C/min and (b) a heating rate of 1.5 °C/min

Further analyses were done on two different heterogeneous polypropylene polymers. The two different heterogeneous, Ziegler-Natta catalysed polymers were analysed. The two polymers were polymerized with different external electron donors. The two external electron donors only differed in the phenyl group in one being exchanged for a methyl group making it less bulky. Characterization details of the polymers can be seen in Table 5-1.

Analysis of the heterogeneous polypropylene, ZNPP-4, synthesized with the bulkier external electron donor, namely DPDMS, is shown in Figure 5.10. The polymer was analysed at three different cooling rates, 1.0 °C/min, 0.6 °C/min and 0.4 °C/min, each followed by a heating cycle of 1.0 °C/min. Firstly it is clear that the lasers show different responses and thus peak temperatures in each case. Comparison of the three different cooling rates only shows slight differences. The difference of the cooling rates can be seen in the succeeding heating profiles. The heating profile effectively shows the dissolution of the polymer back into solution or otherwise stated the melting in solution. As said the heating rate is the same and thus any differences seen must be due to the former cooling cycle. Heating following the 1 °C/min cooling rate shows a slight shoulder, at the lower temperature side. This shoulder becomes a definite peak after 0.6 °C/min cooling and becoming slightly more defined after 0.4 °C/min cooling.

This indicates that the crystals formed during the cooling step will directly affect the solution melting. Just as the cooling step, either slow cooled or quenched cooled, in the bulk has a direct effect on the melting behaviour afterwards. Thus the thermal history in solution is just as important as in the bulk.

SCALLS data of the heterogeneous polypropylene, ZNPP-7, synthesized with the less bulky external electron donor MPDMS can be seen in Figure 5.11. There is a definite difference that can be seen for the cooling plots for this polymer. A shoulder on the cooling curves at the higher temperature side becomes more prominent as the cooling rate decreases. In the heating profiles there is a definite lower temperature peak for all three analyses. The heating profiles that follow the slower cooling rates of 0.6 °C/min and 0.4 °C/min shows the formation of a shoulder on the higher temperature peak.

The analysis of these more complex polymer shows that differences are detected by the improved instrument. Differences are not only seen for the same polymer at different cooling rates but also between different polymers. Even between polymers that are relatively similar, according to known solution crystallization techniques such as Crystaf, as shown by the two heterogeneous polypropylene samples, shown in SCALLS analysis in Figure 5.10 and Figure 5.11 compared to the Crystaf analysis shown in Figure 5.9.

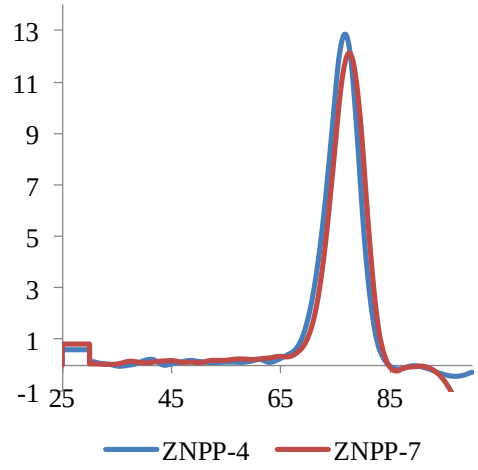

Figure 5.9: Crystaf results for the ZNPP-4 and ZNPP-7 sample

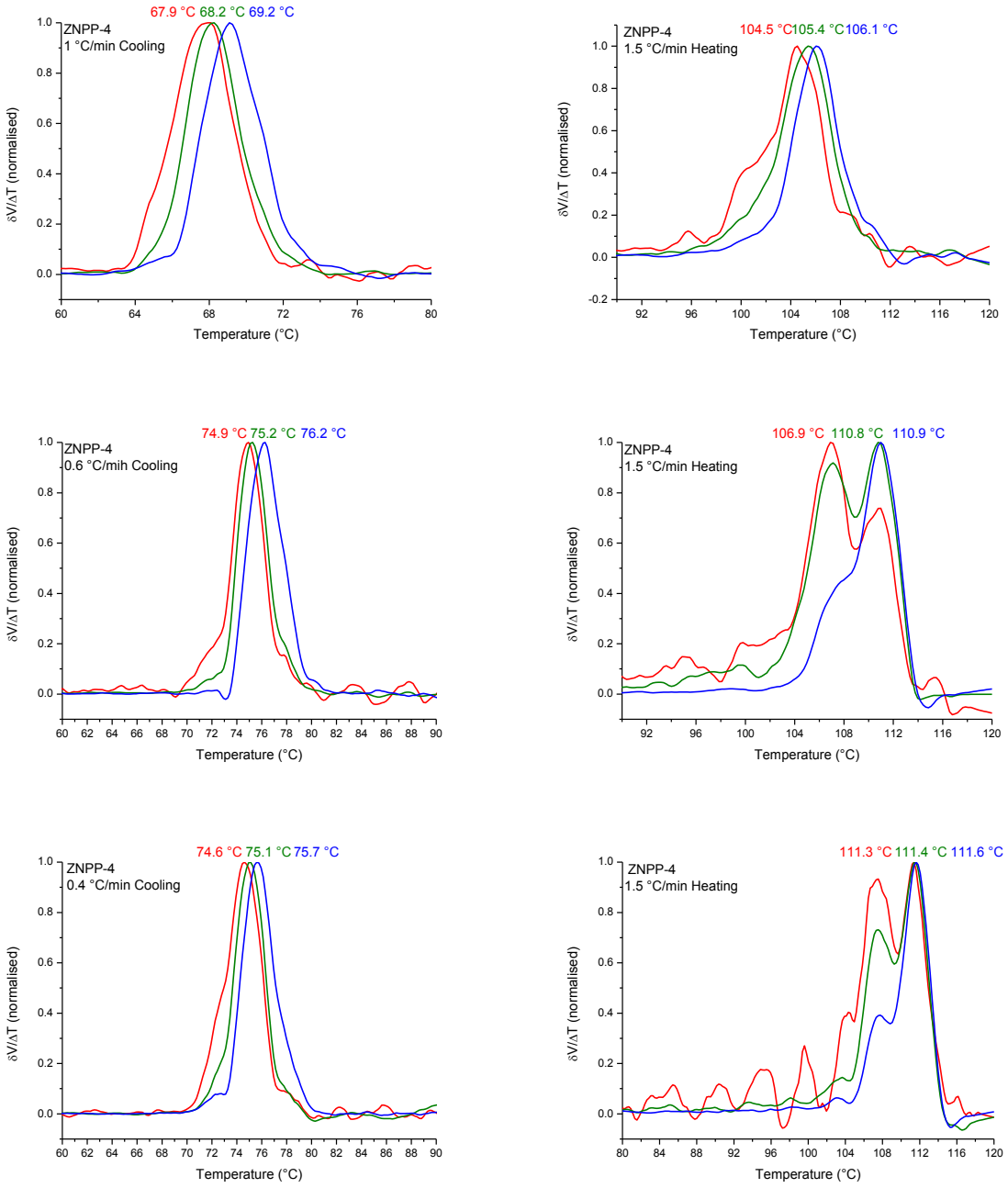

Figure 5.10: SCALLS analysis of a heterogeneous polypropylene, ZNPP-4, synthesized in the presence of DPDMS as an external electron donor, at cooling rates of (a) 1 °C/min, (b) 0.6 °C/min and (c) 0.4 °C/min with subsequent heating analysis at a rate of 1.0 °C/min

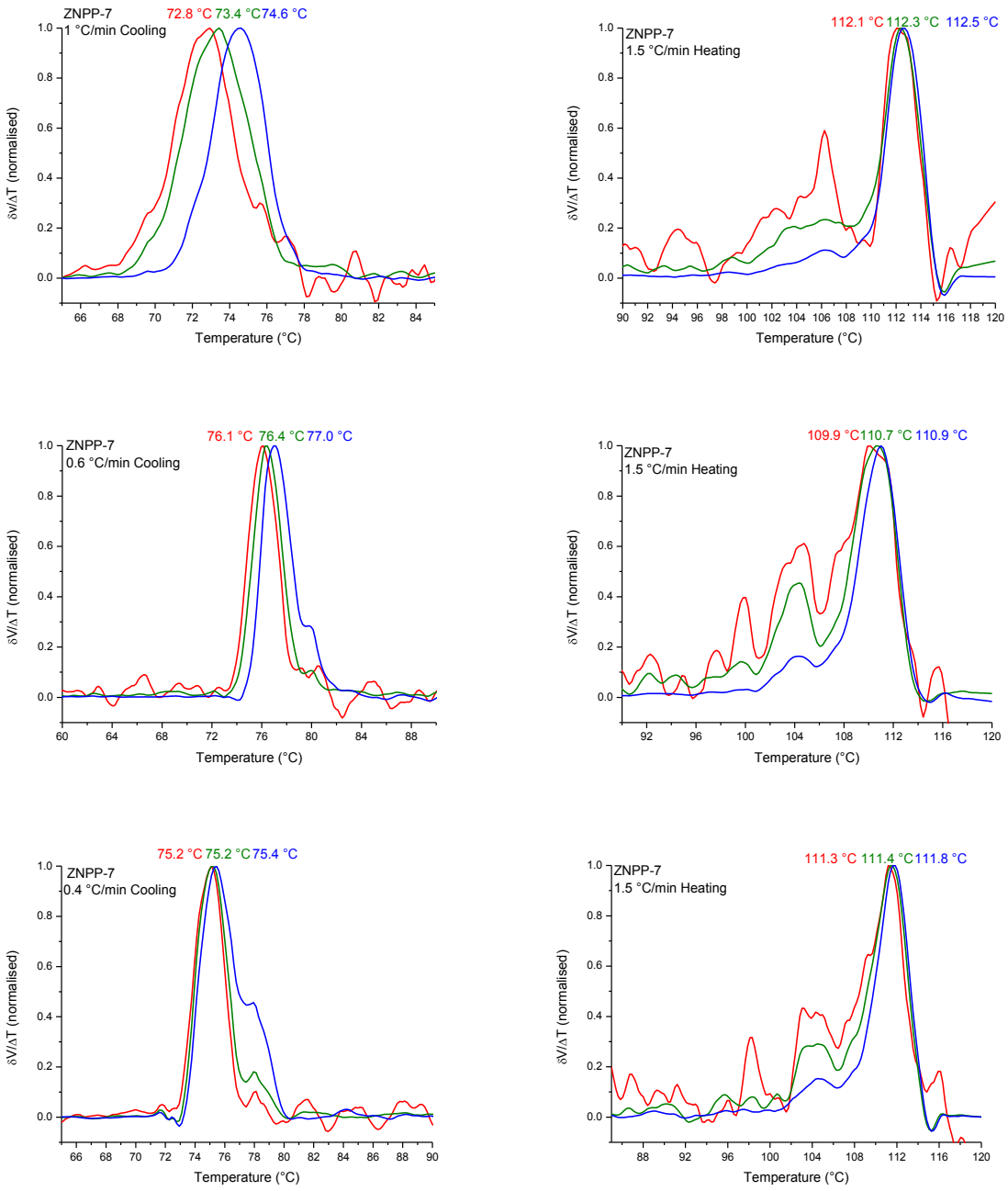

Figure 5.11: SCALLS analysis of a heterogeneous polypropylene, ZNPP-7, synthesized in the presence of MPDMS as an external electron donor, at cooling rates of (a) 1 °C/min, (b) 0.6 °C/min and (c) 0.4 °C/min with subsequent heating analysis at a rate of 1.5 °C/min

Table 5-2: Peak temperatures for the reproducibility runs for the samples discussed in this chapter

Sample name	Cooling or Heating rate	Peak temperature (°C) of the 635 nm laser	Peak temperature (°C) of the 532 nm laser	Peak temperature (°C) of the 405 nm laser
Homogenous PP	0.4 °C/min Cooling	70.4	70.9	71.5
	1.5 °C/min Heating after 0.4 °C/min Cooling	102.5	102.6	103.0
	0.2 °C/min Cooling	73.4	73.8	74.5
	1.5 °C/min Heating after 0.2 °C/min Cooling	102.4	102.6	103.2
ZNPP-9	1 °C/min Cooling	76.0	76.2	76.8
	1.5 °C/min Heating after 1 °C/min Cooling	118.0	118.0	118.1
ZNPP-4	1 °C/min Cooling	67.5	67.7	68.8
	1.5 °C/min Heating after 1 °C/min Cooling	104.0	105.2	105.9
	0.6 °C/min Cooling	74.8	75.1	76.1
	1.5 °C/min Heating after 0.6 °C/min Cooling	106.9	110.8	110.9
	0.4 °C/min Cooling	74.6	75.1	75.7
	1.5 °C/min Heating after 0.4 °C/min Cooling	111.3	111.4	111.6
ZNPP-7	1 °C/min Cooling	72.9	73.5	74.7
	1.5 °C/min Heating after 1 °C/min Cooling	112.1	112.3	112.5
	0.6 °C/min Cooling	76.1	76.4	77.0
	1.5 °C/min Heating after 0.6 °C/min Cooling	109.9	110.7	110.9
	0.4 °C/min Cooling	75.1	75.2	75.4
	1.5 °C/min Heating after 0.4 °C/min Cooling	111.2	111.4	111.8

5.5 Conclusions

It is shown that the addition of a 532 and 405 nm laser to the existing 635 nm lasers increases the sensitivity of the instrument. Addition of dichroic mirrors to direct the laser light to the relevant detectors and broad pass filters to ensure that only the relevant laser light passes through enabled the simultaneous use of all three lasers. It was shown that a relatively fast cooling rate of 1 °C/min can be used without significant loss of sensitivity. Lastly it was shown that the instrument produces reproducible results.

5.6 References

[1] Soares, J.B.P.; Anantawaraskul, S. : Crystallization Analysis Fractionation. J.Polym.Sci., Part B: Polym.Phys. **, 43**, 1557-1570 (2005).

[2] Soares, J.B.P.; Hamielec, A.E. : Temperature Rising Elution Fractionation of Linear Polyolefins. Polymer **, 36**, 1639-1654 (1995).

[3] Monrabal, B.; Sancho-Tello, J.; Mayo, N.; Romero, L. : Crystallization Elution Fractionation. A New Separation Process for Polyolefin Resins. Macromol.Symp. **, 257**, 71-79 (2007).

[4] Cong, R.; DeGroot, A.W.; Kilnker, C.M.; Yau, W.; Hazlitt, L.; Lyons, J.W.; Monrabal, B. : Investigation of Cocrystallization in Polyolefins by Crystallization Elution Fractionation. Abstracts of Papers, 236th ACS National Meeting, Philadelphia, PA, United States, August 17-21, 2008 , ANYL-248 (2008).

[5] Monrabal, B. : Crystallization Based Separations for Semicrystalline Polymers. Abstracts of Papers, 236th ACS National Meeting, Philadelphia, PA, United States, August 17-21, 2008 , ANYL-247 (2008).

[6] van Reenen, A.J.; Brand, M.; Rohwer, E.G.; Walters, P. : Solution Crystallization Analysis by Laser Light Scattering (SCALLS). Macromolecular Symposia **, 282**, 25 (2009).

[7] van Reenen, A.J.; Rohwer, E.G.; Walters, P.; Lutz, M.; Brand, M. : Development and use of a Turbidity Analyzer for Studying the Solution Crystallization of Polyolefins. J Appl Polym Sci **, 109**, 3238-3243 (2008).

[8] Margaretha Brand. : Investigation of molecular weight effects during the solution crystallisation of polyolefins. University of Stellenbosch (2008).

[9] Harding, G.W.; van Reenen, A.J. : Fractionation and Characterisation of Propylene-Ethylene Random Copolymers: Effect of the Comonomer on Crystallisation of Poly(Propylene) in the γ-Phase. Macromol.Chem.Phys. **, 207**, 1680-1690 (2006).

Chapter 6

Sample analysis on the SCALLS: Examples

6.1 How to interpret the laser signals.

Detection of changes in the polymer solution during a cooling or heating of cycle is achieved by using a laser combined with an appropriate detector to follow the process of crystallization or dissolution. The laser light intensity will decrease if scattering occurs. There are three types of scattering that can occur namely, Rayleigh, Mie and Geometric scattering. The type of scattering is determined by the dimensionless size parameter α which can be determined by Equation 6-1 and its relative relationship to the scattering. Mie scattering occurs when $\alpha \ll 1$ and Rayleigh scattering occurs when $\alpha \approx 1$.

Equation 6-1: Particle size measurement

$$\alpha = \frac{\pi D_p}{\lambda}$$

Where D_p is the diameter of the particle and λ is the wavelength of the light.

In the case of this study the transmission of the laser light is measured. An increase in scattering will thus lead to a decrease in the transmission signal strength. The amount of scattering is determined by the size of the particle and the wavelength of the laser light. The intensity of the scattered light varies as the sixth power of the particle size and varies inversely with the fourth power of the wavelength[1]. Laser light with shorter wavelengths will thus be scattered by smaller particles, i.e. the sensitivity towards smaller particles increases. In this study three lasers with decreasing wavelength were used namely, 635, 532 and 405 nm. The 405 nm laser will thus detect smaller particles than 635 nm or 532 nm. There is an upper limit in detection size for the lasers, this is reached when the effectiveness of the scattering blocks any light passing through to the transmission detector. This point will vary for each laser due to scattering being wavelength dependant. The wavelengths of the three lasers only stretch from 635 nm to 405 nm, which is a relatively small range. The range of particles each laser can detect will thus overlap to a certain degree. Analysing the peak temperatures is easier when the first derivative of the raw data is taken. If crystallization is slow (measured as the rate at which the size of the particle grows), there would be a clear distinction between the three laser responses. Slow particle growth will mean a time difference between the detection of the different particle sizes i.e. the laser responses. A faster crystallization, (fast growing particles/spherulites) will lead to the three lasers responses being very close to each other and in certain cases even overlapping completely.

6.2 Ziegler-Natta catalysed polymers.

Polymers previously synthesized and fully characterised[2] were used in this part of the study. This is a reverse of a more traditional study, where the sample is unknown but the technique is fully understood. Polypropylene made by a Ziegler-Natta catalyst results in polymers with a broad molecular weight distribution. In this study a range of Ziegler-Natta catalysed polymers were analysed. The range of heterogeneous polymers synthesized differ in two ways; first the type of external donors used and, second, the Ti:Si ratio used in the polymerization. ZNPP-5 is an example of a polymer synthesized with no external donor. This polymer is the standard to which all other samples will be compared. Two types of external

donors were used, namely diphenyl-dimethoxysilane (DPDMS) and methyl-phenyl-dimethoxysilane (MPDMS), DPDMS is the range of ZNPP-1 to ZNPP-4 and MPDMS is the range of ZNPP-6 to ZNPP-9.

As said numerous times this is a new technique and to be able to give an absolute explanation, in isolation, for results obtained would be foolish, as is the case for many other analytical techniques. As mentioned fully characterized polymers were analysed and will be discussed briefly before the discussion of the SCALLS analysis. The polymers were characterized by means of NMR, DSC, HT-GPC, CRYSTAF and prep-TREF.

Characterization data obtained from NMR, DSC and HT-SEC is summarised in Table 6-1. ZNPP-4, 7 and 9 were discussed in previous sections so will not be discussed here again. All the Ziegler-Natta catalysed polymers were fractionated by means of prep-TREF. Referring to the prep-TREF elution curves shown in Figure 6.2 it can be seen that ZNPP-5, a polymer synthesized without any external donor, elutes at a relative lower temperature with the major fractions between 110 °C and 115 °C while the major fractions for ZNPP-1, ZNPP-2 and ZNPP-3 polymers, polymerised in presence of the DPDMS, is between 115 °C and 120 °C. It was shown that the amount of polymer eluting at lower temperatures is dependent on the amount of external donor used[2]. The amount of polymer eluting at the lower temperature fractions decreased as the external donor/catalyst ratio increased. The two major fractions, with smaller but still significant fractions in the lower temperature intervals eluting in prep-TREF is mirrored in the CRYSTAF analysis, Figure 6.1, of ZNPP-5, showing a broad, bimodal curve. The peak crystallization temperatures according to CRYSTAF analysis, follows a trend according to molecular weight and not tacticity. The range of polymers synthesized with MPDMS as an external donor shows a much broader distribution in molecular heterogeneity. Fractionation with prep-TREF, Figure 6.4 shows that the major fractions are distributed in the 110 °C, 115 °C and 120 °C fractions. CRYSTAF analysis, Figure 6.3 shows that the onset of crystallization is higher for the higher molecular weight polymers.

Table 6-1. Summary of the data of the heterogeneous polypropylene samples

Sample Code	Si:Ti	Tm(°C)	Crystallinity(%)	M_w (g/mol)	PD	mmmm (%)
ZNPP-1	40	162.66	64.83	321000	4.9	96.11
ZNPP-2	16	162.80	63.73	288000	5.0	94.78
ZNPP-3	8	160.99	73.30	246000	5.2	95.13
ZNPP-4	4	161.27	74.64	226000	5.9	94.56
ZNPP-5	0	157.05	54.21	158000	7.5	83.84
ZNPP-6	40	161.44	66.12	262000	6.5	96.00
ZNPP-7	16	159.30	66.75	192000	8.8	95.44
ZNPP-8	8	159.35	74.80	182000	8.7	93.72
ZNPP-9	4	159.49	69.04	183000	8.5	94.57

These samples were then analysed with the SCALLS instrument. As said previously with the improvement of the instrument it is now possible to not only accurately control the cooling but also the heating cycle, and thus both can be used to gain valuable information.

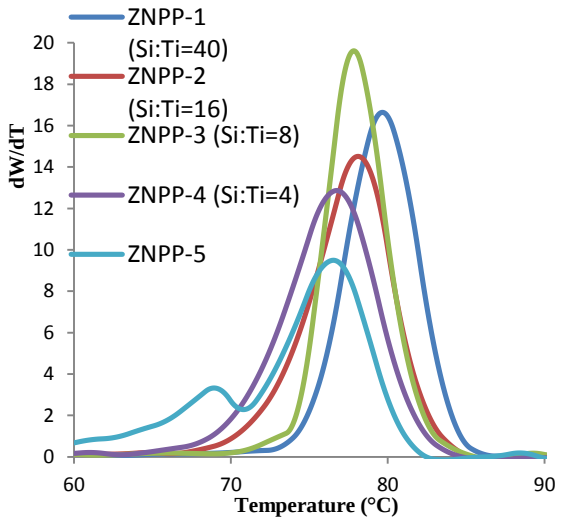

Figure 6.1: Crystaf analysis for ZNPP-1 to ZNPP-5

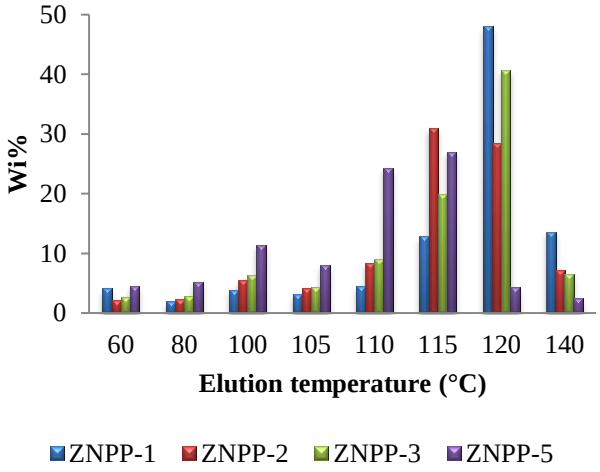

Figure 6.2: prep-TREF analysis of ZNPP-1 to ZNPP-3 and ZNPP-5

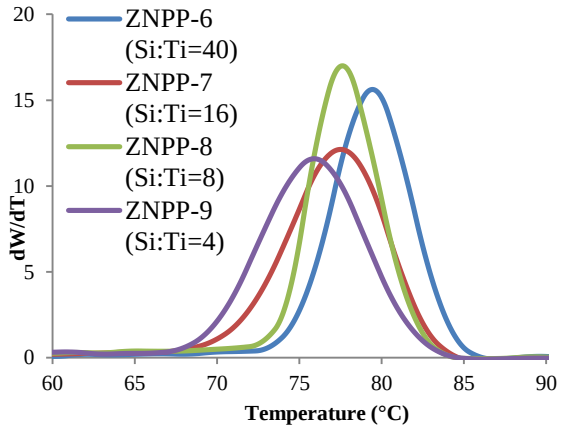

Figure 6.3: Crystaf analysis for ZNPP-6 to ZNPP-9

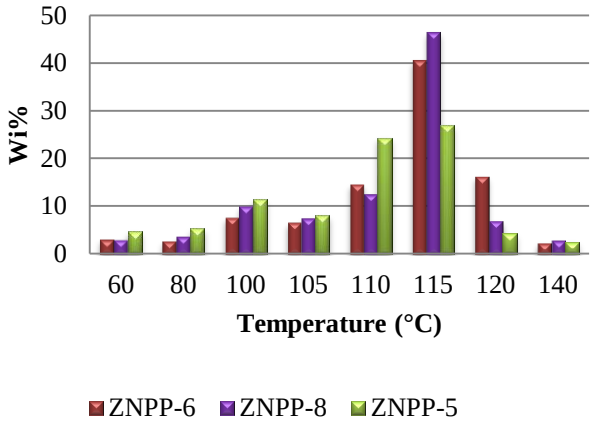

Figure 6.4: prep-TREF analysis of ZNPP-5, ZNPP-6 and ZNPP-8

6.2.1 Cooling cycle as analysed with SCALLS

The cooling cycle gives information on the crystallization of the polymer from solution. The standard cooling rate used for analysis of the SCALLS instrument is quite fast. The effect of cooling rate was determined previously for one laser [3-5] but the relative effect between lasers will be discussed. To determine if any loss of detail occurs due to the fast cooling rate the analysis of three heterogeneous polypropylene samples, namely ZNPP-1, ZNPP-2 and ZNPP-3, was repeated at slower cooling and compared. At a cooling rate of 0.4 °C/min, Figure 6.7 (a,c,e), it can be seen that not only does the general shape of the curve stay the same, but also the relative shift between lasers does not change significantly in comparison with a cooling rate of 1 °C/min, Figure 6.5. It would seem that an even slower cooling rate of 0.2 °C/min, Figure 6.7 (b,d,f), does show more detail regarding the crystallization at first glance. But it is probably more likely, that the very slow cooling rate offers the polymer time to start secondary crystallization events depicted by these jagged profiles that at first glance seem to indicate more detailed information. Important to note is that the slow cooling data of 0.4 °C/min does not significantly differ from the 1 °C/min cooling data and thus shows that for solution crystallization a fast cooling rate can be used. The standard cooling analysis of 1 °C/min can thus also be used for the three laser set-up.

First a discussion of the polymers catalysed with DPDMS as external donor. The solution crystallization temperature increases with an increase in Si:Ti ratio up to a value of 16 after which it stays constant. The solution crystallization temperature stays relatively constant between ZNPP-2 and ZNPP-1 even though the Si:Ti ratio more than doubles. There is however a difference in the shape of the graphs. In sample ZNPP-1 the red laser response shifts away from the green laser, not evident in the previous samples. This is an indication of slower particle growth. The molecular weight increases as the Si:Ti ratio increases, corresponding with the increase in the solution crystallization temperature. The tacticity does not follow the same trend and in this case it would seem that the dominating effect on the solution crystallization is the molecular weight. This is also corroborated with the CRYSTAF data, Figure 6.1, which was discussed earlier. The overall appearances of the graphs, ignoring the peak temperatures are very similar, but keep in mind the only difference is the amount of external donor. Comparing these samples with a polymer

synthesized without any external donor, namely ZNPP-5, shows significant differences. Solution crystallization of ZNPP-5 is shown in Figure 6.5(d), it can be seen that crystallization is over a broader temperature range relative to the series, ZNPP-1 to ZNPP-3, and a significant shift in peak temperature is seen. The red laser response of ZNPP-5 shows bimodality that can be seen as shoulders on the green and blue lasers. Comparing the SCALLS data with the prep-TREF and CRYSTAF data it can be seen that phenomenon seen during SCALLS analysis is mirrored in the other two techniques as well. CRYSTAF analysis, Figure 6.1, shows a broad, bimodal curve for ZNPP-5 and in the prep-TREF analysis it can be seen that there is two mayor fractions between 110 °C and 115 °C with smaller, but still significant fractions in the lower temperature intervals. The heating analysis, Figure 6.6, also shows the significant difference of a polymer synthesized in the presence and absence of an external donor. It can be seen that the solution melting of ZNPP-2, Figure 6.6(a), is more homogenous than ZNPP-5, Figure 6.6(b). There are multiple peaks visible in the analysis of ZNPP-5, which is expected when referring to the solution crystallization graph. It would seem that different size particles formed during crystallization will lead to different melting temperatures in the heating cycle.

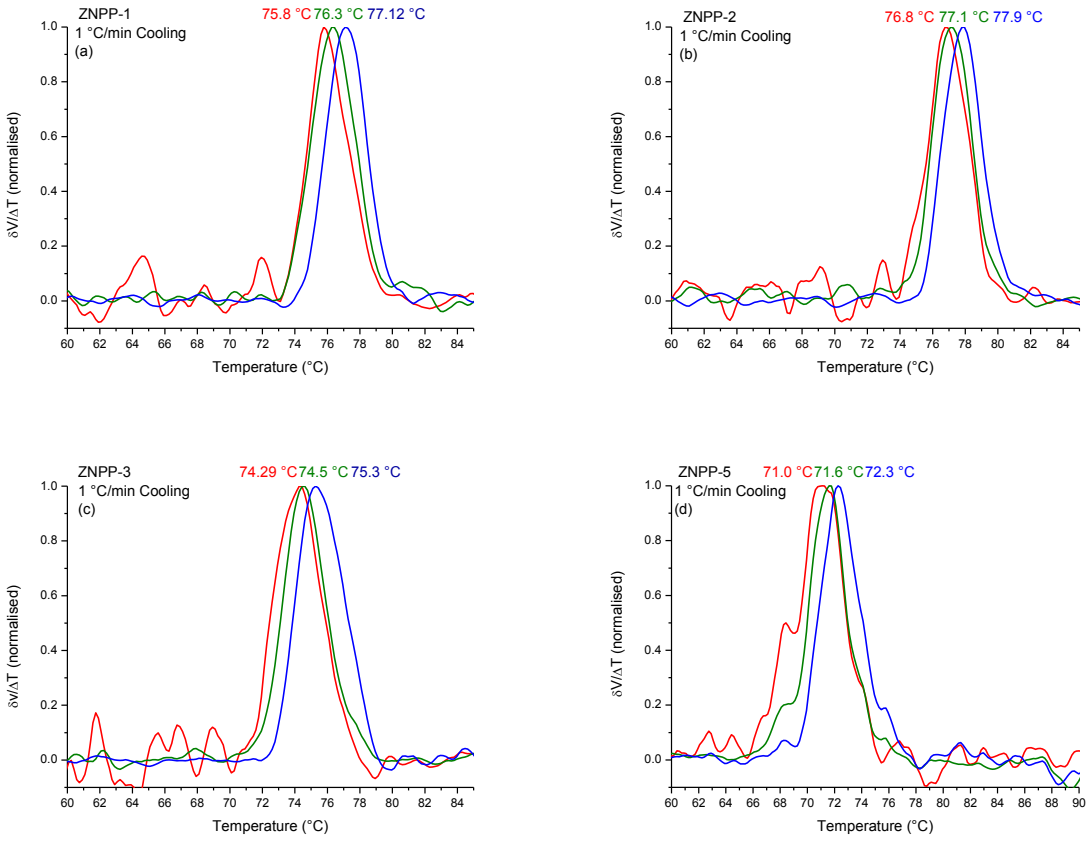

Figure 6.5: SCALLS data for ZNPP-1 to ZNPP-3 and ZNPP-5 at a cooling rate of 1 °C/min

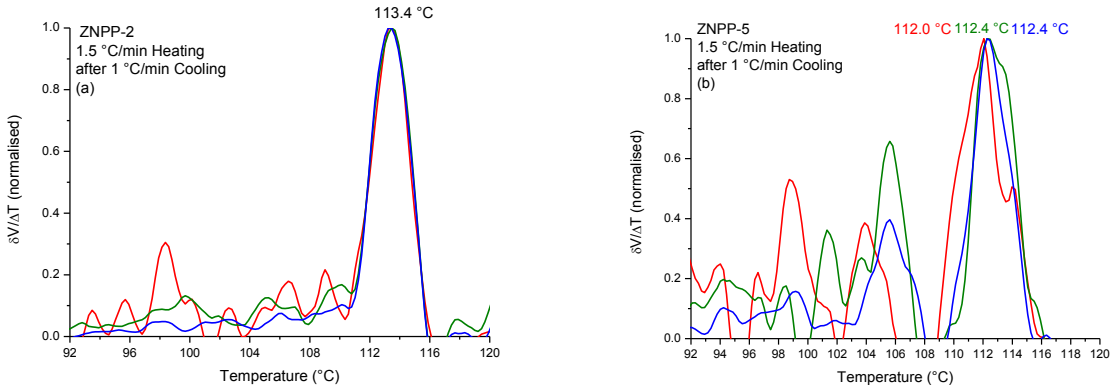

Figure 6.6: SCALLS data for ZNPP-2 and ZNPP-5 at a 1.5 °C/min heating rate after 1 °C/min cooling

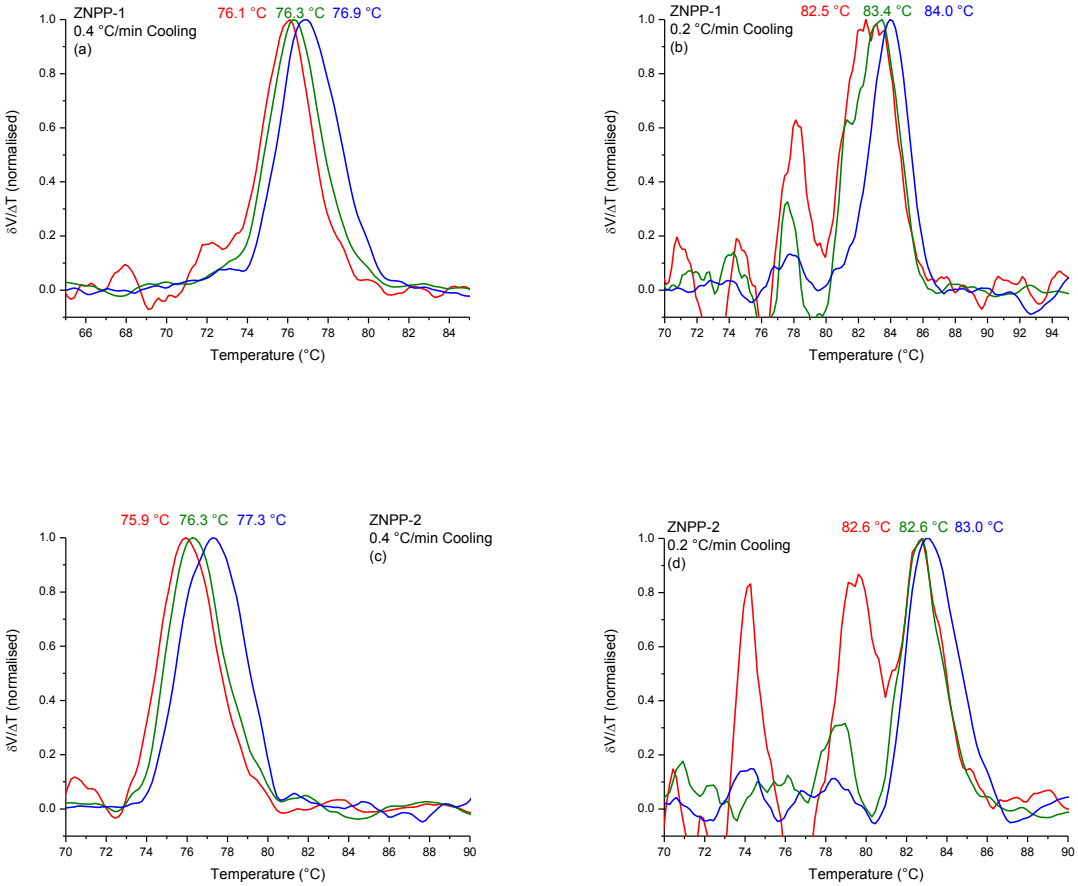

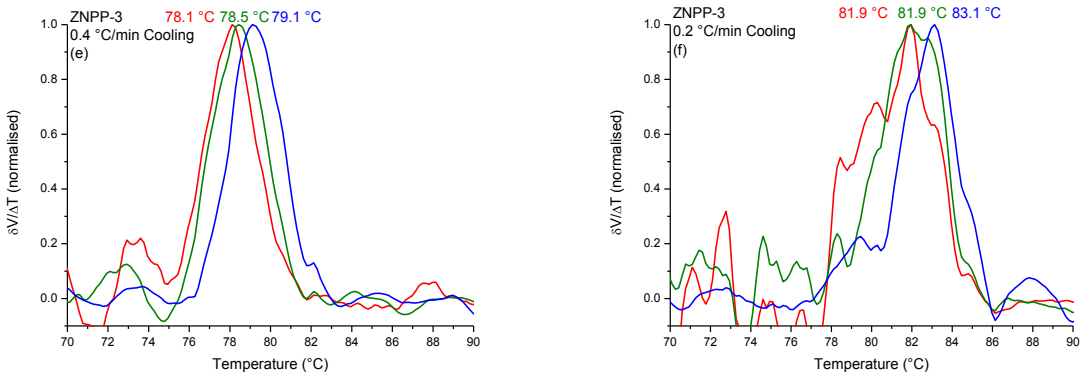

Figure 6.7: SCALLS slower cooling analysis of ZNPP-1, ZNPP-2 and ZNPP-3

SCALLS cooling analysis of two heterogeneous polypropylene samples, ZNPP-6 and ZNPP-8, catalysed with MPDMS as an external electron donor is shown in Figure 6.8 for the 1 °C/min cooling and Figure 6.9 for the 0.4 °C/min and 0.2 °C/min. The slower cooling rate does not show any significant data not present in the faster cooling profile. This is more proof that a faster cooling rate can give significant results without compromise to detail for the cooling analysis. These two polymers, catalysed with MPDMS as an external donor, show much more heterogeneity during the cooling as well as the heating cycles, if compared with the polymers with DPDMS as an external donor, seen in Figure 6.5(a-c). Especially in the case of the heating cycle for ZNPP-8, there are quite a few peaks visible in the lower temperature region. To ensure that this is a true representation this analysis was repeated four times and in each case the same response was seen. The prep-TREF analysis also shows that there is a significant amount of polymer eluting between 100 °C and 120 °C, thus indicating the molecular heterogeneity that is reflected during SCALLS analysis. The fact that the SCALLS analysis reflected what was observed in the prep-TREF analysis indicated that the SCALLS could be used to possibly predict elution temperatures for prep-TREF. This is discussed in the following section.

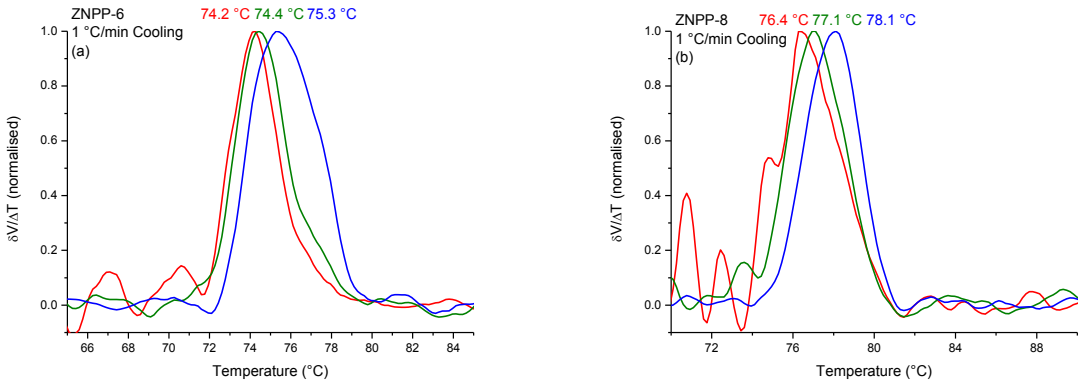

Figure 6.8: SCALLS cooling analysis, 1 °C /min, of ZNPP-6 and ZNPP-8

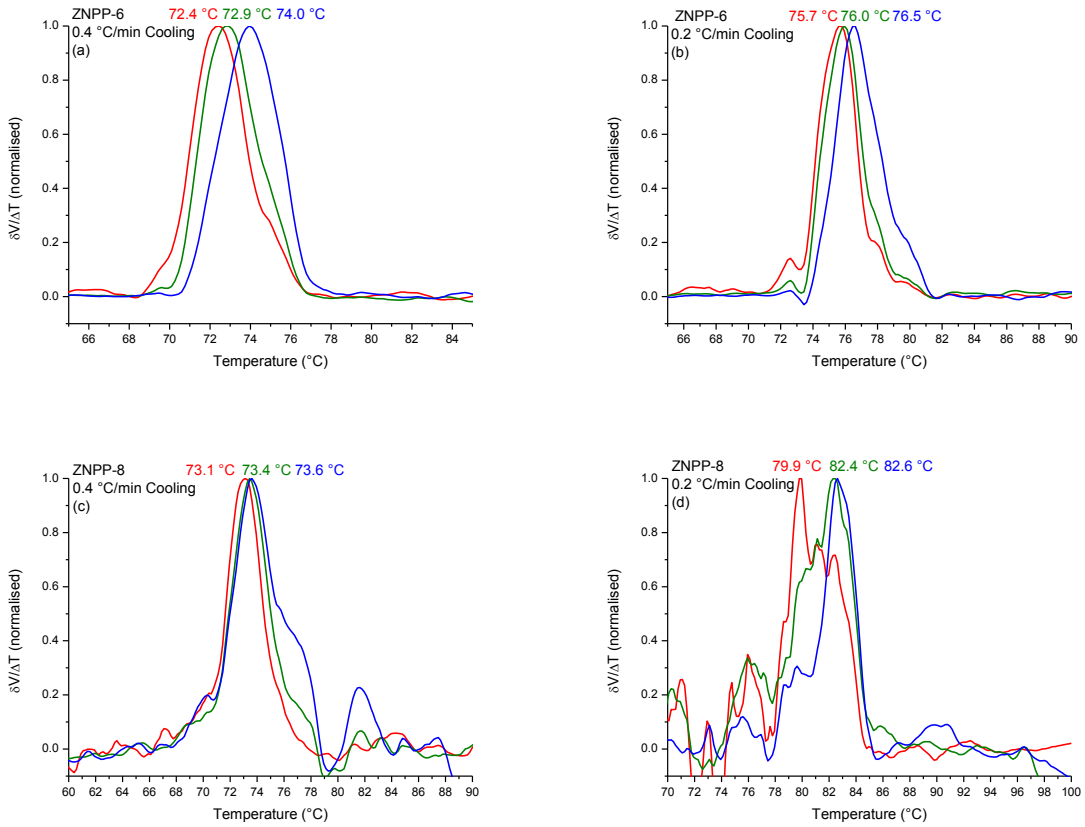

Figure 6.9: SCALLS analysis at a slower cooling rate for ZNPP-6 and ZNPP-8

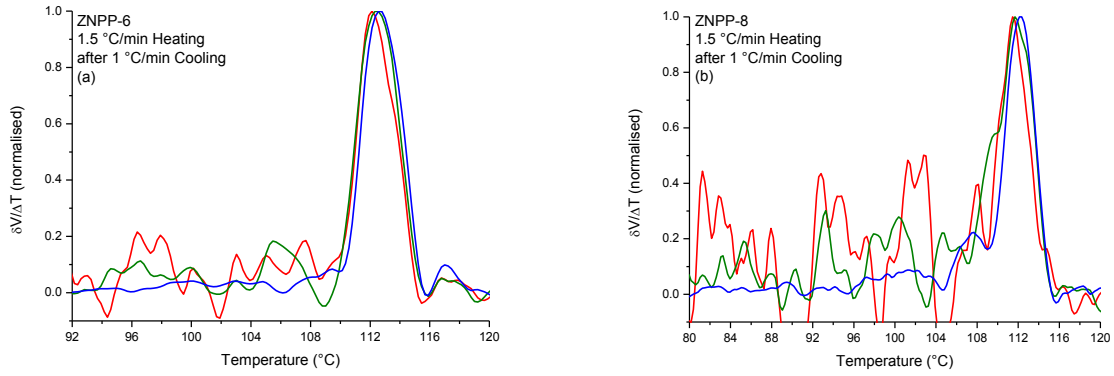

Figure 6.10: SCALLS heating analysis at a rate of 1.5 °C/min after 1 °C/min cooling

6.3 SCALLS as an Analytical TREF

Fractionation of polymers can be a tedious process, as in the case of preparative TREF (prep-TREF). Fractionation temperatures are chosen beforehand and further analysis might prove that certain fractions are not as homogeneous as required. Ideally a fast pre-screening method is needed to be able to choose the fractionation temperatures more informatively. Analysis of certain bulk polymers, previously fractionated, were done to determine if a correlation is possible between the peak temperatures found in the heating analysis of SCALLS and the prep-TREF data. In Figure 6.11 an overlay of two heterogeneous catalysed

prep-TREF data is shown with SCALLS data, indicating a good fit. The TREF and SCALLS data are represented by the bar and line graph respectively. To visually show the correlation the graphs were plotted on two x-axes and shifted by 4 °C. The TREF bar graph is a representation of the amount of polymer, given as a weight percentage, eluted at predetermined temperatures. Visually it would seem that there is a good correlation but for a more comprehensive correlation the relative area of the same temperature intervals found in TREF needed to be determined for SCALLS. The area underneath the graphs, split into 5 °C intervals, was calculated with the aid of Origin®. It is represented as a percentage of the total area, to correspond to the weight percentage of TREF. A very good fit is obtained for ZNPP-1, indicating that SCALLS analysis can help in determining elution temperatures for prep-TREF. At first glance it would seem that this method did not work for ZNPP-6. The main fraction temperature does not correspond between the two techniques. However it can be seen in Figure 6.11(b) that the TREF elution temperature was chosen that the main fraction is split in two, indicating the discrepancy between the values found in SCALLS and prep-TREF. It would seem that SCALLS can be used as a possible pre-screening method to decide elution temperatures for prep-TREF.

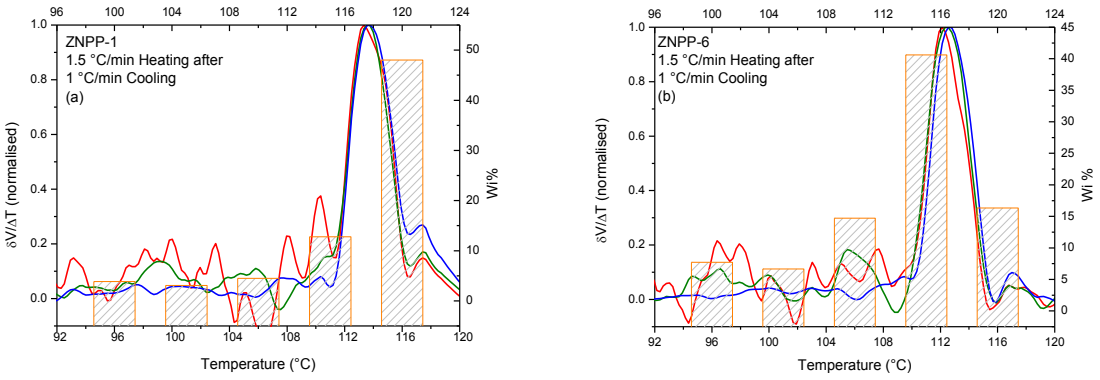

Figure 6.11: prep-TREF overlay with SCALLS analysis

Table 6-2: Integrated area of ZNPP-1 for the SCALLS analysis compared to TREF data

SCALLS Temperature	ZNPP-1 SCALLS %	ZNPP-1 TREF %	ZNPP-6 SCALLS %	ZNPP-6 TREF %	TREF Temperature
30 °C ➔95 °C	28.98	18.02139	26.02901	19.25	30 °C ➔ 105 °C
95 °C ➔100 °C	7.05	3.067843	10.12042	6.67	105 °C
100 °C ➔105 °C	5.11	4.49366	3.76487	14.72	110 °C
105 °C ➔110 °C	2.58	12.77976	8.837523	40.63	115 °C
110 °C ➔115 °C	46.27	48.02197	50.34659	16.33	120 °C
115 °C ➔120 °C	10.01	13.61538	0.901598	2.40	140 °C

6.4 Impact polypropylene samples analysed with SCALLS

Impact polypropylene samples are extremely complex materials consisting of a mixture of ethylene-propylene random copolymers (EPR), iPP and semicrystalline ethylene-propylene copolymers (EPC). Polymerization takes place in a two-step sequential gas-phase process. In the first step isotactic polypropylene is produced, the polymer is then transferred to a second reactor where more catalyst and monomer is added to form the copolymer. Two sets of reactor grade polymers, in powder form, were obtained from Sasol Polymers, Secunda, South Africa. The main difference between the sets was the technology used for synthesis. Each set consisted of a range of samples that were taken from the second reactor at regular intervals, thus the samples only differed in the amount of ethylene present.

6.4.1 First series of impact polypropylene samples analysed

Molecular weight data determined by HT-GPC and the ethylene content, calculated by means of FTIR, is summarised in Table 6-3 and the CRYSTAF analysis is shown in Figure 6.12. The ethylene content increases from 0 %, thus isotactic polypropylene, to 7.8 %, determined with FTIR. CRYSTAF analysis shows that the peak temperature decreases relative to the ICPP2 t0 sample, up to ICPP t60 (3.6 % ethylene) after which the peak temperature increases again, showing that there is molecular heterogeneity in the samples. SCALLS analysis were performed to determine if the three laser setup could detect differences between the polymers that in essence only differed regarding the amount of ethylene content. With increasing levels of ethylene, peak temperature shifts slightly higher and changes in crystallization behaviour are also seen by the broadening of the peak. This is quite remarkable if it is taken into account that the only difference is the ethylene content that varies between 0% and 7.8%. The heating profiles show a slight increase in dissolution temperature with the increasing ethylene content, up to the ICPP2 t90 sample after which the peak temperature shifts lower for the ICPP2 t120 sample.

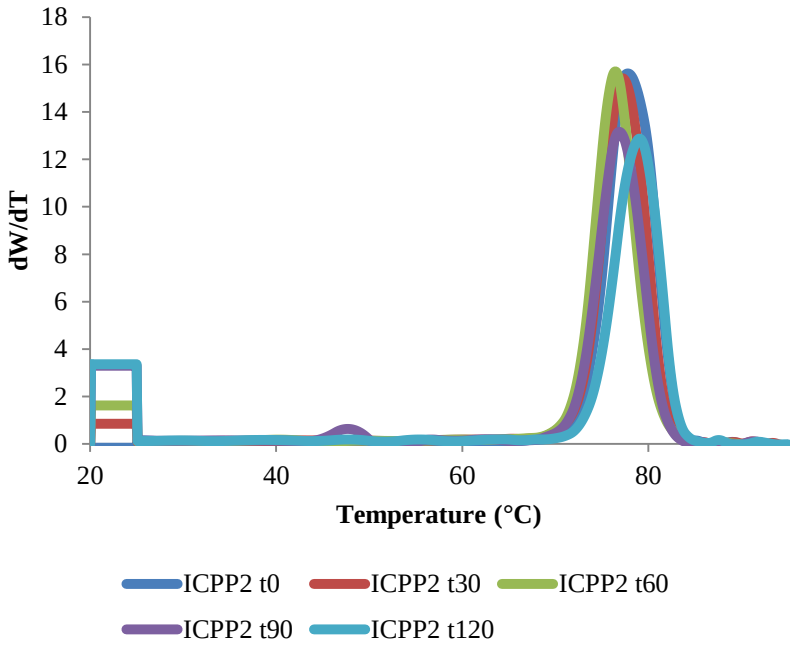

Figure 6.12: CRYSTAF analysis for the ICPP2 range

Table 6-3: Characterization data for the impact polypropylene samples

Sample	Mw	PDI	Ethylene content (%)[a]
ICPP2[b] t0[c]	419606	10.51	0
ICPP2 t30	420803	9.30	2.0
ICPP2 t60	487928	10.51	3.6
ICPP2 t90	456688	9.03	6.8
ICPP2 t120	518560	9.36	7.8

[a] *As determined by FTIR*
[b] *Number distinguishes between the two different technologies used to synthesize the impact polypropylene samples*
[c] *Number denotes the time, in minutes, the sample spent in the second reactor.*

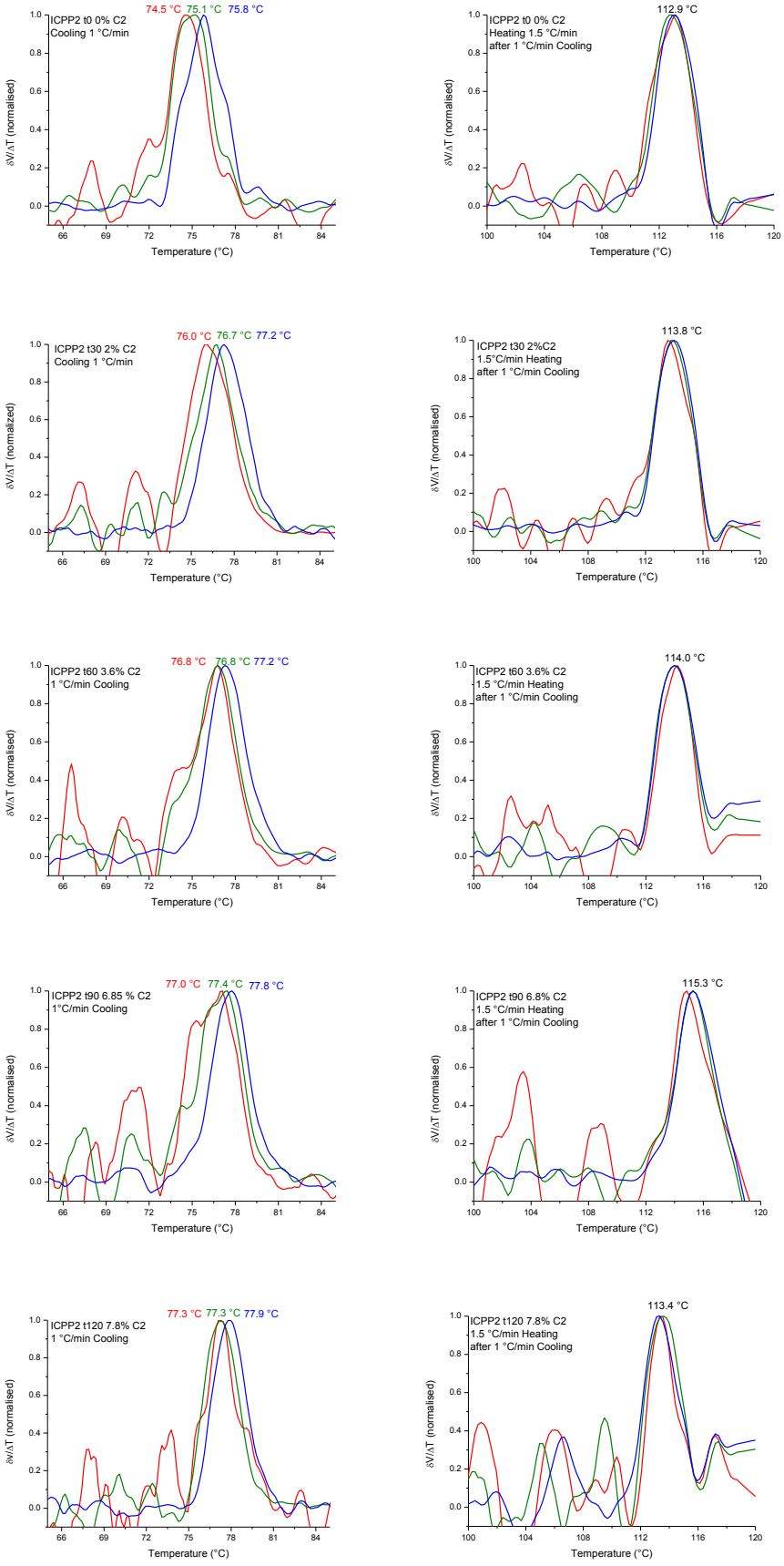

Figure 6.13: SCALLS analysis of the ICPP2 impact polypropylene samples with increasing ethylene content as indicated on graphs, cooled at 1 °C/min (left column) and heated at 1.5 °C/min (right column)

From this first series it could be seen that even slight differences can be detected by means of SCALLS and further analysis were done on a different series of impact-PP samples.

6.4.2 Second series of impact-PP samples analysed

A second series of impact-PP samples (ICPP1 range), polymerized with a different technology were obtained from Sasol polymers. These samples were studied in more detail. The polymers were analysed by means of HT-SEC, prep-TREF, NMR and CRYSTAF. CRYSTAF analysis, Figure 6.12, showed a decrease in peak crystallization temperature with addition of ethylene, up until ICPP1 t180 after which the peak crystallization temperature increased again. Prep-TREF analysis showed that the less crystalline fractions, eluting between 30 °C and 80 °C, for ICPP1 t240 and ICPP t360, increases with the increasing ethylene content, while a decrease in the amount of polymer eluting between 90 °C and 120 °C is seen. This relative decrease is an indication that these fractions consists mainly of polypropylene. In contrast with this the fractions eluting at 130 °C and 140 °C increases with the increase in ethylene content, indicating the possible presence of highly crystalline polyethylene. The fractions were analysed by means of ^{13}C NMR to ascertain if this theory is correct.

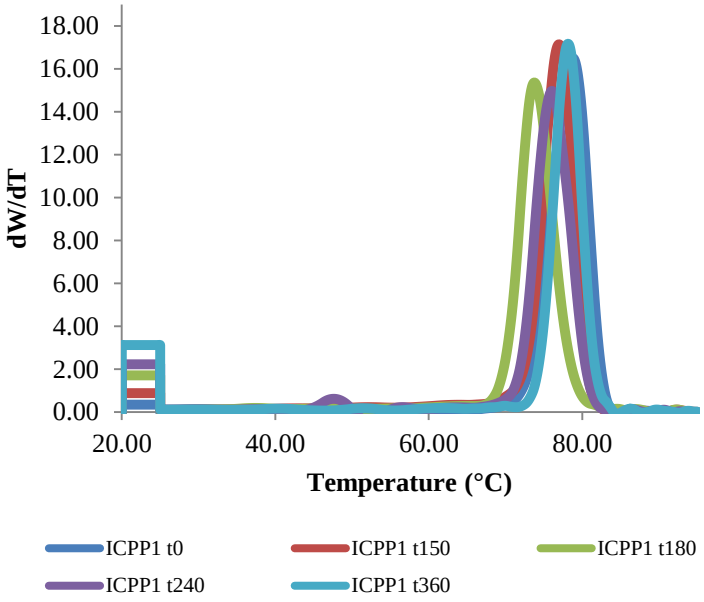

Figure 6.14: CRYSTAF analysis of the ICPP1 series

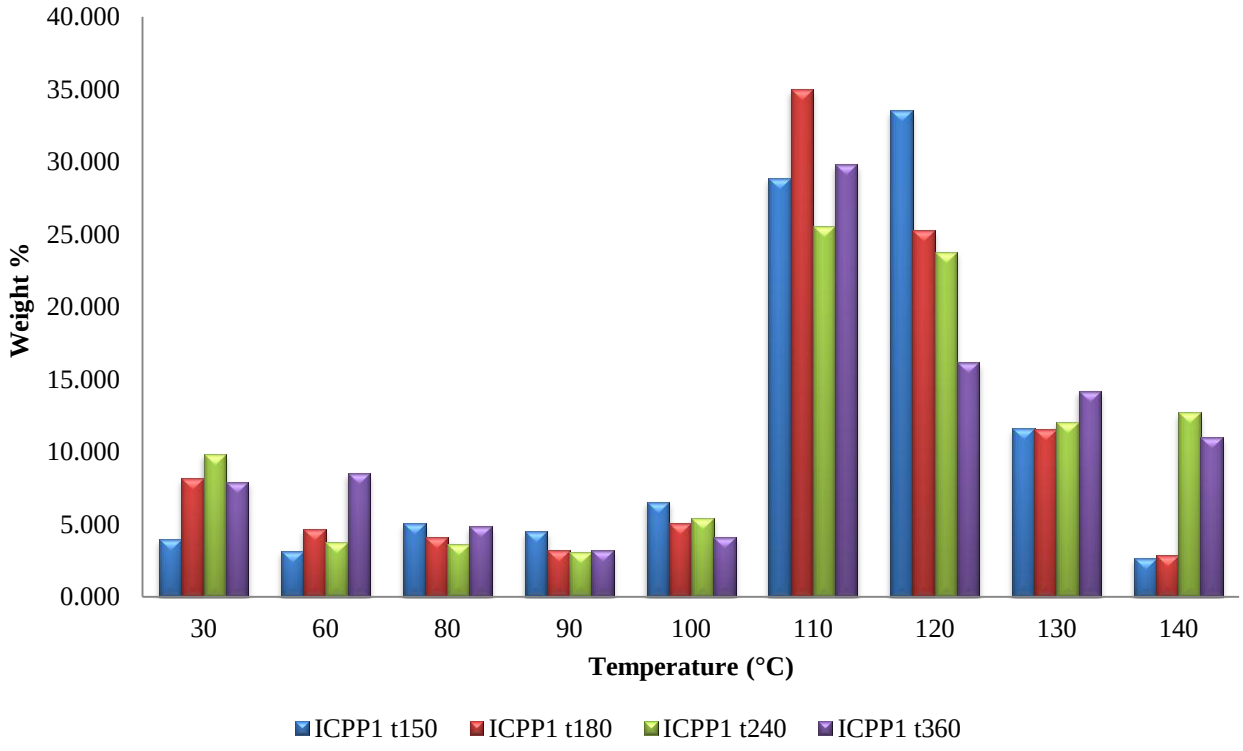

Figure 6.15: TREF elution data for the ICPP1 series

Analysis was done to determine where ethylene incorporates into the polymer. It was seen, as shown in Figure 6.16, that continuous ethylene sequences grew preferentially above alternating propylene and ethylene sequences. At low ethylene contents, alternating sequences are present, causing the initial decrease in the crystallization peak temperature seen during CRYSTAF analysis. The peak temperature increase seen from ICPP1 t240 to ICPP1 t360 is due to the preferential incorporation of ethylene into longer continuous sequences forming highly crystalline polyethylene sequences.

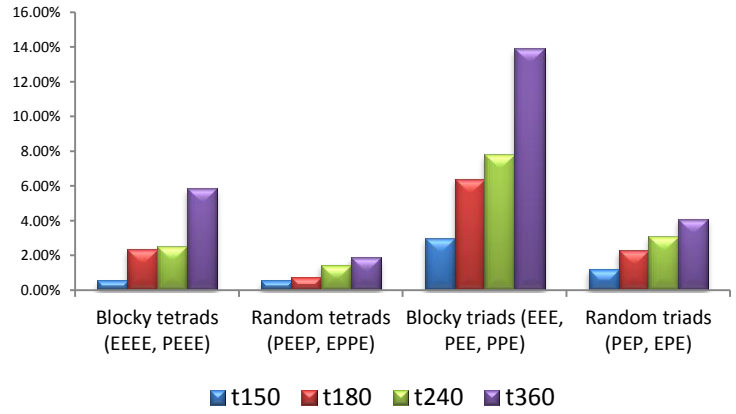

Figure 6.16: Distribution of blocky, random and tetrad sequences in the ICPP1 series

The ICPP1 range of polymers were then analysed with SCALLS using the standard 1°C/min cooling followed with 1.5°C/min heating profile. The samples were analysed as a powder, received from the reactor, and also analysed after it was pressed into a film. The film samples were also analysed with HT-SEC, DSC

and FTIR. A definite change in the molecular mass data of the polymers can be seen after heat treatment. Possible degradation could have taken place and to determine if this is the case FTIR analysis, Figure 6.23, were done. For clarity only one sample, ICPP1 t360, is shown. A broad carbonyl peak can be seen at 1715 cm^{-1} for the heat treated sample not seen with the powder sample. This falls in the area where carbonyl vibration occurs and is thus an indication of degradation. The cooling analysis for both the powder and heat treated samples are shown in Figure 6.17 to Figure 6.21. The majority of the samples show a significant decrease in crystallization temperature after heat treatment, as well as a decrease in the broadness of the graphs. The heating analysis of these samples explains why the degradation causes such a significant drop in solution crystallization temperature.

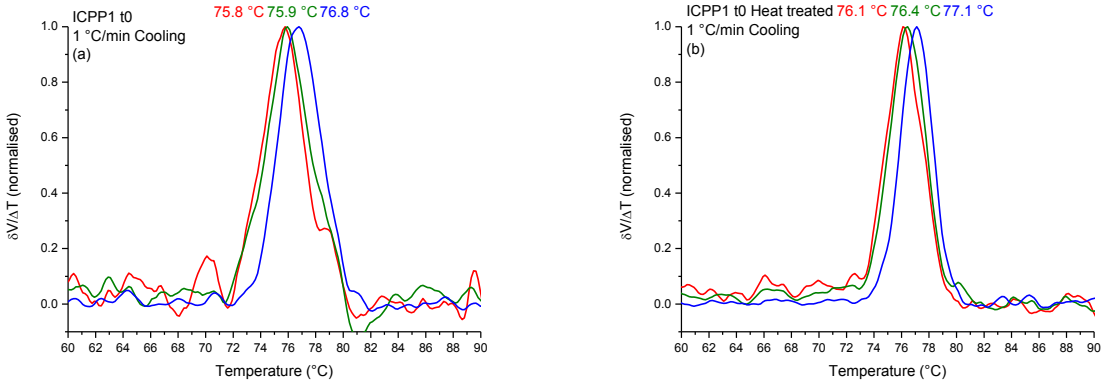

Figure 6.17: ICPP1 t0 cooling data obtained from SCALLS sample analysed (a) in powder form and (b) heat treated

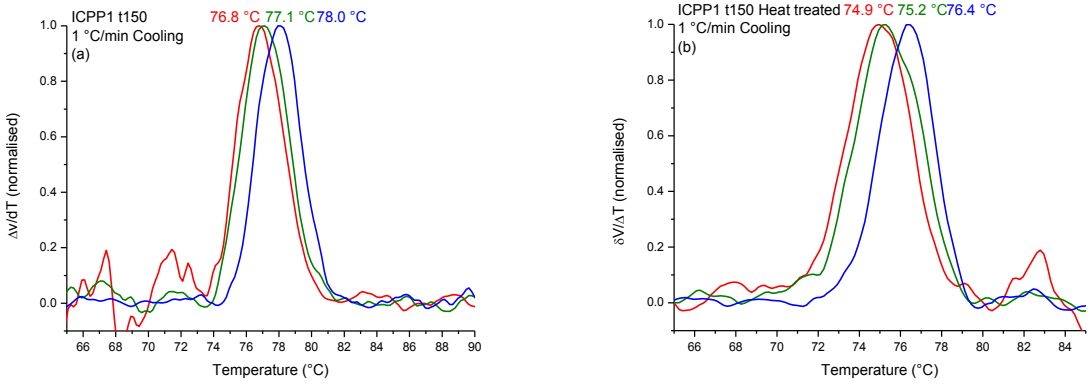

Figure 6.18: ICPP1 t150 cooling data obtained from SCALLS sample analysed (a) in powder form and (b) heat treated

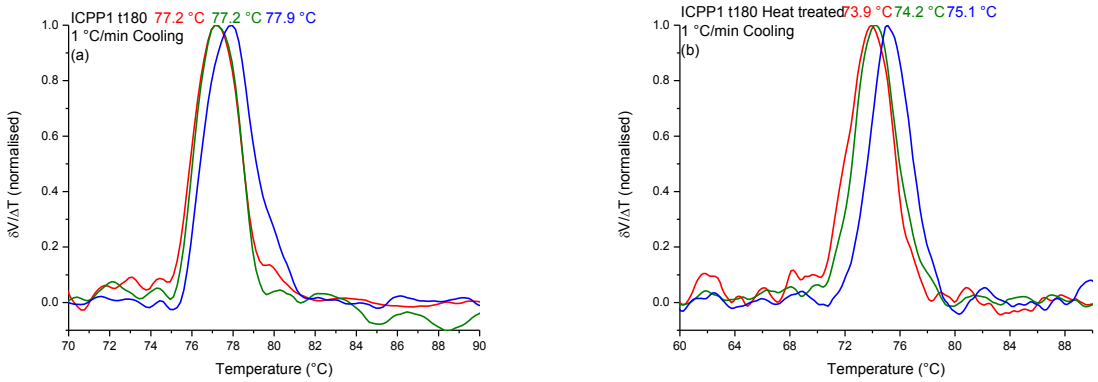

Figure 6.19: ICPP1 t180 cooling data obtained from SCALLS sample analysed (a) in powder form and (b) heat treated

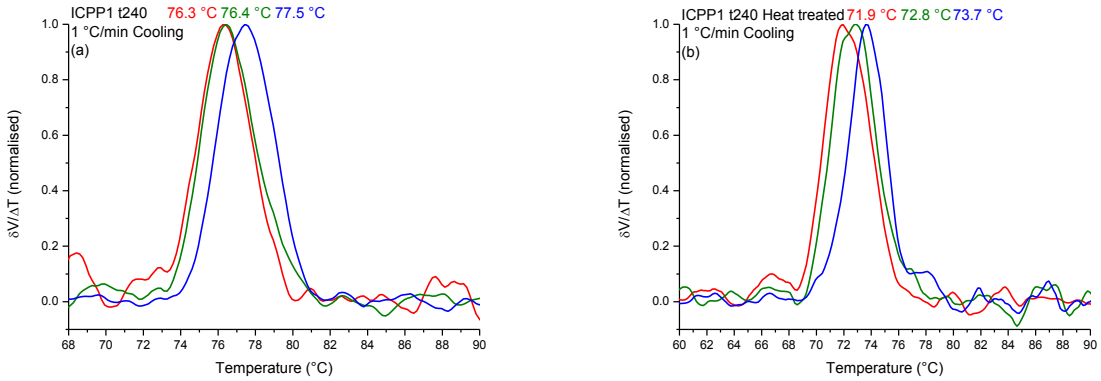

Figure 6.20: ICPP1 t240 cooling data obtained from SCALLS sample analysed (a) in powder form and (b) heat treated

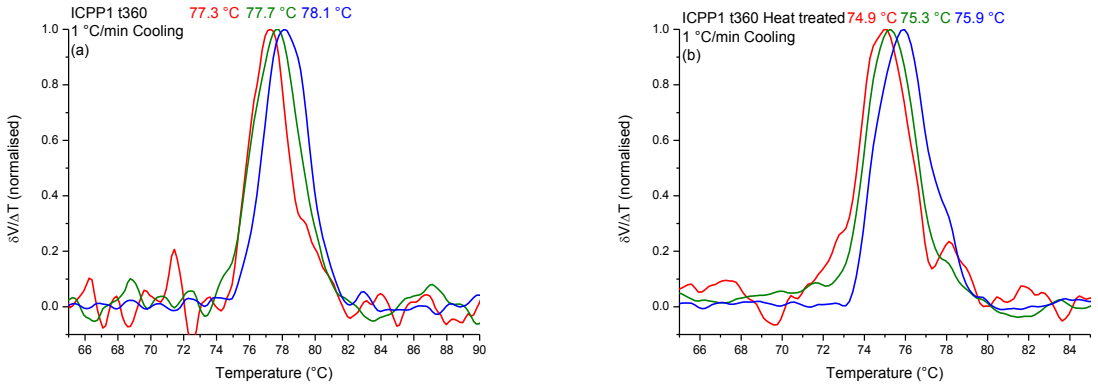

Figure 6.21: ICPP1 t360 cooling data obtained from SCALLS sample analysed (a) in powder form and (b) heat treated

The heating curves of these samples show a distinct difference between the powder and film samples, not only in the peak temperatures but the overall form of the curves. In each case there is a distinct bimodality in the heating analysis of the powdered samples. This bimodality, more specifically the higher peak temperature, disappears after heat treatment. This is due to degradation of the samples, which was confirmed previously by FTIR and DSC analysis seen in Figure 6.23 and Figure 6.22 respectively. The fraction of polymer melting at this higher temperature was more than likely the cause of a nucleation effect

causing the polymer to crystallize out of solution at a higher temperature during cooling analysis and thus the degradation of the polymer causes the shift to a lower peak crystallization temperature.

Table 6-4: Molecular mass data for the ICPP1 powder and heat treated samples determined by HT-SEC

	Mw	Mn	PDI
ICPP1 t0 Heat treated	157506	33401	4.71
ICPP1 t150 Heat treated	249921	32913	7.59
ICPP1 t180 Heat treated	233096	33576	6.94
ICPP1 t240 Heat treated	254469	14046	18.11
ICPP1 t360 Heat treated	164373	26247	6.26
ICPP1 t0 powder	349387	48722	7.17
ICPP1 t150 powder	337185	47036	7.16
ICPP1 t180 powder	340082	42963	7.91
ICPP1 t240 powder	336365	38088	8.83
ICPP1 t360 powder	359046	45194	7.94

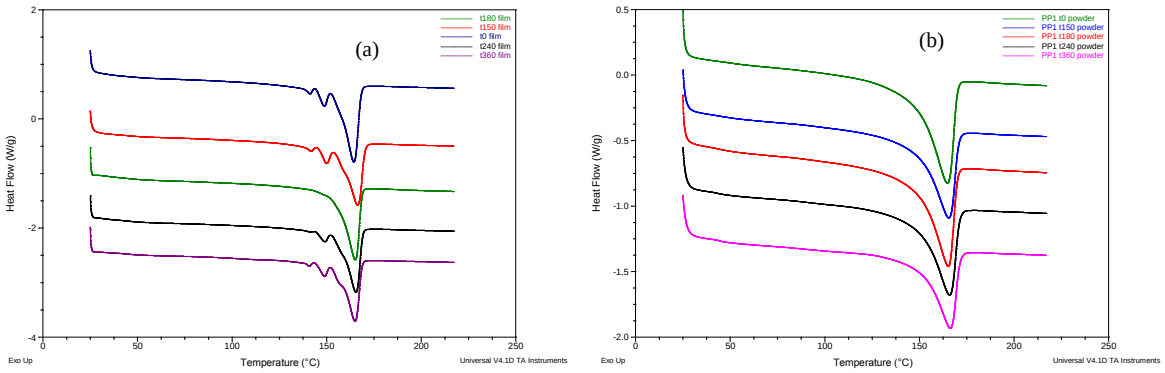

Figure 6.22: DSC first heating thermogram of (a) heat treated ICPP1 samples and (b) powder ICPP1 samples with increasing ethylene content from top to bottom

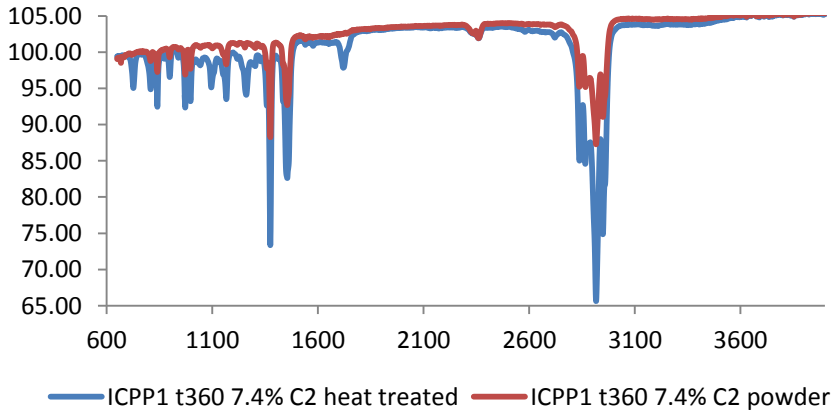

Figure 6.23: FTIR analysis of the ICPP1 powder and film sample

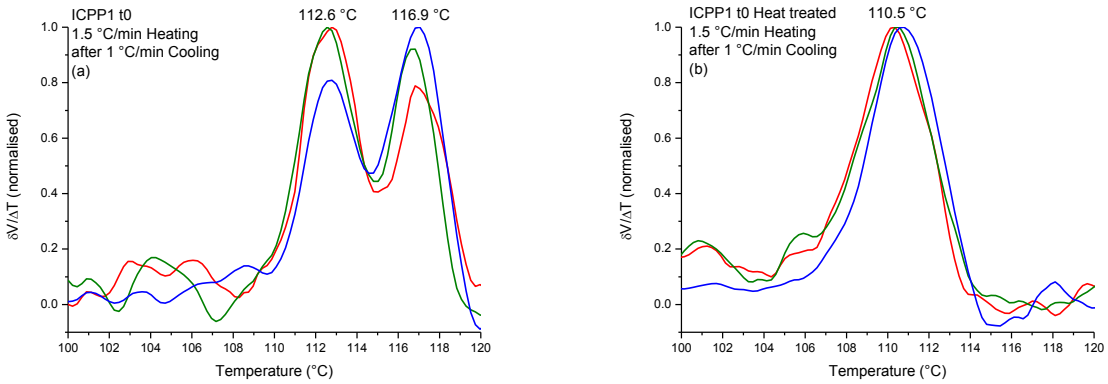

Figure 6.24: Impact polypropylene sample, ICPP1 t0, heating cycle analysed on the SCALLS (a) powder form and (b) after heat treatment

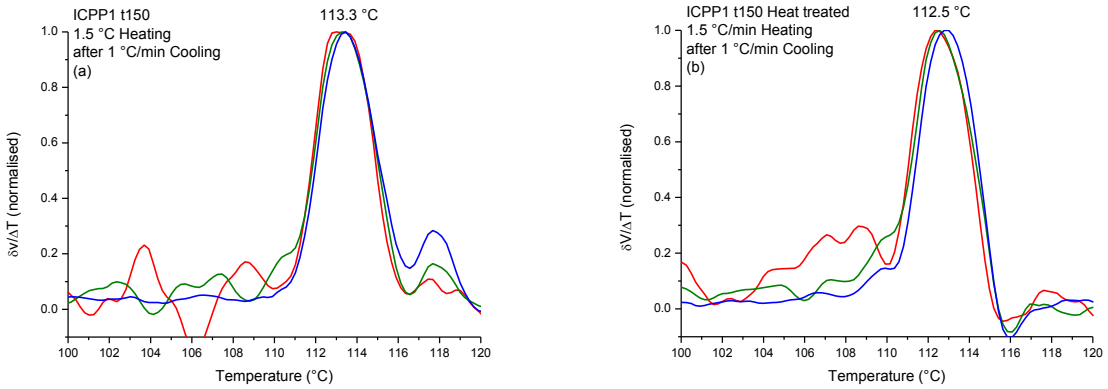

Figure 6.25: Impact polypropylene sample, ICPP1 t150, heating cycle analysed on the SCALLS (a) powder form and (b) after heat treatment

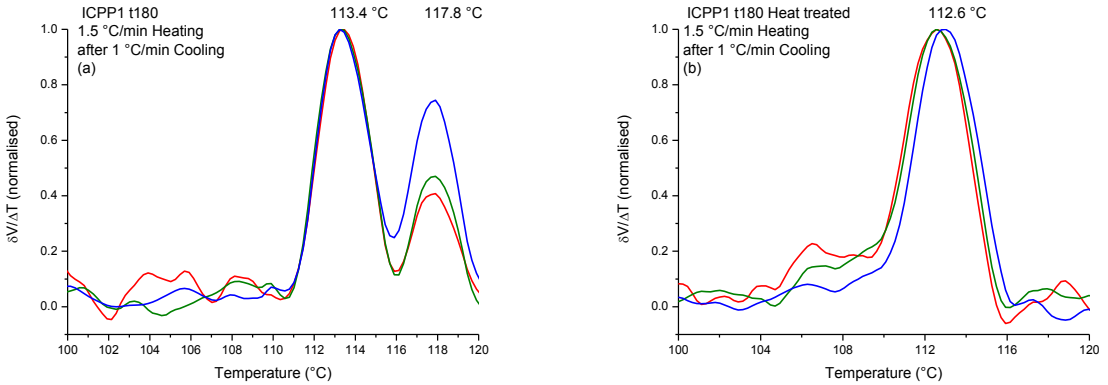

Figure 6.26: Impact polypropylene sample, ICPP1 t180, heating cycle analysed on the SCALLS (a) powder form and (b) after heat treatment

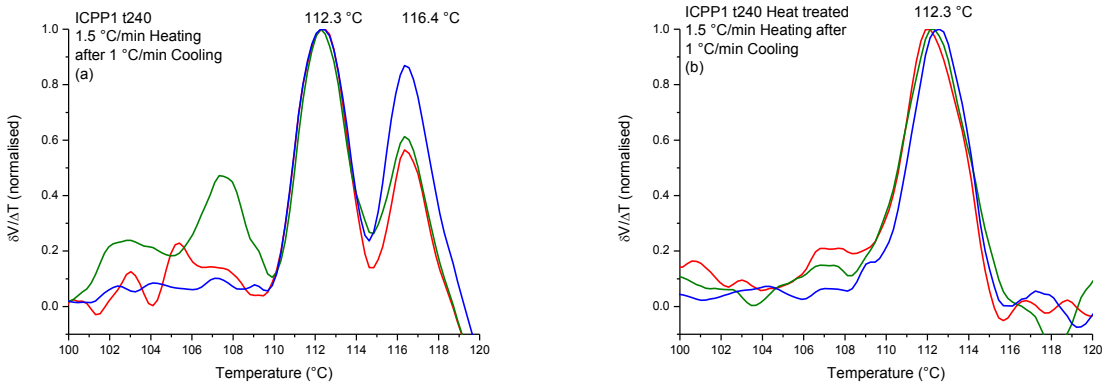

Figure 6.27: Impact polypropylene sample, ICPP1 t240, heating cycle analysed on the SCALLS (a) powder form and (b) after heat treatment

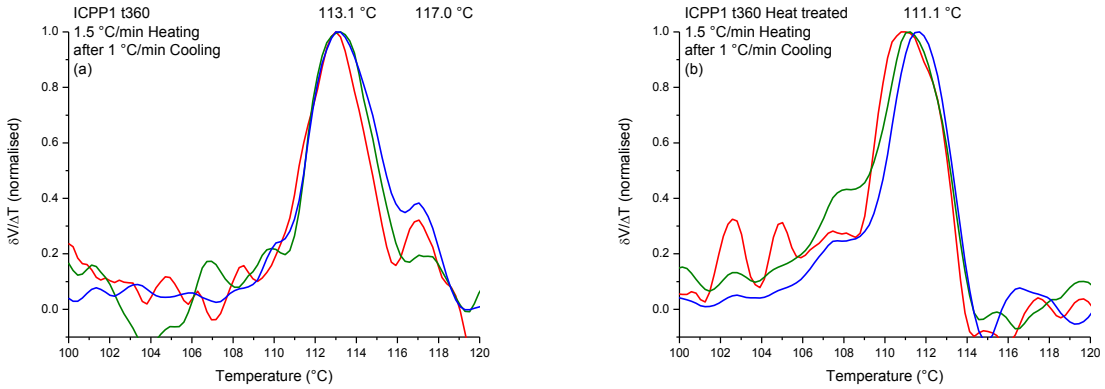

Figure 6.28: Impact polypropylene sample, ICPP1 t360, heating cycle analysed on the SCALLS (a) powder form and (b) after heat treatment

The data from the three lasers were used to determine the relative particle growth. Peak temperatures were plotted against wavelength, Figure 6.29(a). This was to determine the temperature at which a trendline will cross the y-axis. This temperature was used as the zero point and the difference between this point and the peak temperature was plotted against the wavelength. This produces a graph, Figure 6.29(b) showing the relative particle growth of each polymer. By comparing the slope of the graphs it can be seen as the ethylene content increases a decrease in the particle growth rate is seen.

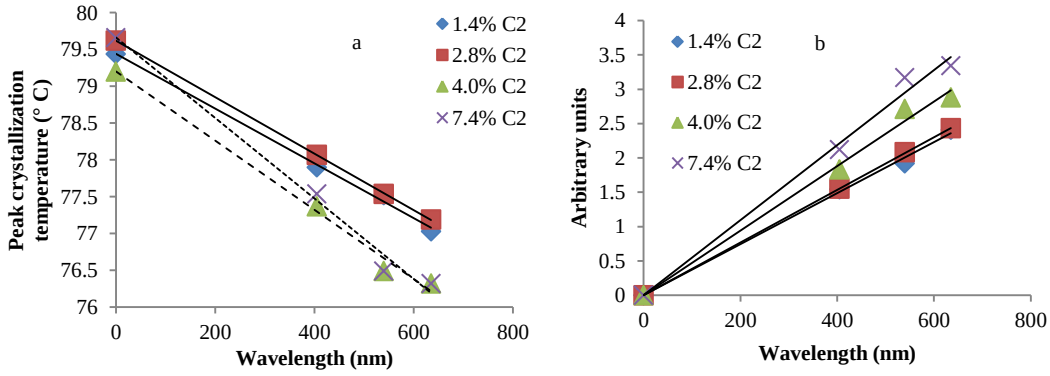

Figure 6.29: Plot of peak temperature against wavelength (a) and (b) the relative particle growth rate.

6.5 Conclusions

The instrument was successful in detecting small differences between complex polymers, in the case of the heterogeneous polypropylene samples it was due to different external donors used during synthesis and for the impact polypropylene samples it was only the amount of ethylene present. It was proven that the instrument can be used as a screening method for prep-TREF to determine the fractionation temperatures. Lastly the relative particle growth rate for impact polypropylene samples were determined.

6.6 References

[1] Barnett, C.E. : Some Applications of Wave-Length Turbidimetry in the Infrared. - J. Phys. Chem. **, 46**, -69 (1942).

[2] Gareth W. Harding. : The structure-property relationships of polyolefins. Stellenbosch : University of Stellenbosch, University of Stellenbosch (2009).

[3] van Reenen, A.J.; Brand, M.; Rohwer, E.G.; Walters, P. : Solution Crystallization Analysis by Laser Light Scattering (SCALLS). Macromolecular Symposia **, 282**, 25 (2009).

[4] Margaretha Brand. : Investigation of molecular weight effects during the solution crystallisation of polyolefins. University of Stellenbosch (2008).

[5] van Reenen, A.J.; Rohwer, E.G.; Walters, P.; Lutz, M.; Brand, M. : Development and use of a Turbidity Analyzer for Studying the Solution Crystallization of Polyolefins. J Appl Polym Sci **, 109**, 3238-3243 (2008).

[6] Supaphol, P.; Spruiell, J.E. : Application of the Avrami, Tobin, Malkin, and Simultaneous Avrami Macrokinetic Models to Isothermal Crystallization of Syndiotactic Polypropylenes. Journal of Macromolecular Science, Part B **, 39**, 257-277 (2000).

[7] T Pradell and D Crespo and N Clavaguera and,M.T.Clavaguera. : Diffusion Controlled Grain Growth in Primary Crystallization: Avrami Exponents Revisited. Journal of Physics: Condensed Matter **, 10**, 3833 (1998).

[8] Tomellini, M.; Fanfoni, M.; Volpe, M. : Spatially Correlated Nuclei: How the Johnson-Mehl-Avrami-Kolmogorov Formula is Modified in the Case of Simultaneous Nucleation. Phys. Rev. B **, 62**, 11300-11303 (2000).

Chapter 7

Conclusions and Future work

7.1 Conclusions

The instrument developed for the studying solution crystallization analysis by laser light scattering (SCALLS) was tested thoroughly, and the first edition of the instrument was used to study the applicability of the Flory-Huggins theory of melting point depression for a series of copolymers.

SCALLS is a technique that offers direct measurement of the solution crystallization or solution melting temperature of polymers. It was successfully used to study the applicability of the Flory-Huggins equation for propylene-higher 1-alkene copolymer systems in solution crystallization. It appears that the solvent interaction parameter for the propylene/higher 1-alkene copolymers (with low comonomer content) is dependent on the comonomer type. The melting point depression is clearly dependent on both the type and amount of comonomer included in the copolymer.

This instrument was then developed to include three lasers (405 nm, 532 nm and 635 nm) which could be used simultaneously to study the solution crystallization and melting behaviour of polyolefins. The construction of the new instrument was successful, and the reliability and reproducibility of the results demonstrated.

Finally, a series of experiments were conducted to illustrate the use and application of the SCALLS instrument. For example, the improved instrument was able to be used as a screening method for prep-TREF, to determine at which temperatures fractionation should occur.

The instrument was successfully used to detect even small differences between more complex materials such as heterogenous polypropylene and impact polypropylene samples. In the case of heterogeneous polypropylene it showed a difference between the samples that only differed in the type of external donor used during synthesis. The impact polypropylene samples only differed by the amount of ethylene content and differences were detected.

So in conclusion; the solution melting temperature of polymers can be measured by SCALLS and the instrument was successfully modified to increase the sensitivity.

7.2 Future work

The work done up to this point have showed that the sensitivity of the instrument can be improved by the addition of lasers with differing wavelengths. The next step will be to further improve the instrument by improving the temperature control to allow the samples to be cooled below the current minimum temperature of 30 °C. Together with this, stronger output voltage lasers should be used to increase the sensitivity and possibly enable earlier detection of the start of crystallization as well as secondary crystallization events.

Development and Use of a Turbidity Analyzer for Studying the Solution Crystallization of Polyolefins

A. J. van Reenen,[1] E. G. Rohwer,[2] P. Walters,[2] M. Lutz,[1] M. Brand[1]

[1]*Department of Chemistry and Polymer Science, University of Stellenbosch, P/Bag X1 Matieland 7602, South Africa*
[2]*Laser Physics Institute, University of Stellenbosch, P/Bag X1 Matieland 7602, South Africa*

Received 21 August 2007; accepted 18 March 2008
DOI 10.1002/app.28390
Published online 23 May 2008 in Wiley InterScience (www.interscience.wiley.com).

ABSTRACT: Cooling a solution of a crystalline polyolefin from 140°C to room temperature causes the dissolved polymer to crystallize. If a laser beam passes through this solution, the crystallization will cause the beam to scatter, which thereby decreases the intensity of the beam. With this principle, it is possible to follow the crystallization of polyolefins under controlled cooling. An instrument capable of doing these analyses was manufactured, and several different polyolefins were analyzed. The effect of the experimental parameters are illustrated for both cooling and reheating experiments. In addition, an interesting dependence on molecular weight was also observed for a series of metallocene polypropylenes. © 2008 Wiley Periodicals, Inc. J Appl Polym Sci 109: 3238–3243, 2008

Key words: crystallization; light scattering; metallocene catalysts; polyolefins; solution properties

INTRODUCTION

Following the article published by Shan et al.[1] on the development of a turbidity fractionation analyzer and having, at the time of the publication of that article, been in the process of designing a similar piece of equipment, we went ahead and designed and built a system similar in general design to that described by Shan et al. The use of fractionation by crystallization to study the molecular heterogeneity of polyolefins (e.g., the short-chain branching distribution) by temperature rising elution fractionation (TREF) is well known and has been covered by some excellent reviews.[2–7] Similarly, the use of Crystaf, developed by Monrabal[8] for the study of the solution crystallization of polyolefins,[6,9,10] is also well known. We have also used preparative TREF to fractionate polyolefins in several studies.[11,12] Both TREF and Crystaf are based on the assumption that the crystallization from solution of a polyolefin is dependent on the crystallizability of the dissolved polymer at a given temperature. In the case of TREF, a polymer solution is slowly cooled and allowed to precipitate onto a support. After cooling, the precipitated polymer is removed by fresh solvent as the temperature is raised. Thus, TREF gives information on the melting of the previously crystallized polymer in the presence of solvent. Crystaf, on the other hand, measures the concentration of a polymer in solution as crystallization occurs. Crystaf has an advantage over TREF in that measurements are made in a single crystallization step, whereas TREF requires both cooling and elution steps. The biggest drawback, according to Shan et al.,[1] of TREF and Crystaf is that both analytical instruments require complex instrumentation and are expensive. The use of a solution turbidity analyzer for the study of polyolefin crystallization behavior in solution seemed to be a logical step, given the reported short analysis times, the ability to crystallize the polymer from solution, and the ability to redissolve the crystallized material from solution (similar to analytical TREF) in a single experiment.[1] In our case, this would be particularly relevant, as we have built up a library of fractionation products of commercial polyolefins and those produced in-house. This article reports the initial results of experiments conducted on this instrument.

Correspondence to: A. J. van Reenen (ajvr@sun.ac.za).

Journal of Applied Polymer Science, Vol. 109, 3238–3243 (2008)

EXPERIMENTAL

Turbidity analyzer

The design of the turbidity fractionation analyzer used in our experiments to measure the turbidity of polymer solutions was based on the design published by Shan et al.[1] The schematic of the experimental setup is given in Figure 1.

The quartz sample holder fit tightly into the four-port aluminum block. The aluminum block was mounted on top of a heater/stirrer, of which the heater coil was connected to the external temperature controller. Thermal paste between the heater/stirrer top and the aluminum block ensured maxi-

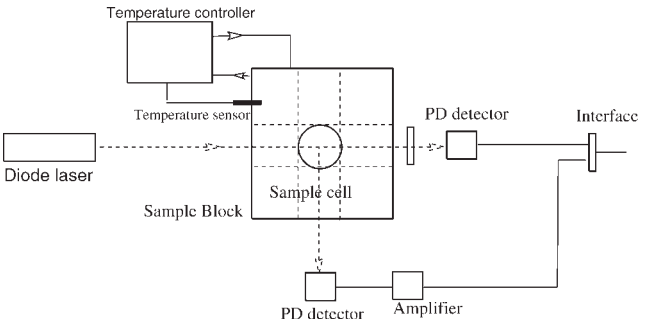

Figure 1 Schematic diagram of the turbidity fractionation analyzer, as viewed from the top.

mum thermal contact. Cooling liquid flowing through the top and bottom sections of the aluminum block allowed for controlled cooling and heating. The laser beam from a 4.5-mW Thorlabs diode laser module CPS 196 (Newton, NJ) at 635 nm was focused in the center of the sample cell. For the preliminary experiments, two UDT-555D Si photodiode detectors were used to detect scattered light. Each was fitted with a preamplifier circuit to boost the signal output. The one photodiode measured the change in the intensity in the forward direction due to scattering. To protect this detector against saturation, a neutral density filter was put in the path of the laser. The second detector was mounted at 90° to the laser beam to monitor the changes in scattering caused by the crystallization of the polymer in the solution with changes in temperature. Because of the lower intensity of this signal, further amplification was required. Because the diode laser output was quite stable, a reference detector was not used in this stage of the investigation. The voltage output of each of the two photodiode detectors was connected to a Stanford Research Systems SR245 interface and a computer for data acquisition and handling. The data acquisition was triggered by a clock pulse of 1 Hz. As the setup did not allow for the amplification of the intensity at the 90° detector, only the direct beam intensity was measured in this preliminary study.

The inside surfaces of the aluminum block were painted matt black to limit scattering and reflections. Furthermore, the interference of room lighting on the detectors was eliminated by tubing between the aluminum block and the detectors.

The temperature-control system was designed in-house and offered special features. To change the temperature at a controlled rate (between 0.2 and 2°C/min) in a heating or cooling range between 30 and 100°C, we used a microprocessor temperature controller (GEFRAN 800 model, Provaglio d'lseo (BS), Italy). As input, from the heater block to the control instrument, we used a resistance thermometer probe (type PT100). Two logic outputs were used, one controlling the hotplate element through a solid-state relay and the other regulating the cooling water flow from a cold water tap through the cooling manifold using a solenoid valve switched by a solid-state relay.

Samples, preparation, and analysis parameters

Several different types of polymers were analyzed on the instrument. Typically, a solution of between 0.5 and 2 mg/mL of the polyolefin was dissolved in 1,2,4-trichlorobenzene at 130°C. The solution, in a quartz sample holder (inside diameter = 21 mm, length = 100 mm), was placed into the receptacle in the aluminum heating/cooling block, and the sample was cooled in a controlled fashion from 100°C to room temperature. Cooling rates varied between 1 and 3.5°C/min. Samples comprised two commercial polyolefins, a propylene-1–pentene copolymer prepared by a heterogeneous transition-metal catalyst and linear low-density polyethylene (LLDPE), and three polypropylenes (PPs) prepared in-house by a suitable C_2 symmetric metallocene catalyst with differing molecular weights but similar tacticities. The latter polymers were produced by the polymerization of propylene with the metallocene catalyst {dimethylesilyl bis[2-methyl-4,5-(benzo)indenyl]zirconium dichloride} and methyl alumoxane (10% solution in toluene) at 25°C and with hydrogen as a transfer agent to control the molecular weight.

Molecular weights were determined with high-temperature gel permeation chromatography. A flow rate of 1 mL/min on a PL-GPC 220 high-temperature chromatograph (Polymer Laboratories, Varian Inc., Amherst, MA) was used, and the measurements were performed at 160°C. The columns used were packed with a polystyrene/divinylbenzene copolymer (PL gel MIXED-B [9003-53-6]) from Polymer Laboratories. The sample concentration was 2 mg/mL, and the solvent used was 1,2,4-trichlorobenzene stabilized with 0.0125% 2,6-di-*tert*-butyl-4-methylphenol. 2,6-Di-*tert*-butyl-4-methylphenol was used as a flow-rate marker. Calibration of the instrument was done with monodisperse polystyrene standards (EasiCal from Polymer Laboratories). The detector used was a differential refractive-index detector. The melting temperature and crystallinity were determined on a TA Instruments Q100 differential scanning calorimetry (DSC) system calibrated with indium metal according to standard procedures. The heating and cooling rates were maintained at a standard 10°C/min. The samples of the standard fractions and original polymers were first subjected to a heating ramp up to 220°C, after which the temperature was kept isothermally at 220°C for 5 min to remove thermal history. The cooling cycle followed the isothermal stage, with the subsequent second heating scan being recorded for analysis. ^{13}C-NMR

TABLE I
Characterization Data for the Polyolefins Used in this Study

Polymer	Comonomer (%)	M_w	PD	T_m (°C)	Crystallinity (DSC)	mmmm%
m-PP-1	n/a	35,962	2.7	150.9	81.0	93.8
m-PP-2	n/a	65,054	2.2	151.3	70.1	93.3
m-PP-3	n/a	141,885	3.1	149.8	55.0	93.5
PP-1–pentene	1-Pentene (1.2)	305,800	4.2	151.8	67.4	n/a
LLDPE	1-Butene (6.0)	278,050	3.8	122.9	nd	n/a

M_w, weight-average molecular weight; T_m, melting temperature; n/a, not applicable; nd, not determined.

spectra were recorded at 120°C on a Varian VXR 300 spectrometer. A pulse angle of 45° and a relatively short repetition time of 0.82 s were used. Some of the samples were also run on a 600 Varian Unity Inova NMR spectrometer equipped with an Oxford magnet (14.09 T) operating at 600 MHz, with a 5-mm inverse detection pulsed field gradient probe. Samples (60–80 mg) for ^{13}C-NMR analyses were dissolved at 110°C in a deuterated 1,1,2,2-tetrachloroethane. Analyses of the ^{13}C-NMR spectra allowed for the calculation of the comonomer content in the copolymers and the tacticity (expressed as mmmm%) of the propylene homopolymers.

RESULTS AND DISCUSSION

Chemically distinct polymers

The purpose of the first set of experiments was to see if chemically distinct polymers would give different responses on the instrument, in other words, whether the technique could distinguish between the crystallization behavior of materials that we knew to be different. To this end, the materials that were used for analyses and their molecular characteristics are listed in Table I.

A typical response is shown in Figure 2. The sharp decrease in the signal from the diode was due to the increased scatter of the incident beam, whereas the scattered signal at the end of the run was due to the crystallites formed during the process of scattering the beam. Data were then analyzed with Origin software (OriginLab Corp., Northampton, MA). To get a peak and have the ability to analyze the peak maximum and peak width, we calculated the first derivative of the voltage data. Data were smoothed as the derivative was calculated. A typical result is shown in Figure 3.

As shown in Figure 3, extensive scatter after crystallization was evident (area marked A in the figure). In other plots presented in this article, extensive smoothing of the data in this area was done before the first derivative was taken. This was done so we could present overlays of different sets of results. The data points collected below 65°C were subject to severe scattering. A minimum voltage was observed around 45°C. Below 45°C, there appeared to be a slight increase in voltage; in other words, we saw an increase in the measured beam intensity. This was caused by the increase in crystallite size as cooling increased and crystalline particles continued to grow. This caused an increased forward scatter and

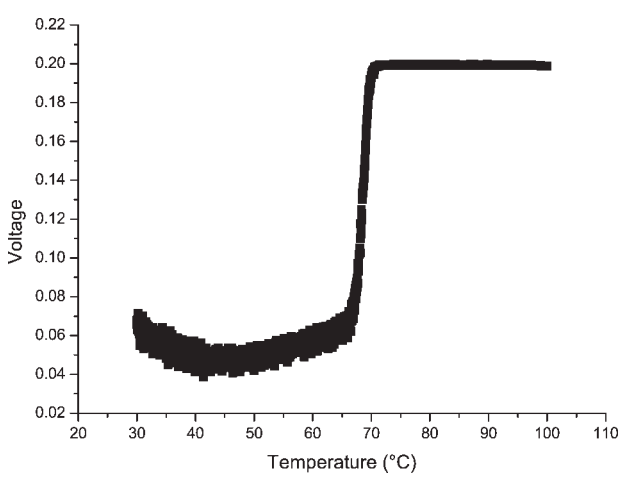

Figure 2 Raw data for the cooling scan of m-PP-3 at 2°C/min and a concentration of 2 mg/mL.

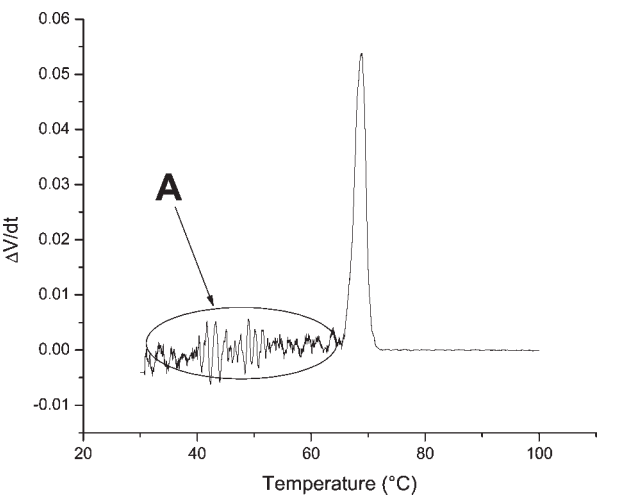

Figure 3 First derivative of the raw data shown in Figure 2. ΔV/dT is the first derivative of the voltage data.

increased the apparent intensity. This is something we believe could be used to good effect in future experiments.

As mentioned, the initial experiments were conducted to see if we could differentiate between chemically different polymers. To illustrate this, we present the scans for two polymers, a commercial LLDPE and a commercial polypropylene-1 (PP-1)–pentene copolymer (see Table I). In each case, a cooling rate of 2°C/min and a polymer concentration of 2 mg/mL were used. An overlay of two of the scans, those of the LLDPE and the PP-1–pentene copolymer, is shown in Figure 4. Comparing this to the scan for metallocene polypropylene-2 (m-PP-2; Fig. 2), we could see that the crystallization behavior of the three polymers were different, not only with respect to the peak crystallization temperatures but also with respect to the range over which crystallization occurred. In particular, the set of conditions selected for the LLDPE led to a very broad peak, with the scattering having a severe influence on the ability to isolate and identify the crystallization peak.

Effect of the experimental parameters

Sample concentration effects

The initial experiments indicated that the crystallization behavior seemed to be dependent on the experimental parameters. This included the concentration of the polymer in solution and the cooling rates. The concentration not only affected the peak crystallization temperature (determined from the first derivative plot) but also the scatter and range of crystallization. The latter is illustrated in Figure 5, where we illustrate the effect of sample concentration on the crystallization profiles of a commercial propylene-1–pentene copolymer. Two solutions, with concentrations of 2 and 0.5 mg/mL, were compared.

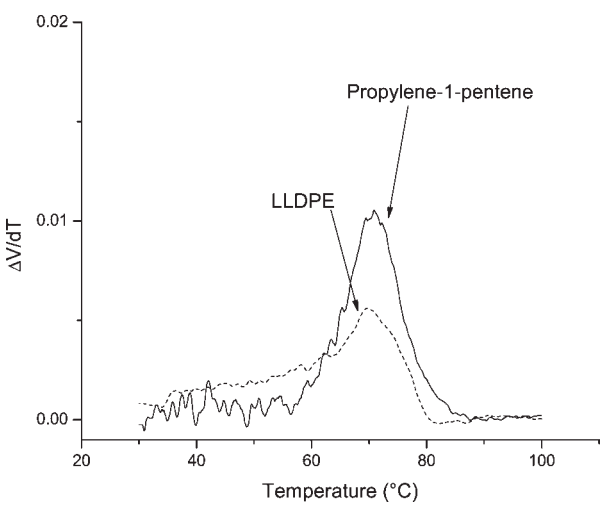

Figure 4 Comparison of a propylene-1–pentene copolymer and LLDPE analyzed under identical conditions (2 mg/mL, 2°C/min).

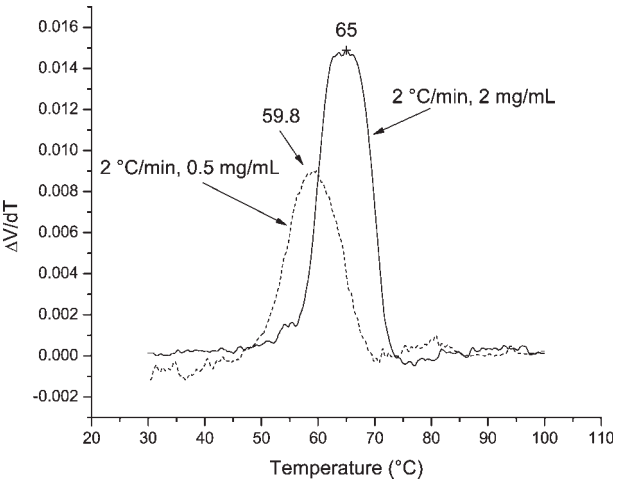

Figure 5 Concentration effects during crystallization from solution for a propylene-1–1-pentene copolymer.

As shown in Figure 5, the higher the concentration was, the higher the crystallization temperature was for a given cooling rate. Intuitively, this was to be expected, as a higher concentration of polymer would lead to more rapid crystallization. It was also noticeable that the peak width for the crystallization of the polymer with the lower concentration was wider than that of the solution with the substantially higher concentration.

Cooling rate

It was expected that the cooling rate would play a role in the data generated by these experiments. As one of the big advantages with these experiments is seen to be the fairly short scan times, we felt it necessary to see how big an effect the cooling rate had on the results. For example, in Figure 6, we illustrate the difference achieved in when cooling rates of 2, 1.4, and 1°C/min were compared.

Even with a relatively small change in the cooling rate, we saw a significant change in the peak temperature of the first derivative peaks of the cooling profiles for three solutions (1 mg/mL) of the propylene-1–pentene copolymer. The peak width of the slower cooling rate was less than that of the slightly faster cooling rate, whereas the crystallization range also appeared to be narrower when the cooling rate was decreased. Unfortunately, the data-capture package used for these experiments precluded the use of even slower cooling rates.

Heating rates

It was obvious that the reverse of the cooling experiments could be done. The suspension of crystallized

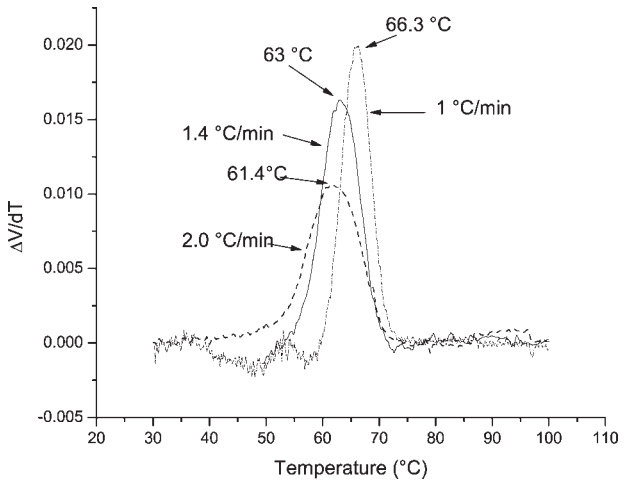

Figure 6 Effect of the cooling rate on the crystallization of PP-1–pentene. Cooling rates of 1, 1.4, and 2°C/min were used. The solution concentration was 1 mg/mL.

material was heated, the disappearance of scattering was recorded, and upon derivation and smoothing, a heating curve was obtained. In Figure 7, the results of the heating experiments of similar solutions of a propylene-1–pentene copolymer are shown.

In Figure 7, the dashed line represents the first derivative of the heating curve of a solution of 1-mg/mL propylene-1–pentene copolymer heated at 1°C/min, whereas the solid line represents the 2°C/min experiment. The peak with an apparent shoulder of the crystallized material heated at 2°C/min was clearly resolved into two maxima when the material was heated at 1°C/min. It is possible that some more peaks might have been present at lower temperatures, but the amount of scatter makes it impossible to make statements in this regard. Similar experiments conducted at 3.5°C/min yielded a very broad peak with a severe tailing toward higher temperatures. There also appeared to be a slight increase in the 2°C/min scan around 40°C, but as this area was severely affected by scattering (crystallites reflecting light), no real conclusion could be drawn about any of the data in this area.

Molecular weight effects

As an additional experiment, we synthesized three metallocene copolymers with the same metallocene catalyst, keeping the catalyst/cocatalyst/monomer ratio constant for all three reactions and while varying the amount of hydrogen introduced into the reaction. The tacticities are given in Table I. In this experiment, we compared two materials with noticeably different molecular weights. The overlay of the crystallization experiment is shown in Figure 8. In this case, it was clear that a molecular weight effect appeared to be present during the solution crystallization of the polymers. This was significant, as molecular weight effects are generally ignored during fractionation crystallization experiments. The effect of the molecular weight on the fractionation was considered by Wild et al.[13] The data obtained by Wild et al.[13] indicated that if the polymer chain ends were considered to be the equivalent of a branch point, the molecular weight dependence on the fractionation mostly disappeared. They also showed that the molecular weight dependence fell away as soon as the molecular weight reached approximately 10^4 g/mol. In our experiment, we concluded that molecular weight did, in fact, play a significant role when two polymers of similar tacticity crystallized from solution.

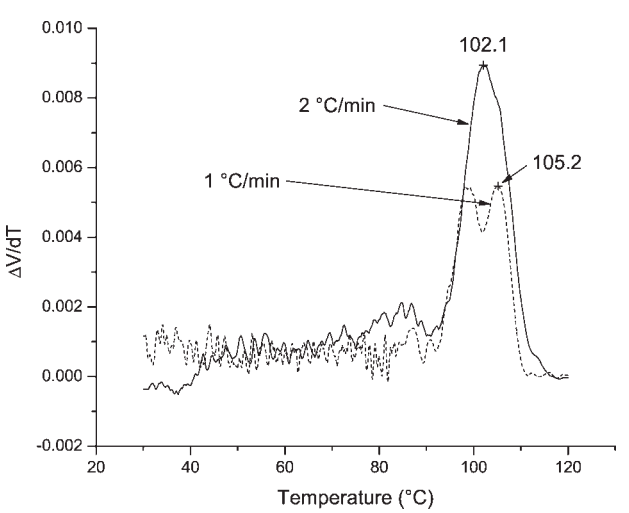

Figure 7 Heating profiles of 1-mg/mL solutions of a PP-1–pentene copolymer. Heating rates of 1 and 2°C/min are shown.

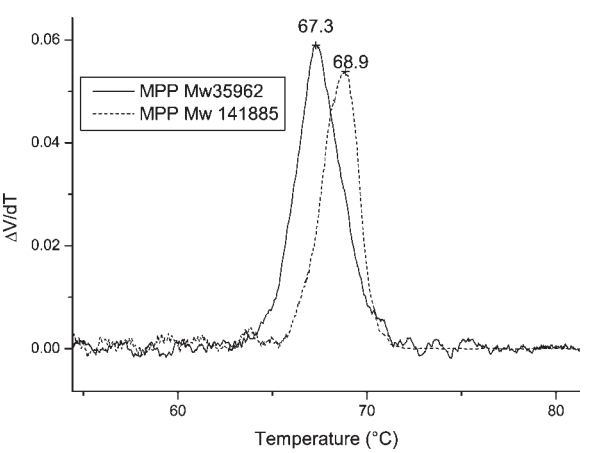

Figure 8 Crystallization profiles of two PPs prepared by a metallocene catalyst. The dashed line represents the polymer with a molecular weight of 141,885, and the solid line represents the polymer with a molecular weight of 35,962. The sample concentration was 2 mg/mL, and the cooling rate was 2°C/min. MPP is metallocene polypropylene.

CONCLUSIONS

It was possible to draw some conclusions regarding the structure/property relationships of the polymers and the results obtained from the initial experiments with the turbidity analyzer. There were, however, some aspects that made us reluctant to make definitive statements in this regard. One aspect that we feel needs further investigation is that of the effect of the forward scatter. In the study presented here, we measured the intensity of the incident beam and attributed the decrease in the detector voltage to the phenomenon of crystallization. However, as soon as the crystallites became large enough, they scattered light very effectively and, as such, should have contributed to the measured light intensity.

Although we are as yet not in a position to make definitive statements about the reasons for the variations that we saw in the crystallization behavior of the polymers that we investigated, we can conclude that we are able, by means of the turbidity analyzer, to differentiate between polymers of different chemical and morphological composition. The first results indicate that the experimental parameters played a big role in this setup. This makes it difficult to compare chemically dissimilar polymers, but with chemically similar polymers, it does appear possible to compare materials. In this regard, we showed an apparent dependence of molecular weight during the solution crystallization of m-PP samples. Both cooling (crystallization from solution) and heating (melting and dissolution) experiments were successfully demonstrated, and it was shown that both cooling and heating rates, as well as polymer concentration, affected the molecular weight.

Shan et al.[1] concluded that there is tremendous potential for the use of a turbidity analyzer for the study of polyolefin crystallization, and we must concur. The method is easy to use, rapid, and allows for both cooling and heating experiments to be conducted in a short space of time. We feel that some work still needs to be done on the data collection aspect, to ensure that what is measured is due to crystallization and not some experimental artifact.

References

1. Shan, C. L. P.; deGroot, W. A.; Hazlitt, L. G.; Gillespie, D. Polymer 2005, 46, 11755.
2. Wild, L. Adv Polym Sci 1990, 98, 1.
3. Soares, J. B. P.; Hamielac, A. E. In Modern Techniques for Polymer Characterisation; Pethrick, R. A.; Dawkins, J. V., Eds.; Wiley: Chichester, England, 1999; p 15.
4. Xu, J.; Feng, L. Eur Polym J 2000, 36, 867.
5. Glockner, G. J Appl Polym Sci Appl Polym Symp 1990, 45, 1.
6. Monrabal, B. Encyclopaedia of Analytical Chemistry; Wiley: Chichester, England, 2000; Vol. 9, p 8074.
7. Soares, J. B. P.; Hamielac, A. E. Polymer 1995, 36, 1639.
8. Monrabal, B. U.S. Pat. 5,222,390 (1991).
9. Monrabal, B. J Appl Polym Sci 1994, 52, 491.
10. Monrabal, B. Macromol Symp 1996, 110, 81.
11. Harding, G.; van Reenen, A. J. Macromol Chem Phys 2006, 207, 1680.
12. Assumption, H. J.; Vermeulen, J. P.; Jarret, W. L.; Mathias, J. L.; van Reenen, A. J. Polymer 2006, 47, 67.
13. Wild, L.; Ryle, T. R.; Knobeloch, D. C.; Peat, I. R. J Polym Sci Polym Phys Ed 1982, 20, 441.

Solution Crystallization Analysis by Laser Light Scattering (SCALLS)

Albert van Reenen,[*1] *Margaretha Brand,*[1] *Erich Rohwer,*[2] *Piet Walters*[2]

Summary: Solution crystallization analysis by laser light scattering offers a direct way of studying the solution crystallization of polyolefins. The technique yields similar results to Crystaf, but in a shorter time and with apparently greater sensitivity in some cases. The use of SCALLS is demonstrated for the study of selected propylene/higher α-olefin copolymers. Some conclusions are also drawn regarding the effect of molecular weight on the solution crystallization of polyolefins.

Keywords: laser light scattering; polyolefins; solution crystallization

Introduction

Crystallization from solution of the polyolefins is used in well-known analytical techniques, to provide information on chemical composition distribution of these important polymers. In this instance, both Crystaf and analytical Tref (*a*Tref) is well-known, and has been extensively reviewed.[1–4] More recently, Monrabal[5] has reported the use of Crystallization Elution Fractionation (CEF), a refinement on the basic Tref technique, and which affords rapid analysis (compared to conventional *a*Tref and Crystaf) and good separation.

Recently we reported the use of solution crystallization analysis by laser light scattering (SCALLS).[6] This technique was previously described by Shan *et al.*,[7] who initially termed the technique ''turbidity fractionation analysis''. In the case of SCALLS, light scattering can be measured (either as intensity of transmitted light or as intensity of scattered light) by taking readings (for example, based on our experimental parameters) as slowly as once every six seconds or as rapidly as ten times per second. This relates to (at a cooling rate of 1.4 °C/min and a temperature range of 70 °C) 500 to 30 000 data points. The technique also affords a direct measurement. Light is scattered as soon as crystallite sizes becomes large enough to scatter the laser light (this would be dependent on wavelength of the light). In addition SCALLS affords the opportunity of measuring the ''solution melting temperature'' of polyolefins, as the solution may be heated in a controlled fashion after crystallization has been completed. This paper reports on the effect of some of the experimental parameters as well as some recent studies on crystallization of propylene copolymers.

Experimental Part

The SCALLS Instrument

The development and layout of the instrument has been reported elsewhere.[6] We added two photodiode detectors to the instrument, at 90° and 270°. The ''in-line'' photodiode detector is denoted as the 180° detector. This detector measures laser light intensity and will record a decrease in intensity as crystallization occurs. The 90° and 270° detectors measure scattered light intensity. In a further development we placed a neutral density filter between the sample cell and the 180° detector. The general layout is shown in Figure 1.

[1] Department of Chemistry and Polymer Science, University of Stellenbosch, South Africa
E-mail: ajvr@sun.ac.za
[2] Laser Physics Institute, University of Stellenbosch, Private Bag X1, Matieland 7602, South Africa

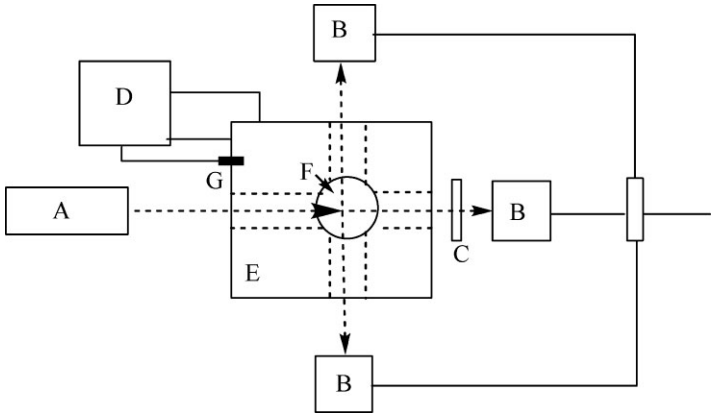

Figure 1.
A schematic layout of the SCALLS instrument. A = diode laser, B = photodiode detectors, C = neutral density filter, D = temperature controller, E = sample block, F = sample cell, G = temperature probe.

The SCALLS Method

Unless otherwise indicated, all heating and cooling experiments in the SCALLS were conducted using a polymer concentration of 1 mg/mL in 1,2,4 trichlorobenzene, and at a rate of 1.4 °C/minute. Polymer solutions were made up at 140 °C and controlled cooling was done from 100 °C to 30 °C.

Polymers

We synthesized a series of isotactic polypropylenes using a suitable C_2 symmetric metallocene catalyst. Hydrogen was used to control molecular weight. Some of these polymers were subjected to preparative TREF experiments[8] and fractions with well-defined molecular weights and tacticity were isolated and used in the molecular weight studies. The propylene copolymers (propylene/octene, propylene/tetradecene and propylene/octadecene) were synthesized using a metallocene catalyst as previously described.[9] The polymers were subjected to standard characterization techniques. Thermal analyses were done on a TA instruments Q100 DSC using a heating and cooling rate of 10 °C/min, while ^{13}C NMR spectra were obtained on a Varian VXR 600 MHz spectrometer in 1,1,2,2-tetrachloroethane-d_2, using δ 74.3 as internal secondary reference. The pulse angle was 45 degrees and the acquisition time was 0.82 seconds (130 °C) and used to determine tacticity, comonomer content and possible 2,1 monomer insertions. Molecular weight determinations were done on a PL 220 GPC at 160° in trichlorobenzene as solvent and using 4 polystyrene/divinylbenzene copolymer packed columns (PL gel MIIXED-B [9003-53-6]). The properties of the polymers that were analyzed are given in Table 1. Crystaf experiments were run on a Model 200 (Polymer Char, Valencia, Spain) in TCB as solvent (cooling at 0.1 °C/min from 100 °C to 30 °C). Where necessary, polymers were fractionated on a preparative TREF instrument built in-house.[8]

Results and Discussion

In Figure 2, the responses of the three different detectors are shown for the same polymer in the same cooling experiment. In this case, a metallocene PP with a molecular weight of 70 000 g/mol and a tacticity of 95.4% was used. There is good correlation between the three detectors. The 180° detector measures a decrease in laser light intensity, while the other two detectors measures an increase in scattered light intensity. The response for the 180° detector is reversed in the plot to allow better differentiation between the derivative curves.

Table 1.
Summary of properties of polymers used in this study.

Polymer	Mw (g/mole)	PD[b]	Comonomer type	[Comon] (mole%)
iPP-1[a]	38000 [92.7%]	2.1	None	–
i-PP-2[a]	35000 [96.6%]	2.2	None	–
i-PP-3[a]	83000 [93.5%]	1.9	None	–
i-PP-4[a]	134000 [93.5%]	2.0	None	–
PP/C8-1	506700	2.4	1-Octene	0.86
PP/C8-2	643500	2.3	1-Octene	0.57
PP/C8-3	722200	2.5	1-Octene	0.47
PP/C14-1	344800	2.5	1-Tetradecene	0.89
PP/C14-2	744900	2.5	1-Tetradecene	0.63
PP/C14-3	308900	3.0	1-Tetradecene	0.50
PP/C18-1	1140000	2.1	1-Octadecene	0.66
PP/C18-2	609000	2.5	1-Octadecene	0.47
PP/C18-3	641100	2.6	1-Octadecene	0.39

[a]: Polymer fractions obtained by p-TREF from metallocene iPP, values in square brackets are isotacticity,
[b]: PD = polydispersity

In Figure 3 and 4 we show the solution crystallization behaviour of 4 polymers obtained by the p-TREF fractionation of metallocene iPPs. In Figure 3 the solution crystallization of two polymers with similar molecular weight but different tacticities is shown. It is quite clear that the polymer with the lowest tacticity crystallizes from solution at a lower temperature, which is to be expected. In this case the molecular weight of the two polymers was quite low (around 35 000 g/mol)

In Figure 4, however, we see the crystallization behaviour of two polymers of similar tacticity (94%) but different molecular weight (83 000 vs 134 000 g/mol) In this case it seems clear that the polymer with the highest molecular weight crystallizes from solution first. The Flory Huggins equation which has commonly been adapted and used to predict the behaviour of polymers in Crystaf and TREF experiments predicts that molecular weight should not have a real effect on the solution crystallization of polyolefins. This result, as well as others that we have observed[6] seems to indicate that, in the case of PP at least, this might not be the case. ^{13}C NMR (spectra not shown

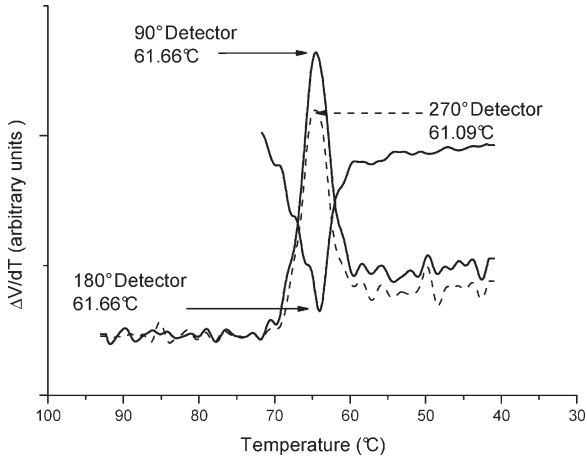

Figure 2.
First derivative SCALLS plots (cooling) of the responses of three different detectors for the same polymer sample. The 180° detector response is inverted for clarity.

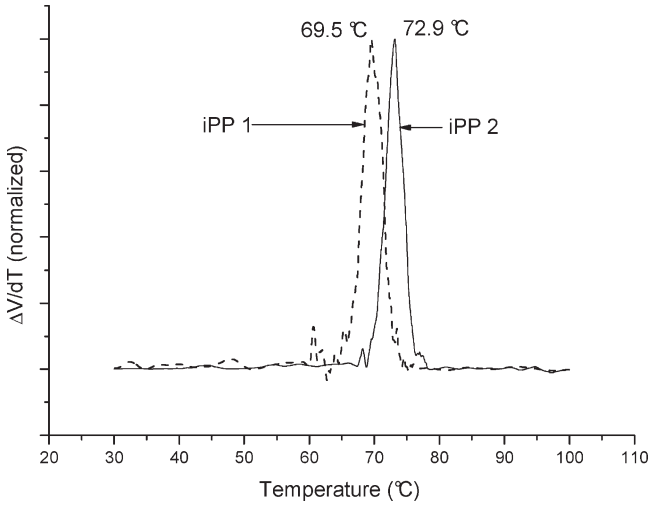

Figure 3.
The normalized first dervative SCALLS cooling plots for iPP 1 and iPP 2.

here) analysis of these two polymers reveal similar but negligible occurrence of 2,1 misinsertions in the polymers. The occurrence of these regioerrors could therefore not account for the difference in crystallization temperatures that we observe. The authors believe that crystallization is a function of both tacticity and molecular weight. Similar effects have been reported for Crystaf.[4]

We compared the use of SCALLS on a series of propylene copolymers with peak crystallization temperatures obtained by Crystaf and DSC. At the same time we also compared ''solution melting'' temperatures obtained by SCALLS with the bulk melting behaviour as measured by DSC. In Figure 5 we present the SCALLS cooling profiles of the C14 copolymers, while the Crystaf profiles for the same polymers are

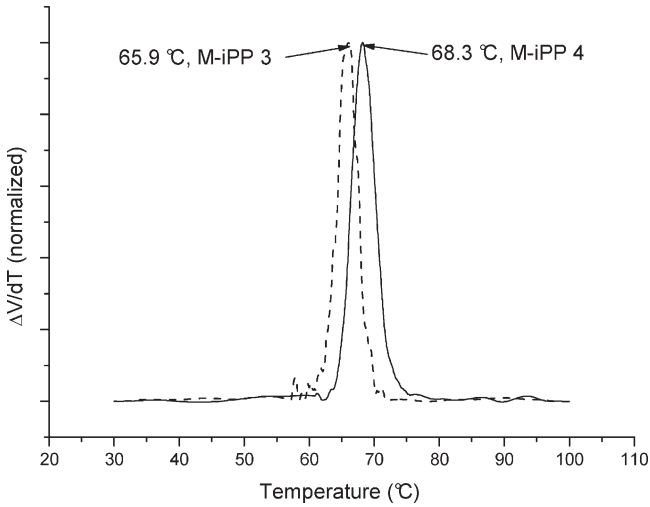

Figure 4.
The normalized first dervative SCALLS cooling plots for iPP 3 and iPP 4. Cooling rate was at 2 °C/minute for this experiment.

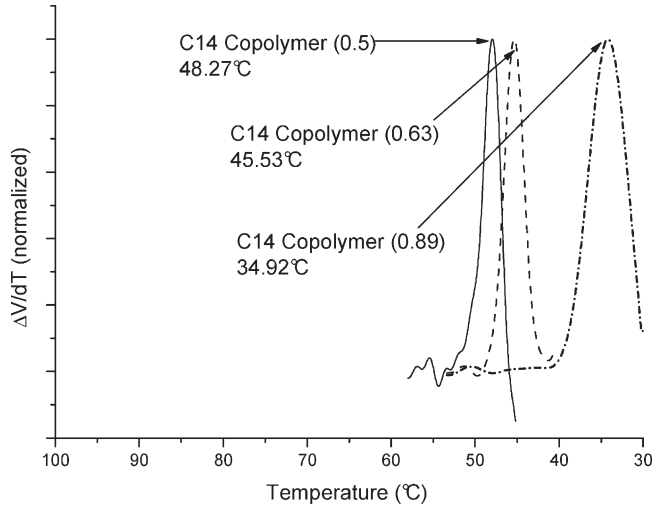

Figure 5.
The normalized first derivative SCALLS plots (ccooling) for 3 C14 copolymers. Comonomer content and peak crystallization temperatures are indicated on the figure.

presented in Figure 6. In this instance, it is interesting to note that SCALLS is able to differentiate between two polymers with small differences in comonomer content (see Table 1) while this appears to be difficult to do with Crystaf. A graphic summary of all the results of this study is presented in Figure 7. Overall the peak crystallization temperatures determined by SCALLS is lower than for Crystaf, largely due to the faster cooling rate used for SCALLS.

In Figure 8 the cooling profile of the C18 copolymers are presented, with the heating profile of the three polymers presented in Figure 9. It is clear that SCALLS

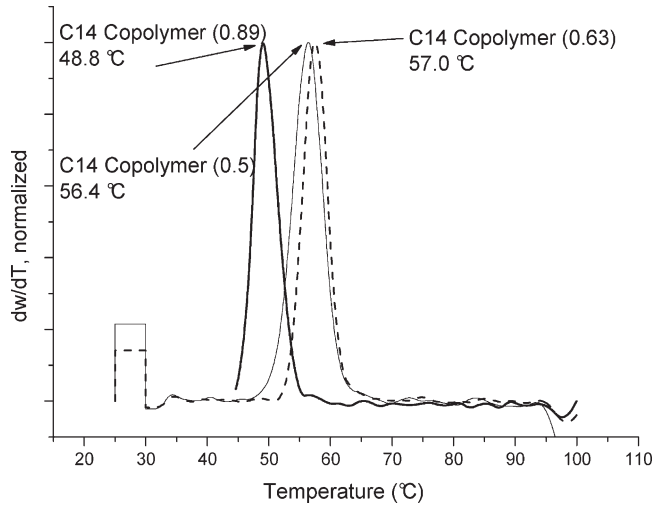

Figure 6.
The Crystaf cooling profiles for 3 C14 copolymers. The peak crystalization temperatures and the comonomer content are indicated in the figure.

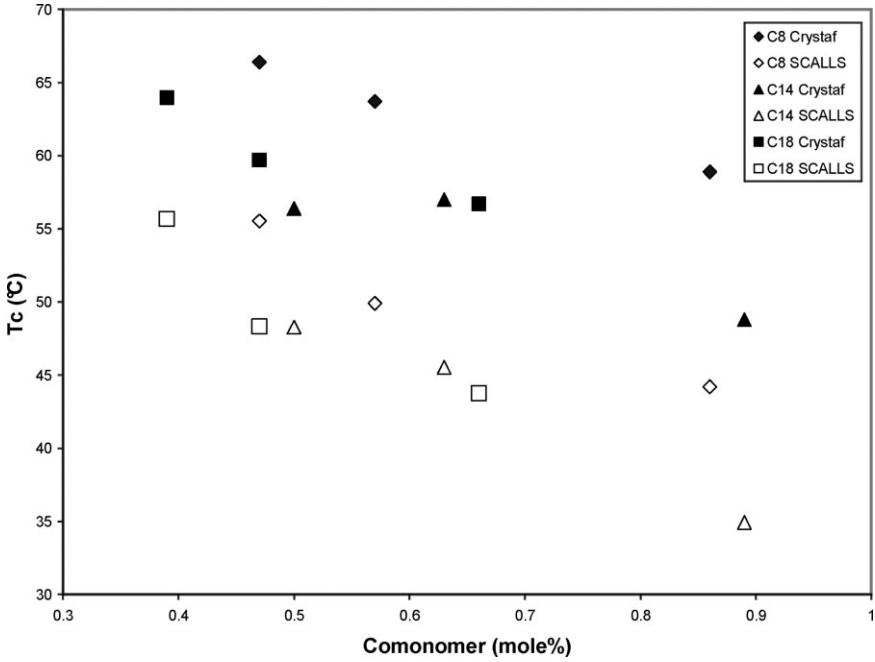

Figure 7.
The peak solution crystallization temperatures of propylene copolymers (C8, C14 and C18) as determined by SCALLS and Crystaf.

presents an opportunity to study the ''solution melting'' behaviour of the polyolefins. A comparison of the solution and DSC melting trends for the C18 and C14 copolymers are presented in Figure 10. A good correlation is observed. It should be possible to study the relationship between the solution melting (T_m) and the bulk melting temperature (T_m^0) as a function of comonomer type and content.

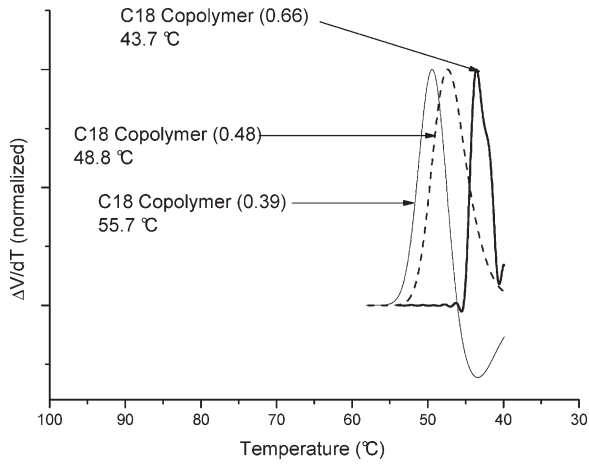

Figure 8.
Normalized first derivative SCALLS plots (cooling) for propylene-octadecene copolymers. The peak crystallization temperatures and the comonomer content are shown in the figure.

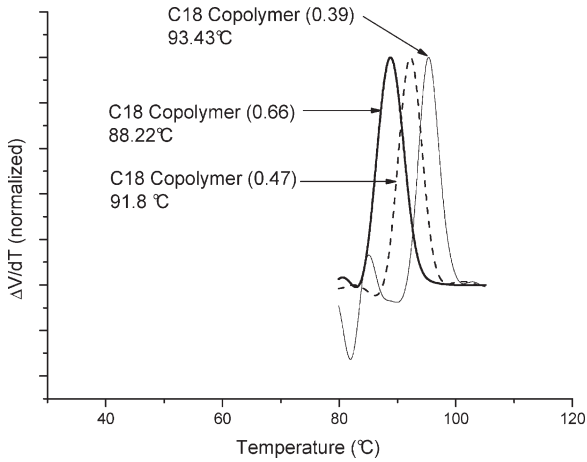

Figure 9.
The normalized first derivative SCALLS plots (heating) for propylene-octadecene copolymers. The peak crystallization temperatures and the comonomer content are shown in the figure.

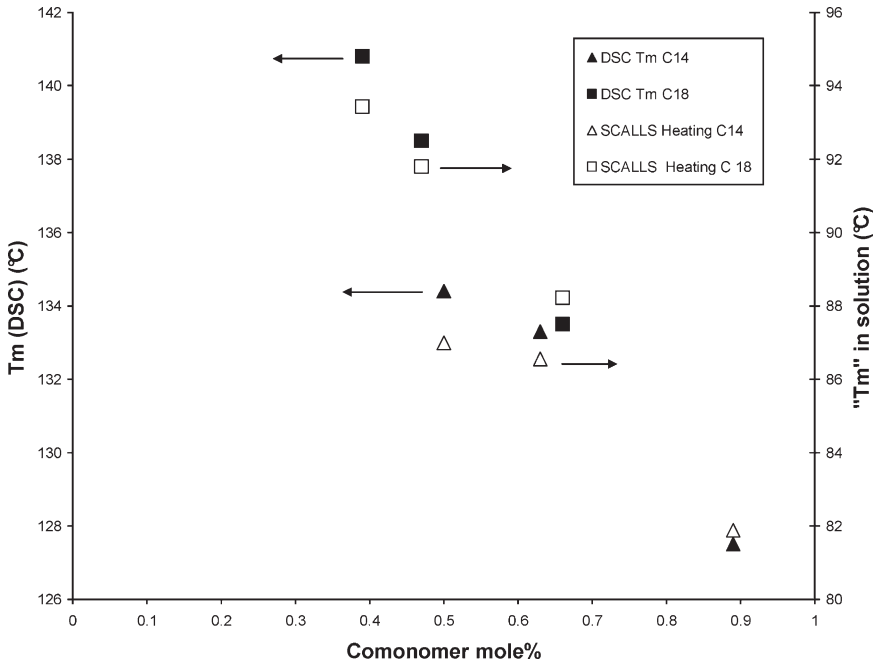

Figure 10.
Comparison of DSC melting temperatures and SCALLS solution melting temperatures for C18 and C14 propylene copolymers.

The data presented here is obviously insufficient to draw conclusions from, but we are at present completing a series of similar measurements on a wide range of propylene-1-alkene copolymers, and will be presenting the results shortly.

Conclusion

SCALLS is a direct method of observing solution crystallization of the polyolefins. The technique is able to clearly differentiate in the crystallization behaviour of

polyolefins with small but distinct differences in chemical composition. In some instances this technique, even with rapid cooling rates, appears to be more sensitive than Crystaf. This could be due to the fact that this is a direct method, which records changes in light intensity and scattering immediately, while Crystaf relies on far fewer measurements which occur after the fact. In Crystaf crystallization occurs first, and thereafter a solution concentration is measured. The authors also believe that SCALLS presents a means of directly investigating the applicability of the Flory-Huggins equation to the prediction of solution crystallization of the polyolefins, in particular the effect of molecular weight and even the solution interaction parameter.

[1] S. Anantawaraskul, J. B. P. Soares, P. M. Wood-Adams, *Adv. Polym. Sci.* **2005**, *182*, 1.
[2] J. B. P. soares, A. E. Hamielec, in: "*Modern techniques for polymer characterization*", R. A., Pethrick, J. V. Dawkins, Eds., Wiley, New York 1999, p. 15.
[3] L. Wild, C. Blatz, in: "*New advances in polyolefins*", T. C. Chung, Ed., Plenum, New York 1993, p. 147.
[4] J. B. P. Soares, S. Anantawaraskul, *J Polym. Sci. B: Polym. Phys.* **2005**, *43*, 1557.
[5] B. Monrabal, J. Sancho-Tello, N. Mayo, L. Romero, *Macromol. Symp.* **2007**, *257*, 71.
[6] A. J. van Reenen, E. Rohwer, M. Brand, M. Lutz, P. Walters, *J. Appl. Polym. Sci.* **2008**, *109*, 3238.
[7] C. L. P. Shan, W. A. deGroot, L. G. Hazlitt, D. Gillespie, *Polymer* **2005**, *46*(25), 11755.
[8] A. J. van Reenen, G. W. Harding, *Macromol. Chem. Phys.* **2006**, *207*, 1680.
[9] A. J. van Reenen, R. Brüll, U. M. Wahner, H. G. Raubenheimer, H. Pasch, *J. Polym. Sci A: Polym. Chem.* **2000**, *38*(22), 4110.

